Studies on the Metabolic Pathway of (-)-Epigallocatechin Gallate by Rat Enterobacteria and the Effect of the Metabolites on Glucose Tolerance in Mice

Takagaki, Akiko

DOCTORAL DISSERTATION

Studies on the Metabolic Pathway of (−)-Epigallocatechin Gallate by Rat Enterobacteria,
and the Effect of the Metabolites on Glucose Tolerance in Mice

ラット腸内細菌による(−)‐エピガロカテキンガレートの代謝経路の解明と、
同代謝産物のマウス耐糖能への影響に関する研究

2020

Gradual School of Agricultural Science, Kobe University

Akiko Takagaki

Student No. 146A471A

1

Contents

Abbreviations

EGCG: (−)-Epigallocatechin Gallate

EGC: (−)-Epigallocatechin;

EC: (−)-Epicatechin;

ECG: (−)-Epicatechin Gallate;

C: (+)-Catechin;

GCG: (−)-Gallocatechin Gallate;

CG: (−)-Catechin Gallate

BM3: 1-(3′,4′,5′-Trihydroxyphenyl)-3-(2″,4″,6″-trihydroxyphenyl)propan-2-*ol*

BM4: 1-(3′,5′-Dihydroxyphenyl)-3-(2″,4″,6″-trihydroxyphenyl)propan-2-*ol*

BM5: 5-(3′,5′-Dihydroxyphenyl)-4-hydroxyvaleric Acid

BM6: 5-(3′,5′-Dihydroxyphenyl)-γ-valerolactone

BM7: 3-(3′,5′-Dihydroxyphenyl) propionic acid

BM8: 4-Dehydroxylated epigallocatechin

BM9: 5-(3′,4′,5′-Trihydroxyphenyl)-4-hydroxyvaleric acid

BM10: 5-(3′,4′,5′-Trihydroxyphenyl)-γ-valerolactone

BM11: 5-(3′,5′-Dihydroxyphenyl)valeric acid

BM12 : 5-(3′-Hydroxyphenyl)valeric acid

BM13: 5-(3′,4′,5′-Trihydroxyphenyl)valeric acid.

BM6-GlcUA: 5-(3′, 5′-Dihydroxyphenyl)-γ-valerolactone -monoglucronide;

BM6-Sul: 5-(3′,5′-Dihydroxyphenyl)-γ-valerolactone -monosulfate

GLUT4: Glucose transporter 4

AMPK: AMP-activated protein kinase

PI3K: Phosphatidylinositol 3′-kinase

aPKC: Atypical protein kinase C

L6: Rat skeletal muscle cell line

AICAR: 5-Amino-4-imidazolecarboxamide-1-β-D-ribofuranoside;

G6PDH: Glucose-6-phosphate dehydrogenase;

2DG: 2-Deoxyglucose;

DMSO: Dimethyl sulfoxide

Chapter1

General Introduction

Green Teas and Catechins

The tea plant (*Camellia sinensis*) is a perennial evergreen tree that belongs to the camellia family, and the origin is said to be the region from Yunnan to Sichuan in southwestern China (1, 2). Thea is one of the oldest drinks in history and one of the most widly consumed bevarages in the world. The history in of green tea in China is more than 2000 years, and it has long been used as a beverage for promote health (2, 3, 4). The first introduction of tea to Japan from Chine was thought to be in the early Heian period (2). During the Heian period, tea was prized at the court and was used among monks for ceremonial purpases and as a way to stay awake. It is considered to be in the Kamakura period that the custom of drinking tea generally became popular. As noted in "Kissa Yojo-Ki" (5) written by Eisai, humans have historically known that green tea is a healthful drink as a healthy cure-all drink (yojo no senyaku). In the middle of the Edo period, the manufacturing method of Sencha greatly progressed. Later, green tea with good taste and aroma became very popular in Edo. In modern times, tea is a popular drink, and various health effects of tea have become known all over the world (6, 7).

There are several different types of tea in the world, and they are traditionally classified as green tea, black tea, and oolong tea due to the differences in how they are processed. One of the key steps in the manufacturing process that determines the type of tea is the degree of fermentation of the leaves. The duration of tea leaf fermentation refers to how long tea is allowed to undergo enzymatic oxidation (8, 9). The fermentation process may be stopped by either frying or steaming the leaves before completely drying them out. Based on the degree of fermentation, teas are classified as non-fermented, semi-fermented, and fully-fermented. Green tea is non-fermented, oolong tea is semi-fermented, and black tea is fully-fermented. Tea leaves contain proteins, tannins, caffeine, saponin, vitamins, etc. The beneficial effects of green tea have been known for a long time, and it is a popular and healthy drink. The benefits of drinking tea are primarily attributed to the presence of flavan-3-ols. In green tea, many monomeric catechins are present in tea leaves, but in black tea, catechins undergo oxidative polymerization and turn into a red pigment theaflavin during fermentation process. Green tea is popular globally due to its health benefits, which are attributed to the tea catechins. Green tea catechins have a skeleton of flavan-3-ols (Figure 1-1), and one of the plant polyphenols, which is an astringent, is known as tannin. Catechins were first isolated from the Indian plant extract catechu (from the plant *Acacia catechu*, a tree of the Fabaceae family, acacia genus).

4

Green tea catechins constitute about 25% of the dry mass of a fresh tea leaf, although total catechin content varies widely depending on species, clonal variation, growing location, season, light variation, and altitude. The predominant constituents of green tea are polyphenols, belonging to the family of catechins, such as (−)-Epigallocatechin gallate [EGCG], (+)-Catechin [C], (−)-Epicatechin [EC], (−)-Epigallocatechin [EGC)], and (−)-Epicatechin gallate [ECG]. A typical brewed green tea beverage (250 mL) contains 50-100 mg of catechins. Green tea leaves contain 12−14% green tea catechins in the first flush and about 14−15% in the second flush (1, 9, 10).
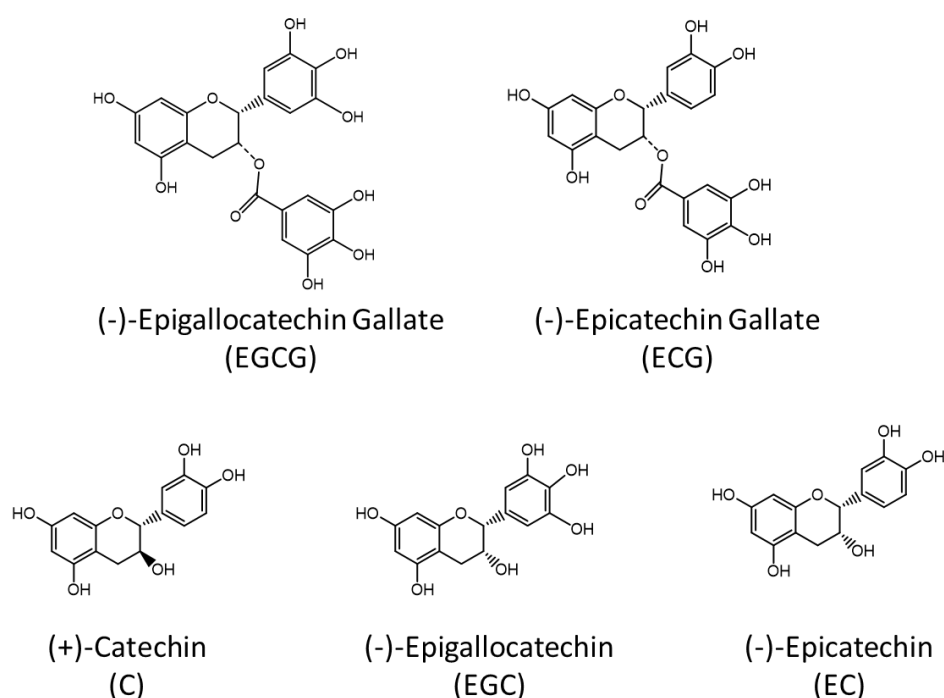

Figure 1-1 Structures of major green tea catechins.
Catechin abbreviations are shown in parentheses.
In this paper, catechins are indicated by abbreviations.

Health Benefits of Green Tea Catechin

Since about 4000 years ago, which is when the health benefits of green tea were recorded for the first time by a Chinese emperor, tea has been used as a medicine (2, 6). In particular, green tea has been known to be good for health and has been consumed on a daily basis for many years. Traditionally tea has been taken to alleviate drowsiness, feverishness, treatment for conjunctivitis; as well as for cough suppression, diuresis, deodorization, as a remedy for hangovers, food poisoning etc. In recent years, many physiologically active effects have been reported from scientific analyses. Many studies on the physiological functions of green tea

catechins have been conducted across the world; with several such studies in particular having been performed in Japan, since the Japanese consume the highest amounts of green tea. In recent years, the many health benefits of green tea have been studied.

Green tea catechins are known for their various activities in the body, including antioxidative, anti-cancer, and the lowering of cholesterol and sugar levels in the blood (10, 11). The major effects of green tea catechins include breath odor eliminating effect and prevention of tooth decay, anti-bacterial effect, and anti-oxidant action. The anti-oxidant effect has been reported to contribute to the prevention of diseases associated with free radicals and reactive oxygen species, such as cancer or cardiovascular and neurodegenerative diseases. In addition to the anti-oxidant properties of green tea catechins, their anti-diabetic, anti-bacterial, anti-inflammatory, and anti-obesity activities have also been reported. Among green tea catechins, EGCG is the most abundant, and there has been a lot of research done on its efficacy. Various pharmacological studies have confirmed that EGCG exhibits anti-oxidant, anti-tumor, anti-inflammatory, and neuroprotective effects (12, 13).
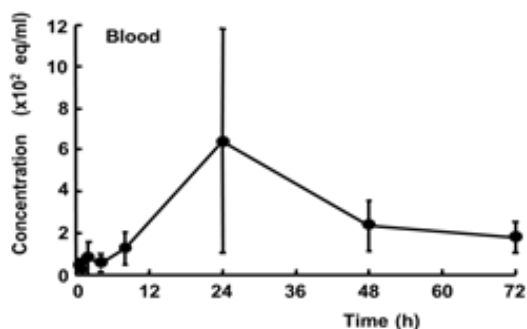

Figure 1-2 Blood level of radioactivity after oral administration of (−)- [4-^{3}H]-EGCG to male wister rat (4 mg, 200íCi/kg, 6weeks, n=4) (15).
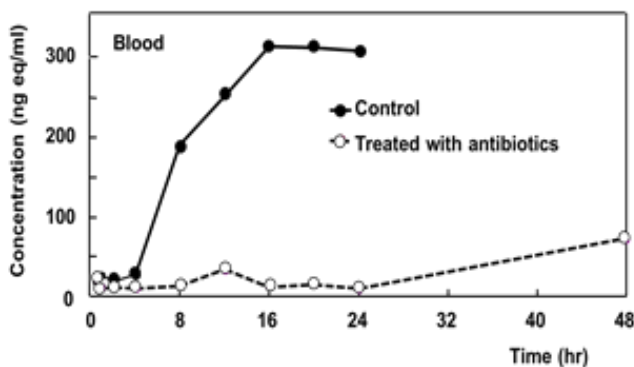
Figure 1-3 Blood of Level radioactivity after oral administration of (−)- [4-^{3}H]-EGCG to rats treated with and without antibiotics (15).

Metabolic Fate of EGCG

Based on the above findings, it is considered important to elucidate the mechanisms responsible for the biological activities of green tea catechins in the body, and thereby a number of studies have been conducted on the kinetics of tea catechins, including their absorption, distribution, and excretion. Li *et al* (14) reported that the human urinary cumulative excretion of major microbial metabolites was as high as 8-25 times the levels of EGC and EC, and accounted for 6-39 % of the amounts of ingested EGC and EC.

My Laboratory has been conducting research on the kinetic study of EGCG after oral administration to rats in order to determine the mechanisms of functions of green tea

catechins in body. These studies demonstrated EGCG dynamics in Wistar rats using (−)-[4-^{3}H]EGCG (15). After oral administration of (−)- [4-^{3}H]EGCG to rats, the radioactivity in the blood, major tissues, urine, and feces was measured. The radioactivity in blood and tissues remained low 4 h post administration, began to increase after 8 hour, peaked at 24 hour, and then, decreased gradually (Figure 1-2). The major urinary excretion of radioactivity occurred after 8-24 hours, and the cumulative radioactivity excreted by 72 hours was 32.1 % of the initial dose. The radioactivity in the feces was 35.2 % of the initial dose within 72 hours post administration. To examine the influence of microbial bacteria on the metabolic fate of EGCG, antibiotic saline solution containing bacitracin, neomycin sulfate, and streptomycin sulfate (200 mg of each antibiotic/kg) were administered to rats by intragastric gavage every 12 hour for 2 days before (−)-[4-^{3}H]EGCG administration to suppress the activity of intestinal bacteria. In the case of rats pretreated with antibiotics (antibiotic-pretreated rats), the blood radioactivity levels were significantly lower than those in rats not pretreated with antibiotics (normal rats) (Figure 1-3). The radioactivity in the antibiotic-pretreated rat urine was estimated to be only 1/100th of that in the normal rat urine. These results showed that the radioactivity detected in the blood and urine of normal rats mostly originated from the degradation products of EGCG metabolized by intestinal bacteria, whereas the amount of intact EGCG absorbed in the body was very low (0.26 % of its dose).

Metabolic fate of (−)- [4-^{3}H]Epigallocatechin gallate in rats was illustrated as indicated in Figure 1-4 (15)**.** A main metabolite in the normal rats was purified and identified as 5-(5′-hydroxyphenyl)-γ-valerolactone 3′-*O*-β-glucuronide (expressed as **BM6**-GluA in Figure 1-4). In feces of the normal rats, EGC (40.8 % of the fecal radioactivity) and 5-(3′,5′-dihydroxyphenyl)-γ-valerolactone (**BM6**, 16.8 %) were detected. These results suggested that **BM6** was absorbed in the body after degradation of EGCG by intestinal bacteria, yielding M1 (Figure 1-4) with EGC as an intermediate. From this study, it was found that the bioavailability of EGCG, which is the most abundant green tea catechin, is very low (0.26 %) although the physiological functions after drinking green tea has been widely reported. While the absorption ration of degrade metabolites of EGCG by intestinal bacteria was found to high. (32.1 %) There have been only few reports of detail examinations concerning of EGCG metabolism in the bod, and of functionality contribution in body brought after green tea intake.

With the elucidation of high bioavailability of ring-fission metabolites produced by intestinal flora, their functions are becoming exceedingly clear. However, studies on the physiological effects of microbial metabolites are still limited.

The Major Urinary Ring Fission Metabolites after Green Tea Drinking

In recent years, γ-valerolactone has been increasingly recognized as the main metabolic compound of flavan-3-ol. Previous reports have described the identification of γ-valerolactone metabolites and their biofunctionality. Unno *et al* (16) reported the urinary excretion of 5-(3′,4′-dihydroxyphenyl)-γ–valerolactone, a ring-fission metabolite of EC synthesized by intestinal microflora, and evaluated its anti-oxidant potential for scavenging radicals in the form of Trolox equivalent anti-oxidant capacity (TEAC). They suggested that 5-(3′,4′-dihydroxyphenyl)-γ-valerolactone, a microbial metabolite of EC, circulating in the body, may exhibit a higher anti-oxidant effect than L-ascorbic acid.

Kohri *et al* (17) identified urinary metabolites after oral administration of ECG to rat. Five major metabolites were excreted in rat urine. These were purified in their deconjugated forms and their chemical structures were determined. The degradation products from ECG included pyrogallol, 5-(3′,4′-dihydroxyphenyl)-γ-valerolactone, 4-hydroxy-5-(3′,4′-dihydroxyphenyl)valeric acid, 3-(3′-hydroxyphenyl)propionic acid, and m-coumaric acid. In addition, they studied metabolic fate of (−)- [4-^{3}H] EGCG in rats, and the main metabolite in the normal rat urine was purified and identified as 5-(5′-hydroxyphenyl)-γ-valerolactone *3′-O-β*-glucuronide (**BM6**-GluA in Figure 1-4). In feces of the normal rats, EGC and **BM6** were detected. These results suggested that **BM6** was absorbed in the body after degradation of EGCG by intestinal bacteria. Furthermore, they speculated that **BM6** underwent glucuronide conjugation in the intestinal mucosa and/or liver, before entering the systemic circulation, and being excreted in the urine.

Li *et al* (14) identified two catechin metabolites in human urine and blood after green tea ingestion to be 5-(3′,4′,5′-trihydroxyphenyl)-γ-valerolactone (**BM10**) and 5-(3′,4′-dihydroxyphenyl)-γ-valerolactone using LC/ESI-MS and NMR analyses. These metabolites peaked 7.5 - 13.5 hours after ingestion of a single dose of green tea, while EGC and EC peaked at 2 hours. In their kinetic study, cumulative urinary excretions of the two metabolites were as high as 8-25 times the level of ingested catechins, which suggested that the microbial metabolites could contribute to cancer prevention and other health effects due to their anti-oxidant activity in the body.

After consumption of green tea beverages, free and conjugated γ-valerolactone has been detected in human urine, plasma, and fecal slurries. Thus, γ-valerolactones were considered as the major ring-fission metabolites produced by intestinal flora in the gut (18-21). In recent years, several reviews have reported flavan-3-ols, phenyl-γ-valerolactones, and phenylvaleric acids as the main colonic metabolites. Among the metabolites of EC, which is a catechol type of catechin, conjugates of 5- (3′, 4′-dihydroxyphenyl) -γ-valerolactone and 5- (3′, 4′-dihydroxyphenyl) 4-hydroxyl-valeric acid are reported as the main colonic metabolites. In these reviews, the importance of focusing investigations on microbial metabolites, such as

8

phenyl-γ-valerolactones, has been proposed because it would help to further elucidate the beneficial properties of dietary flavan-3-ols. It is reasonable to assume that green tea catechins undergo degradation by intestinal bacteria in the gut in addition to being metabolized by phase II enzymes in the body after absorption. However, there is still limited information on the green tea catechin metabolism in the intestine and the contribution of metabolites to beneficial effects in the body.
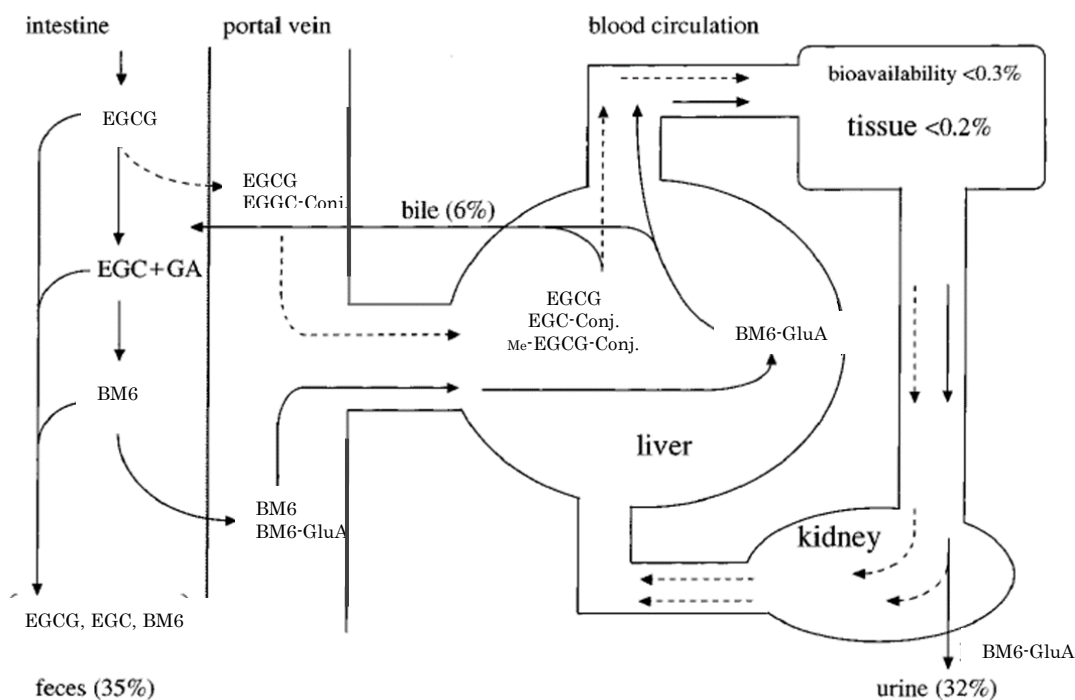
Figure 1-4 Possible metabolic route of EGCG orally administered to rats (15).
GA, gallic acid; BM6, 5-(3',5'-dihydroxyphenyl)-γ-valerolactone; BM6-GluA, 5-(5'-hydroxyphenyl)-γ-valerolactone 3-O-glucuronide; EGCG-Conj, EGCG conjugates; Me-EGCG-Conj,methylated EGCG conjugates; feces (35 %), mean radioactivity excreted in feces by 72 h after a dose of (-)[4-^{3}H]EGCG; urine (32 %),mean radioactivity excreted in urine by 72 h after a dose of (-)-[4-^{3}H]EGCG; bile (6 %), mean radioactivity excreted in bile by 48 hafter an dose of(-)- [4-^{3}H]EGCG.

9

Antidiabetic Effect followed by Green Tea Drinking

Due to changes in daily lifestyle habits, the number of patients with lifestyle diseases (hyperlipidemia, hypertension, diabetes) is increasing. Lifestyle diseases are increasing not only in Japan but also on a global scale. Therefore, it is expected that medical expenses will increase, and each country needs to take urgent measures against lifestyle diseases. In general, exercise and a controlled diet are what are required for the treatment and improvement of metabolic syndrome, but due to the demands of everyday life, it is often difficult to keep up such good lifestyle habits. Recent studies have suggested that abnormal production of adipocytokine resulting from hypertrophy of fat cells due to obesity is a common onset factor for diabetes, hypertension and hyperlipidemia, inducing insulin resistance and renal dysfunction, and it is believed to be a progression factor.

Several epidemiological studies have been conducted on the anti-diabetic effect of green tea drinking on humans (22-25). Iso *et al* (22) reported that green tea intake reduces the risk of onset of type 2 diabetes in an epidemiological study targeted at the Japanese population. Shizuoka prefecture is the largest green tea production area, accounting for about 40% of total green tea production of Japan. This area is known for its low number of obesity and metabolic syndrome cases, and a low cancer mortality rate. Since it is speculated that high levels of green tea consumption benefit the health, the relationship between green tea drinking and lifestyle diseases was investigated in an epidemiologic study in Kakegawa City. An epidemiological survey of the effects of green tea on lifestyle-related diseases has been conducted in several trials. In Shizuoka prefecture of Japan, it has been reported that when green tea extract was ingested by 60 people (age range 32-73 years old, 49 males, 11 female) with high blood glucose level, their blood hemoglobin Alc (HbA1c) value significantly decreased (23).

Blood Glucose Regulation by the Green Tea Catechins in the Body

The mechanisms for regulating blood glucose concentrations of EGCG were studied from several functional aspects, that is, for Inhibition of α-glucosidase and other carbohydrate digestive enzymes (26, 27), stimulation of insulin secretion from pancreatic beta cells (28), inhibition of gluconeogenic enzymes in the liver (29, 30). There are several reports on the gluconeogenesis inhibitory action by EGCG. Addition of EGCG to rat normal hepatocytes and hepatoma cells suppressed the generation of genes for producing enzymes involved in gluconeogenesis, and it was revealed that the amount of enzymes decreased. It has been reported that as EGCG suppresses the expression level of specific transcription factors related to gluconeogenesis, the expression level of gluconeogenic enzyme decreases and the production of glucose decreases (31).

However, considering the low absorptivity of green tea catechins, it is difficult to explain that such blood glucose regulation effects following green tea consumption were attributable only to green tea catechins. There are no reports concerning the microbial metabolites degradation of green tea catechins by intestinal flora, with respect to the effect on antidiabetic effects.

Glucose Uptake in Skeletal Muscle during Regulation of Blood Glucose Level

Skeletal muscle is the largest tissue in the human body and plays an important role in the metabolism of energy sources such as glucose or lipids. The heat consumption by skeletal muscle during basal metabolism is said to be 30 % of that consumed by the whole body (32), making it the most energy consuming organ in the human body. Then, addition to the function as a motor organ, the function as a metabolic organ of skeletal muscle has attracted much attention (33). In diabetic patients, peripheral glucose uptake by insulin decreases making them insulin resistant. Insulin resistance in skeletal muscles not only causes type 2 diabetes and metabolic syndrome, it also causes macrovascular complications, such as myocardial infarction and stroke. It is known that accelerating glucose consumption of skeletal muscle by moderate exercise contributes to elimination of obesity and prevention/improvement of diabetes. Since it is known that patients with type 2 diabetes exhibit a marked reduction in glucose uptake ability in skeletal muscle, research has focused on the skeletal muscle as a target tissue for improvement of type 2 diabetes and obesity (34).

It is known that glucose transporter 4 (GLUT4) is important for incorporating blood glucose into skeletal muscle cells. GLUT4 is normally present in the intracellular pool. When stimulated, it migrates to the cell membrane and becomes a transporter for uptake of glucose into the cell. Recent reports explaining the mechanism of hyperglycemic glycosuria have focused on the insulin-sensitive GLUT4 as a novel target for an antidiabetic agent. GLUT4 is expressed in adipose tissue, skeletal muscle and cardiac muscle. Of these, skeletal muscle is a particularly effective target for hyperglycemia, because skeletal muscle accounts for approximately 80 % of insulin-stimulated glucose uptake in the postprandial state and plays a vital role in maintaining glucose homoeostasis (32).

There are two types of signaling pathways that promote GLUT4 translocation to membrane, insulin-dependent and insulin-independent pathways as illusitated in Figure 1-5. In the insulin dependent type, the endogenous tyrosine kinase is activated and autophosphorylated by insulin binding to the insulin receptor on the cell membrane. Insulin receptor substrate 1 (IRS1) binds to phosphorylated tyrosine and is phosphorylated. The phosphorylated IRS1 binds to and activates phosphatidylinositol (PI)-3-kinase (PI-3-kinase), and the activated PI-3-kinase further attracts protein kinase B (PKB) to the cell membrane to activate it. Activated PKB promotes glycogen synthesis in the liver by transferring GLUT4 to the cell

membrane and incorporating glucose into the cell, simultaneously inactivating glycogen synthase kinase 3 and activating glycogen synthase. AMPK is known for its insulin-independent action; AMPK is activated by several stimuli, such as exercise, and causes migration of GLUT 4 to the membrane (35).

It has been already reported that EGCG can facilitate the GLUT4 translocation both in skeletal muscle of mice and rats *ex vivo*, and in insulin-resistant L6 myotubes (36). Further EGCG has the potential to significantly increase glucose uptake accompanying GLUT4 translocation in L6 myotubes at a concentration as low as 1 nM (36). Further, treatment with EGCG could improve glucose uptake by increasing GLUT4 translocation in dexamethasone-induced insulin resistant L6 muscle cells through activation of both AMPK and PI3K/Akt pathways (37).

Thus, research on the glucose uptake ability of EGCG has already been conducted, but there are no reports on an antidiabetic effect of microbial metabolites degraded from green tea catechins yet.
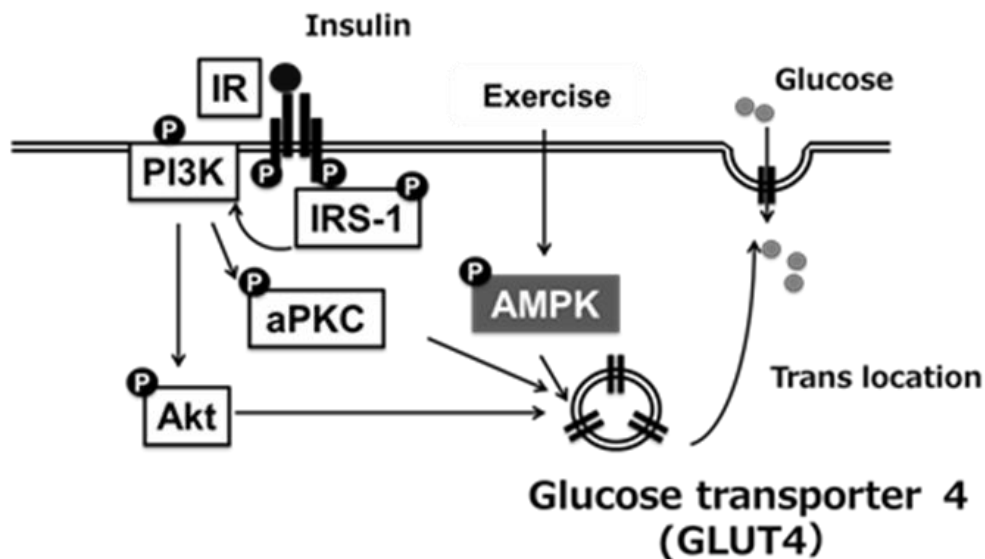
GLUT4: Glucose transpoter type 4, IR: Insulin receptor,
IRS: Insulin receptor substrate 1, PI3K: Phosphatidylinositol-3-Kinase,
aPKC: atypical Protein kinase C, AMPK: 5'-AMP-activated protein kinase

Figure 1-5 Mechanism of glucose uptake in skeletal muscle cell.
Contraction triggers GLUT4 translocation in skeletal muscle through the activation of AMP-activated protein kinase (23).

Aim of This Study

It is well known green tea catechins favorably exhibit beneficial effects in body, however EGCG is reported to be slightly absorbed in the body (0.26 % of dose). On the other hand, metabolites derived from EGCG by intestinal bacteria were found to be detected abundantly in urine (32.1 % of dose). However there are no reports concerning the microbial metabolites degradation from green tea catechins by intestinal flora, with respect to the effect on antidiabetic effects. In addition, there are only a few reports on EGCG metabolism in gut tract, isolation and identification of enteric bacteria involved in EGCG metabolism, and physiological functions of these microbial metabolites in the body. Therefore, the author started investigating the metabolism of green tea catechin, mainly focusing on EGCG in the rat. In this study, the author examined with the aim of clarifying the metabolism of EGCG in rat enterobacteria, isolation and identification of EGCG-metabolizing bacterium, and further investigated to determine whether the metabolite contributes to functions in the body after intake of EGCG.

In **Chapter 2**, to elucidate the EGCG metabolism by rat enterobacteria, repeated incubation of EGC with rat intestinal flora under anaerobic condition was examined. Several kinds of EGCG metabolites were identified by LC-MS and NMR analyses, and these suggested a metabolic pathway of EGCG in rat intestine.

In **Chapter 3**, anaerobic bacteria associated with degradation of EGCG were isolated and identified from rat fecal and cecum samples. In addition, EGC metabolism by several isoflavone-converting bacteria commercially obtained were tested. The results in this Chapter 3 suggested that EGC-metabolizing bacteria are common in isoflavone-metabolizing bacteria. In addition, it was found that EGC metabolizum by ring fission bacteria are susceptible by symbiotic bacteria.

In **Chapter 4**, the author conducted *in vivo* experiments of EGCG metabolism in order to determine the main metabolite derived from EGCG *in vivo*. Examinations were conducted on 5-(3′,5′-dihydroxyphenyl)-4-hydroxyvaleric acid (**BM5**) produced in gut tract would be underwent conversion to form lactonized 5- (3′, 5′-dihydroxyphenyl) -γ-valerolactone (**BM6**) during blood circulation process to exertion in urine, or absorption process of passage through the large intestine digestive tract.

In **Chapter 5**, the potential of EGCG microbial metabolites to contribute to the beneficial effects following green tea consumption was investigated. In this study, evaluation of metabolites has focused on antidiabetic ability. The author examined the ability of EGCG metabolites to increase glucose uptake ability into L6 skeletal muscle cells. Furthermore, the main metabolite **BM6** was observed in GLUT4 translocations and glucose tolerance tests in mice to investigate its anti-hyperglycemic effect *in vivo*.

As an appendix (**Chapter 6**), the effect of 5- (3′,4′, 5′-trihydroxyphenyl) -γ-valerolactone (**BM10**), which is an EGCG urinary metabolites detected in human urine, was examined according to improvement of glucose tolerance was examined in Chapter 6.

In **Chapter 7**, comprehensive discussion throughout the research in this doctoral thesis was descrived.

Chapter 2

Metabolism of EGCG by Rat Enterobacteria

INTRODUCTION

As described in Chapter 1, green tea catechins are known for their various activities in the body (38-41). The metabolism of the major catechin of EGCG has been the focused to determine the mechanisms behind these physiological activities. Many of such studies have addressed the metabolism of EGCG in mammalia such as rat, mouse and human. After oral administration of EGCG to rat and human, metabolites detected in plasma were examined (43-46). There have also been reports on the excretion and distribution of EGCG (15, 47, 48) as well as pharmacokinetics studies (15, 48). The EGCG metabolites excreted in bile and urine were further identified (14, 47, 50, 51). Furthermore, excreted EGCG metabolites such as 5-(3′,4′-dihydroxyphenyl)-γ-valerolactone, **BM10** and **BM6** found in human (14, 50) and rat urine (15) were identified. These are regarded to be the ring-fission metabolites of EGCG and/or EGC formed in the intestinal microbiota. Results of such studies have pointed to the metabolic pathways of EGCG in the gut tract (15), while Hattori *et al* (52, 53) has proposed the first stage of EGCG metabolism by identifying EGCG metabolites produced in the human intestinal bacteria. However there is still much to be done to elucidate the full metabolic pathway, and therefore this author has conducted this *in vitro* study to discover more about the role of rat intestinal bacteria in the metabolic pathways of EGCG.

MATERIALS AND METHODS

Chemicals

EGCG and EGC were purchased from Sigma-Aldrich Japan (Tokyo). Methanol-*d*4 and tetramethylsilane (TMS) were obtained from Kanto Chemical Co. Ltd. (Tokyo, Japan). All other chemicals were commercially available products of analytical grade or HPLC grade in this study.

Cultures

General anaerobic medium (GAM) was obtained from Nissui Pharmaceutical (Tokyo, Japan). All cultures in this doctoral study were conducted under anaerobic condition at 37 ⁰C

with an Anaero Pack (anaerobic cultivation) system (Mitsubishi Gas Chemical Company, Inc., Tokyo, Japan) unless otherwise stated.

Animal Treatment

Male Wistar rats, from Charles Liver Laboratories Inc. (Yokohama, Japan) were housed in a room temperature facility at $23 \pm 3^{\circ}C$ and 50 ± 5 % relative humidity, with a 12 hour light-dark cycle, and given normal pelleted food (Oriental Yeast Ltd., Tokyo, Japan) during the experimental period. All experimental procedures in animal studies in Chapter 1, 2 and 3 were in accordance with the guidelines for animal experiments of R&D group of Mitsui Norin Co., Ltd. In Chapter 2, the 15-21 weeks of age rats were used.

Screening of Enteric Bacteria with EGCG Hydrolyzing Capability

EGCG solution (1 mL, 10 mg/mL) was sterilized by filteration with DISMIC-25cs, 0.2 μm (Toyo Roshi Kaisha Ltd., Tokyo, Japan). Added the EGCG solution to 9mL of pre sterilized 0.1 M phosphate buffer (pH 7.1). Each bacterial strain (22 genera, 169 strains) was inoculated into this solution and then 2 mL of sterile mineral oil was layered over. After incubation at $37^{\circ}C$ for 24 hours the mixture was centrifuged at $3500 \times g$ for 10 min at room temperature. In order to select the enterobacteria capable of hydrolyzing EGCG the supernatant was analyzed by HPLC. Analytical HPLC was conducted with a $250 \times 4.6mm$ i.d., 5 μm, Capcell Pak C18 UG120 (Shiseido Co.Ltd.,Tokyo, Japan) in an Waters 2695 Separations Module (Nihon Waters, Tokyo, Japan) apparatus equipped with a Waters 2489 UV/VS Detector (270 nm). Elution was carried out with distilled water/methanol/acetonitrile/phosphoric acid (85/10/5/0.01, v/v/v/v) at a flow rate of 1 mL/min at 40 $^{\circ}C$.

Analysis of Metabolite Formation from EGC by Rat Enterobacteria

Incubation of EGC with rat intestinal bacteria was done according to the method of Meselhy R.M *et al* (54). Fresh cecal contents (3.3 g) obtained from three male Wistar rats (16 weeks of age) were incubated in 300 mL of GAM broth at $37^{\circ}C$ under anaerobic condition with an Anaeropack system (Mitsubishi Gas Chemical). The culture was centrifuged after 3 days by Avanti TM J-25 (Beckman Coulter, Tokyo, Japan) at $15000 \times g$ for 20 min at $4^{\circ}C$. Harvested cells were washed once with sterile water (200 mL) and then suspended in 150 mL of pre-filtered 0.1 M phosphate buffer (pH 7.2). Then 200 mg of EGC in 20 mL of 5 % aqueous methanol pre-filtrated with the sterilized membrane filter was added to the cell suspension. Incubation of the mixture was done under anaerobic condition with the Anaeropack system. Aliquots (1 mL) of the incubation mixture were taken out in an anaerobic glove box under CO_2 atmosphere at 24, 48, 72, 96 and 168 hours after incubation, and the samples were centrifuged by MX-301 centrifuge (TOMY Seiko, Tokyo, Japan) at $15000 \times g$ for 10 min at $4^{\circ}C$. The resulting supernatants were filtered using the membrane filter and

analyzed by Surveyor HPLC and LCQ Deca XPplus system (Thermo Fisher Scientific, USA). The above experiment was repeated more than 15 times with the cecal samples from different rats (15-21 weeks).

Purification of EGCG Metabolites

Formation of EGC metabolites by rat intestinal flora was done according to the incubation procedure as described above. After incubation for 24, 48 and 96 hours, 50 mL samples were taken from the incubation mixture using the anaerobic glove box. Each sample was centrifuged at $15000 \times g$ for 20 min at 4^oC in order to remove bacterial cells. The resulting supernatant was adjusted to about pH 3.5 with 5 M HCl and then it was extracted three times with an equal volume of ethyl acetate. The resulting ethyl acetate fraction was evaporated to dryness under reduced pressure. The residue obtained from the 24 hour incubation mixture was used for the isolation of 1-(3′,4′,5′-trihydroxyphenyl)-3-(2",4",6"-trihydroxyphenyl)propan-2-*ol* (**BM3**) and 4-dehydroxylated epigallocatechin (**BM8**), and the residue from the 48 hour mixture was used for 1-(3′,5′-dihydroxyphenyl)-3-(2",4",6"-trihydroxyphenyl)propan-2-*ol* (**BM4**). Similarly, the isolation of **BM5** to 3-(3′,5′-dihydroxyphenyl) propionic acid (**BM7**) was performed with the 96-hour incubation mixture. Each residue obtained from the 24- and 48-hour incubation mixtures was dissolved in 3 mL of 5 % aqueous methanol and the solution underwent preparative HPLC for purification of **BM3**, **BM4** and **BM8**. Preparative HPLC was conducted with a 150 mm × 20 mm i.d., 5 μm, Capcellpak C18 MG column (Shiseido Co.Ltd., Tokyo, Japan) in a JASCO HPLC 800 series system (JASCO, Tokyo, Japan). The column was eluted with a linear solvent gradient, starting with 10 % (v/v) methanol aqueous solution containing 1 % (v/v) acetic acid and finishing with 60 % (v/v) aqueous methanol containing 0.5 % (v/v) acetic acid, at a flow rate of 9.7 mL/min at 40 ^oC. The absorbance at 270 nm was measured to monitor the elution pattern. Each fraction which contained metabolites was collected and evaporated to dryness, and this residue was dissolved in 5 mL of distilled water then concentrated to dryness. This procedure was repeated again twice to completely remove acetic acid. The resultant residues were each dissolved separately in a small amount of distilled water and freeze-dried to obtain **BM3** (17 mg), **BM4** (15 mg) and **BM 8** (5 mg). To isolate **BM5** to **BM7,** the ethyl acetate fraction obtained from the 96 hours incubation mixture was extracted with one-fifth the volume of 20 mM aqueous Na_2CO_3 solution. According to this process, **BM6** remained in the organic layer, and **BM5** and **BM7** were distributed in the aqueous layer. Metabolite **BM6** in the ethyl acetate fraction was purified in the same way as **BM3** to yield 5 mg of purified **BM6**. The aqueous solution containing **BM5** and **BM7** was evaporated down to approximately 5 mL and the concentrate was adjusted to around pH 5.0 with 5 M acetic acid. The precipitate (probably sodium acetate) was removed by

centrifugation, and the supernatant was subjected to preparative HPLC performed under the same conditions as described above except mobile phases without acetic acid were used. Metabolite **BM7** fraction was evaporated under reduced pressure and then freeze-dried to yield purified **BM7** (3 mg). Metabolite **BM5** fraction was concentrated to remove the organic solvents, and the resulting concentrate was applied to an ion exchange column 10×65 mm, 5.1 mL of Diaion SK1B Na^+ form (Mitsubishi Chemical, Tokyo, Japan) equilibrated with distilled water. The column was eluted with 5 volume of distilled water. The eluate was concentrated to approximately 3 mL and then lyophilized to yield 21 mg of **BM5** as sodium salt.

With the use of different intestinal flora, 5-(3′,4′,5′-trihydroxyphenyl)-4-hydroxyvaleric acid (**BM9**) to 5-(3′-hydroxyphenyl)valeric acid (**BM12**) were formed from EGC in addition to **BM3**, **BM5** and **BM6** (Figure 2-2A). Then, to isolate **BM9** and **BM10** the 24-hours incubation mixture was adjusted to pH 1.5 with 5 M phosphoric acid and the metabolites were extracted 3 times with the same volume of a mixture of ethyl acetate / n-butanol (1/1, v/v). The organic layer was then treated twice with half volume of 100 mM aqueous Na_2CO_3 containing 0.1 % sodium ascorbate. In this procedure, **BM9** passed into the aqueous layer, while **BM10** remained in the organic layer. The aqueous layer was adjusted to around pH 7.0 with 5 M HCl and then concentrated to about 15 mL. Ethanol (75 mL) was added to the concentrate, which was then centrifuged to remove insoluble material. The supernatant was concentrated to 1mL, then the resulting concentrate was adjusted to pH 2-3 with 2 M HCl and subjected to preparative HPLC. The same HPLC conditions were used as for **BM5** mentioned above. Metabolite **BM9** fraction was collected and concentrated to remove the organic solvent. The resultant solution was treated with the Diaion SK1B Na^+ form column in the same way as for **BM5**. The eluate was concentrated and lyophilized to yield 5 mg of purified **BM9**. The ethyl acetate-n-butanol layer containing **BM10** was concentrated to dryness. The resultant residue was treated in the same way as was **BM3** to yield 3 mg of purified **BM10**. 5-(3′,5′-Dihydroxyphenyl)valeric acid (**BM11**) and **BM12** were purified respectively from 72 hours and 168 hours incubation mixtures, using the same procedure as for **BM3**, to finally yield 10 mg of **BM11** and 19 mg of **BM12**. Metabolite 5-(3′,4′,5′-trihydroxyphenyl)valeric acid (**BM13**) was also transformed from EGC by different rat intestinal flora (Figure 2-2B). This compound was also purified from 24 hoyrs incubation mixture using the same method as for **BM11** to obtain 8 mg of purified **BM13**.

Analysis of Fecal Metabolites after Oral Administration of EGCG

Fecal metabolites after oral administration of EGCG were analyzed. Male Wistar rats (15 weeks of age, n=4) were orally administered EGCG (25 mg in 1 mL of saline). The rats were then put in stainless steel metabolic cages. Fecal samples were collected at time intervals of

18

0-8, 8-24, 24-32, 32-48 hours respectively after dosing. After freezing at -30°C, the samples were lyophilized. The resulting fecal powder (1 g) was added to 0.8 mL of 10 % aqueous methanol and 0.2 mL of 1 M sodium acetate buffer (pH 3.5) containing 1 % ascorbic acid and 0.15 mM EDTA. This mixture was well homogenized with a vortex mixer (Scientific Industries, NY, USA) and ultrasonic bath for 1 hour. After the mixture was centrifuged at $25000 \times g$ for 20 minutes at 10 °C, the resulting supernatant was analyzed by LC-MS.

Inter-Conversion between BM5 and BM6

Interconversion between **BM5** and **BM6** was examined in the pH range of 1-10. Buffers used were 0.2 M potassium-hydroxy chroride buffer (pH 1.0 and 2.0), 0.2 M citrate-phosphate buffer (pH 3.0-8.0), 0.2 M borate-sodium hydroxide buffer (pH 9.0-10.0). Each buffer (0.9 mL) was placed in an individual tube, and 0.1 mL each of 1 M **BM5** or **BM6** aqueous solution was added. The mixture was incubated under CO_2 gas at 37°C, and after 24 hours, the incubation mixture was analyzed with HPLC.

Analysis of Metabolites Formed from EGC in Rat Cecum

Male Wistar rats (21 weeks of age, $n = 6$) underwent a laparotomy after intraperitoneal injection of 25 mg thiopental sodium (Ravonal; Mitsuibishi Takeda Pharma Co., Ltd.).The segment of junction between the cecum and large intestine was ligated. Then, EGC solution (3 mg/ 0.5 mL of saline) was directly injected into the cecum and the rats were kept under the anesthesia gas. After 5 hours, cecal contents were harvested. To the cecal contents (1 g) was added 0.8 mL of 10 % aqueous methanol and 0.2 mL of 1 M sodium acetate buffer (pH 3.5) containing 1 % ascorbic acid and 0.15 mM EDTA. After sonication for 30 minutes at 40°C, the mixture was centrifuged at $25000 \times g$ for 20 min at 10 °C. The supernatant was analyzed by the LC-MS system as described above.

LC-MS Analysis Method

LC-MS analysis of EGC metabolites by rat intestinal flora *in vitro* was performed using a Finnigan Spectra System which consisted of a Surveyor HPLC system and an LCQ Deca XPplus system (Thermo Fisher Scientific, USA). HPLC was conducted with a 100×2.0 mm i.d., 5μm, Capcell pack MG column at a flow rate of 0.2 mL/min at 40°C. The column was eluted with a flow rate of 0.2 mL/min at 40°C using 100 % buffer A (distilled water/acetonitrile/acetic acid; 100/2.5/0.2, v/v/v) for 2 min, and then linear increases in buffer B (distilled water/acetonitrile/methanol/acetic acid; 33/2.5/66/0.2, v/v/v) from 0 to 80 % for 2 to 25 min. Then the mobile phase was re-equilibrated with 100 % buffer A for 5 min. The column elute was monitored with the diode array detector and after that was directed to the LCQ Deca XPplus ion trap mass spectrometer incorporated with ESI interface. The negative

ion polarity mode was set for the ESI source. Initially analysis was carried out using full scan, data-dependent MS/MS scanning from m/z 100 to 1000. LC-MS analysis for quantification of metabolites in cecum and feces was done using a 150×2.0mm i.d., 4μm, Synergi MAX RP-18 column (Phenomenex, Macclesfield, U.K.) (55). Column was eluted using buffer A (distilled water/acetonitrile/acetic acid; 98/2/0.3, v/v/v) and buffer B (distilled water/acetonitrile/acetic acid; 60/40/0.3, v/v/v) at a flow rate of 0.2 mL/min at 40 °C. The column was eluted first with 100% buffer A for 2 min, followed by linear increases in buffer B to 100 % from 2 to 20 min, and with 100 % buffer B up to 24 min. The column was lastly equilibrated with buffer A for 6 min. Quantification of the metabolites in cecum and feces was done using the selected ion monitoring (SIM) mode. The separated [M-H]$^-$ ion chromatograms were selected at *m/z* 305, 307, 291, 225 and 207 for the specific parent ions of **BM1**, **BM3**, **BM4**, **BM5** and **BM6**, respectively. Metabolites in cecum and feces were identified based on the standard calibration curves obtained with the metabolites purified in this study.

NMR and Optical Rotation Analyses

NMR analysis was conducted using a Bruker Ultrashield 400 plus system. (^{1}H, 400 MHz; ^{13}C, 100 MHz : Bruker BioSpin, Ibaragi, Japan). All samples were dissolved in methanol-d_4 (Kanto Chemical, Tokyo, Japan). Chemical shifts were referenced with tetramethylsilane (TMS) as an internal standard. Specific rotation $[\alpha]_D^{20}$ of two metabolites (**BM5** and **BM6**) was measured by a P-1020 polarimeter (JASCO, Tokyo, Japan). Metabolite **BM5** was dissolved in distilled water (c 0.225) and **BM6** in methanol (c 0.355).

RESULTS

Screening of Enteric Bacteria Capable of Hydrolyzing EGCG

The metabolism of galloylated catechins such as ECG and EGCG by intestinal bacteria has been thought to be initiated by the release of gallic acid from the catechins (15, 17, 54). Related to this, Hackett and Griffiths (56, 57) have also reported that unlike (+)-catechin, 3-*O*-methyl-(+)-catechin did not undergo ring fission by intestinal flora. Thus for the metabolism of catechins by intestinal flora, the free hydroxy group at the 3 position has been found to be important. Accordingly, this author first screened enteric bacteria with the capability of hydrolyzing EGCG. Among 169 stains of commercially available bacteria, four bacterial strains, *Enterobacter aerogenes*, *Raoultella planticola* (*Klebsiella planticola*), *K.peneumoniae* susp.p*neumoniae*, and *Bifidobacterium longum* subsp. *infantis* (*B. infantis*) were found to have EGCG hydrolyzing capabilities. Since these bacteria are known to exist commonly in the intestinal tract, it is considered EGCG could be easily hydrolyzed to yield EGC and gallic acid in the gut.

Time-course Analysis of Metabolites by Rat Enterobactera.

After hydrolyzing EGCG to EGC (**BM1**) and gallic acid, subsequent metabolic processes are degradation of EGC by intestinal bacteria. In this study, **BM1** was incubated with intestinal bacteria from rat fecal contents in 0.1 M sodium phosphate buffer (pH 7.2) and transformation of **BM1** over time was examined by LC-MS analysis. The author performed the *in vitro* experiments more than 15 times, and finally found that degradation of **BM1** by rat intestinal flora occurred through at least three different metabolic pathways. These three metabolic routes are referred to as Route I, Route II, and Route III.

Figure 2-1 shows time-course analysis of EGC metabolites produced by rat intestinal flora through the pathway of Route I. In this route, **BM1** (EGC) was first converted to **BM3** within 24 hours incubation, along with a small amount of **BM8**. Conversion into the second metabolite (**BM4**) peaked at 48 h incubation accompanied by a decrease in **BM3**. Subsequently, after incubation for 48 h **BM5** began to increase gradually accompanied by a decrease in **BM4**. **BM5** production reached a plateau after about 96 h incubation and it remained as the main product throughout the incubation periods (168 hours). Two other small peaks (**BM6** and **BM7**) were also detected during the same incubation period in which **BM5** was produced.

In Route II (Figure 2-2A), the first metabolic step of EGC was conversion into **BM3,** as it was in Route I. However, **BM3** was converted to **BM9** at the second step in route II, and then **BM9** to **BM5**. Metabolite **BM5** was further converted to **BM11** and finally **BM12** was produced from **BM11**. Thus, **BM5** was produced from **BM3** through **BM9** by route II, while

in the case of Route I, it was converted from **BM3** via **BM4**. Metabolite **BM5** was produced in Route I, but was converted to **BM12** via **BM11** and hence **BM12** is regarded as the major product in Route II. **BM6** and **BM 10** were also found to be formed.

In route III (Figure 2-2B), as in Routes I and II, EGC was first converted to **BM3**. During incubation for 24 to 48 hour, **BM3** was observed to be converted to **BM9**; and thereafter **BM9** was converted to **BM13** then successively **BM 13** was converted to **BM11**. Metabolite **BM10** was also produced after 48 hours incubation. Metabolite **BM11** showed hardly any conversion to other metabolites even after extension of incubation time to 168 hours, and therefore this compound was regarded as the major product in Route III. This metabolic route is very similar to Route II.

This author has revealed three routes of the EGC metabolic pathway by rat intestinal flora in the *in vitro* experiments. Among the three routes, Route I was shown to be the more dominant pathway compared to Routes II and III because the conversion of EGC into the compounds shown in Route I occurred with high frequency (probability with more than 90 %) in the repeated experiments *in vitro*.
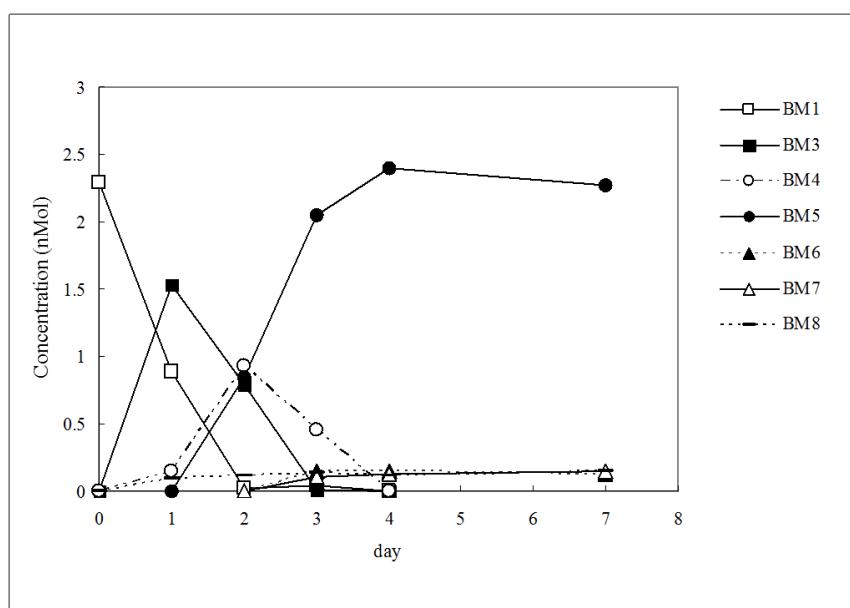

Figure 2-1

Time profile of EGC metabolism by rat intestinal flora via the o Route I.

Quantitative analysis way performed with LC-MS instrument.

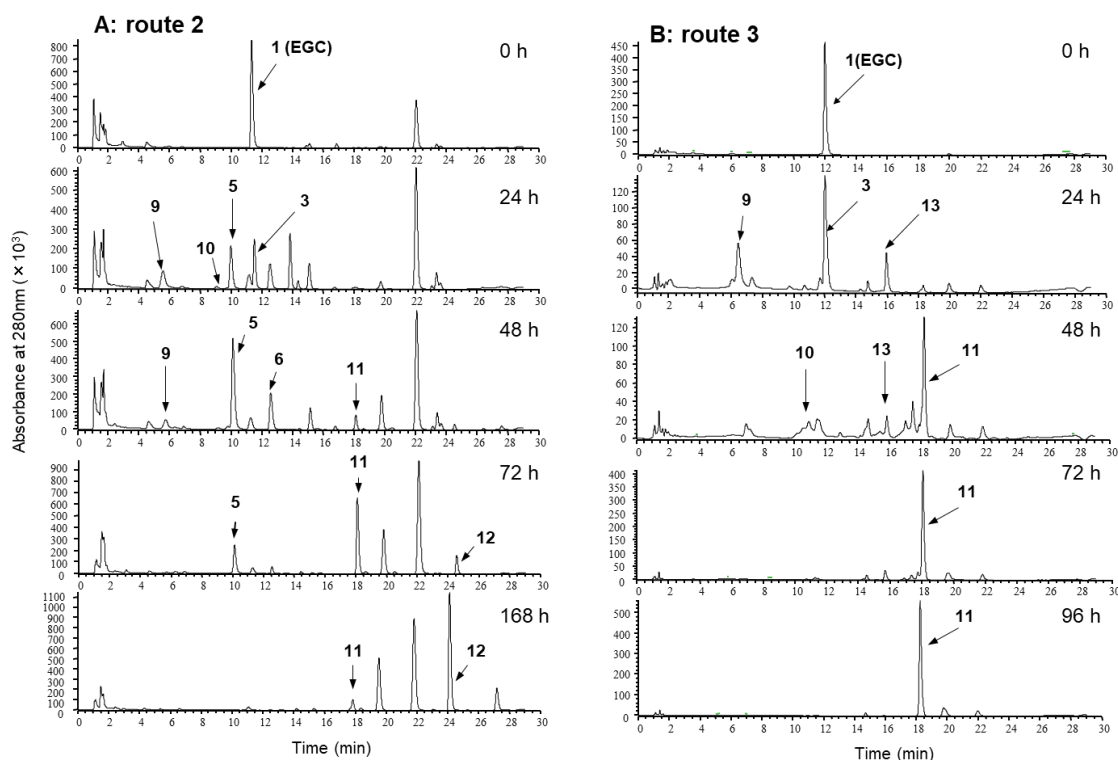EGC (BM1 : □), BM3(■), BM4(○), BM5(●),BM6(▲), BM7(△), BM8(─)

Figure 2-2　HPLC chromatograph profile of Route II and Route III metabolic pathway.
(A): Route II. (B): Route III. The numbers on the chromatogram indicates BM number.
UV detection by HPLC was performed at a wavelength of 270 nm.

Structural Analysis of Metabolites Produced in Routes I, II, and III.

EGC metabolites found in each of the metabolic routes described as above, were then purified by preparative HPLC and their structures were determined by LC-MS and NMR analyses. Thus, six metabolites (**BM3 – BM8**) in Route I, four metabolites (**BM9 - BM12**) in Route II, and **BM13** in Route III were purified and identified. In the case of **BM5** and **BM9**, extraction and purification processes were somewhat complicated.

BM3 showed a pseudomolecular ion peak at m/z 307 [M-H]⁻ in its electoronspray ionization (ESI)-MS analysis, 2 mass units larger than that of EGC. ¹H- and ¹³C-NMR spectra of **BM3** were very similar to those of 1-(3′,4′-dihydroxyphenyl)-3-(2″,4″,6″-trihydroxyphenyl)propan-2-*ol* (54) and 1-(3′,5′-dihydroxyphenyl)-3-(2″,4″,6″-trihydroxyphenyl)propan-2-*ol* (52) except for their aromatic signal patterns. Two aromatic rings in **BM3** were found to have substitution patterns resembling those of EGC. Together with ¹H-¹H shift correlation spectroscopy (COSY), heteronuclear multiple quantum coherence (HMQC) and heteronuclear multiple bond correlation (HMBC) experiments, **BM3** was identified as 1-(3′,4′,5′-trihydroxyphenyl)-3-(2″,4″,6″-trihydroxyphenyl)propan-2-*ol*.

23

Metabolite **BM4** showed an [M-H]$^-$ ion peak at *m/z* 291 in negative ESI-MS analysis, which was 16 mass units less than that of **BM3**. The ^{1}H- and ^{13}C-NMR data of **BM4** could be superimposed with those of 1-(3′,5′-dihydroxyphenyl)-3-(2″,4″,6″-trihydroxyphenyl)propan-2-*ol* reported by Wang *et al.* (52). Consequently, **BM4** was determined to be 1-(3′,5′-dihydroxyphenyl)-3-(2″,4″,6″-trihydroxyphenyl)propan-2-*ol*.

The ^{1}H- and ^{13}C-NMR data of **BM5** closely resembled that of 5-(3′,4′-dihydroxyphenyl)-4-hydroxyvaleric acid reported in our previous paper (39) except for the aromatic signal patterns. The aromatic pattern of **BM5** was very similar to that of the 3', 5'-dihydroxyphenyl moiety in **BM4**. Also the appearance of [M-H]$^-$ ion peak at *m/z* 225 in the negative ESI-MS data of **BM5** was consistent with data of 5-(3′,4′-dihydroxyphenyl)-4-hydroxyvaleric acid. From these data together with COSY, HMQC and HMBC experiments, the chemical structure of **BM5** is determined to be 5-(3′,5′-dihydroxyphenyl)-4-hydroxyvaleric acid. The optical rotation value, [α]$_D^{20}$ (c 0.225, H$_2$O) is -18.1^o.

The MS, ^{1}H-NMR, and ^{13}C-NMR data of **BM6** agreed with previously reported data of 5-(3′,5′-dihydroxyphenyl)-γ-valerolactone (15). Accordingly, **BM6** is found to be 5-(3′,5′-dihydroxyphenyl)-γ-valerolactone. The optical rotation value, [α]$_D^{20}$ -8.9 ^{o} (c 0.355, CH$_3$OH), of **BM6** was very similar to that ([α]$_D^{20}$ -12.9 ^{o} (c 0.4, CH$_3$OH)) of the same compound identified previously (25). Thus it is reasonable to conclude that **BM6** has 4*R* configuration.

Metabolite **BM7** showed a pseudomolecular ion peak at *m/z* 181 [M-H]$^-$ in negative ESI-MS analysis. Molecular mass of this compound was 16 mass units bigger than that of 3-(3′-hydroxyphenyl) propionic acid (39). Aromatic signal patterns of **BM7** in ^{1}H-NMR and chemical shifts of the aromatic ring in ^{13}C-NMR were analogous to those of **BM6**. From these observations together with results of HMQC and HMBC experiments, **BM7** is determined to be 3-(3′,5-dihydroxyphenyl) propionic acid.

Negative ESI-MS data of **BM8** exhibited an [M-H]$^-$ ion peak at *m/z* 289, 16 mass units less than that of EGC, suggesting that relative to RGC the compound lacked one hydroxyl group. The ^{1}H- and ^{13}C-NMR data were very similar to those of EGC, except for chemical shifts in the B ring. The chemical shifts of **BM8** were comparable to those in the 3′,5′-dihydroxyphenyl moiety of **BM4**. With further experiments with HMQC and HMBC, **BM 8** is identified as 4'-dehydroxy EGC.

A pseudomolecular ion peak at *m/z* 241 [M-H]$^-$ in negative ESI-MS was seen in **BM9**. The ^{1}H- and ^{13}C-NMR data showed good resemblance to those of **BM5**, except for its aromatic signal patterns. The aromatic chemical shifts of **BM9** were quite similar to those in the 3′,4′,5′-trihydroxyphenyl group of **BM3**. Therefore, it is concluded that metabolite **BM9** is

24

5-(3′,4′,5′-trihydroxyphenyl)-4-hydroxy-valeric acid. This discovery was further substantiated by COSY, HMQC, and HMBC experiments.

Negative ESI-MS data of **BM10** showed an [M-H]⁻ ion peak at *m/z* 223, 18 mass units less than that of **BM9**, suggesting the compound was dehydrated from **BM9**. The ¹H- and ¹³C-NMR spectra implied that **BM10** has γ-valerolactone structure as well as **BM6**. The signal patterns and chemical shifts of the aromatic ring in **BM10** were found to be almost identical with those in **BM9**. Combined with COSY, HMQC, and HMBC experiments, **BM10** was determined to be 5-(3′,4′,5′-trihydroxyphenyl)-γ-valerolactone.

In the case of **BM11**, a pseudomolecular ion peak at *m/z* 209 [M-H]⁻ was observed, 16 mass units less than that of **BM5**, suggesting the compound lacked one hydroxyl group relative to **BM5**. The ¹H- and ¹³C-NMR data of **BM11** were compatible with those of 5-(3′-hydroxyphenyl)valeric acid previously reported by Meselhy *et al* (54) apart for the aromatic signal patterns of **BM11**. The aromatic patterns of **BM11** were observed to be very similar to those of **BM7**. These observations suggested that this compound is 5-(3′,5′-dihydroxyphenyl)valeric acid. This suggestion was confirmed with more experiments with COSY, HMQC, and HMBC.

The ¹H- and ¹³C-NMR data of **BM12** and **BM13** were analogous to those of **BM11**, except that the signal patterns and chemical shifts of aromatic rings in three compounds were different from each other. The whole signal patterns and chemical shifts in **BM12** were superimposable on those of 5-(3′-hydroxyphenyl)valeric acid reported by Meselhy *et al* (54). The ESI-MS data of **BM12** showed a pseudomolecular ion peak at *m/z* 193 [M-H]⁻, which was 16 mass units less than that of **BM11**. These observations clearly showed that **BM12** is 5-(3′-hydroxyphenyl)valeric acid. In **BM13**, the ESI-MS data exhibited a pseudomolecular ion peak at *m/z* 225 [M-H]⁻, 16 mass units larger than that of **BM11**. The ¹H-NMR and ¹³C-NMR spectra of the aromatic signal patterns of **BM13** were very analogous to those of **BM3** and **BM9**. Therefore, metabolite **BM13** was identified to be 5-(3′,4′,5′-trihydroxyphenyl)valeric acid. This result was further supported with results of COSY, HMQC, and HMBC experiments.

The ¹H-NMR and ¹³C-NMR spectroscopic data for the purified metabolites are summarized in Tables 2-1 and Table 2-2, respectively. On the basis of the time-course analysis of the metabolites derived from EGCG and their structural identification, the author proposed three metabolic pathways of EGCG by rat intestinal bacteria (Route I to III) as illustrated in Figure 2-3 with each of metabolite's cemical structure.

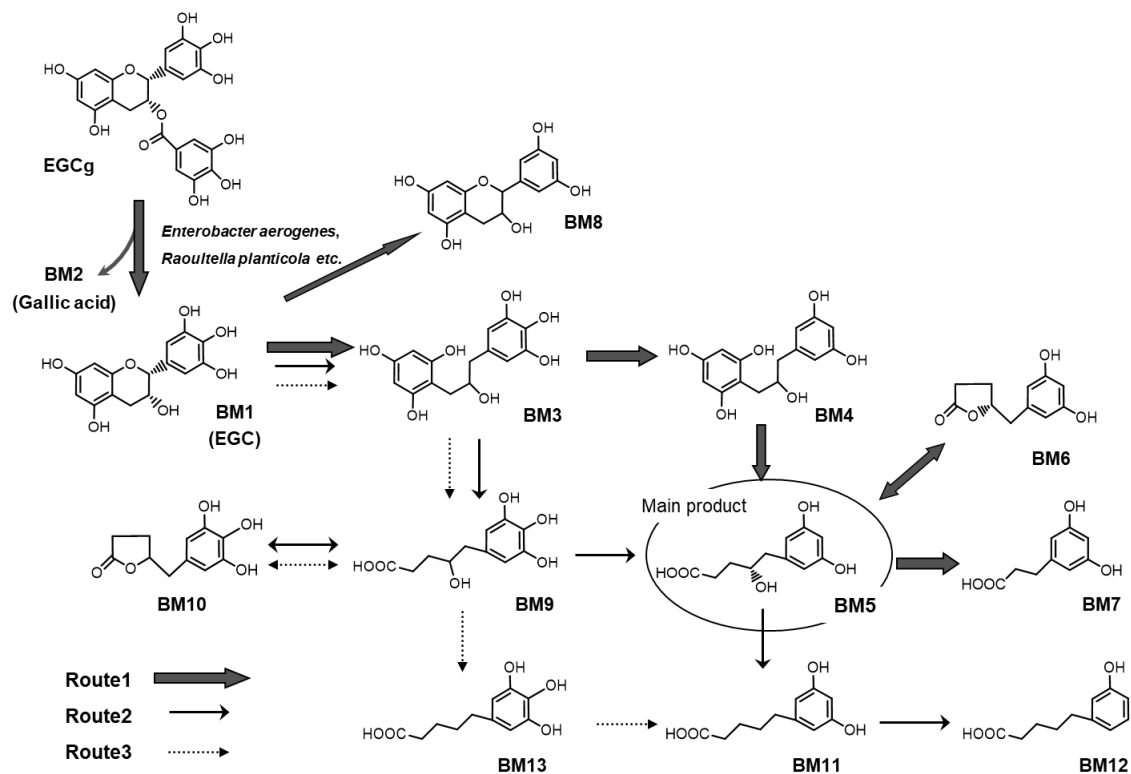**Figure 2-3** Putative metabolic pathway of EGCG by rat intestinal bacteria via route I, route II and route III by repeated in vitro metabolism examination.

Route I is suggested the primary EGC metabolic route by rat intestinal flora. Eleven kinds of EGCG metabolites were purified and identified by EGC cultured medium with rat intestinal flora. Metabolites structures were identified by LC-MS and NMR analysis.

Table 2-1 ¹H NMR spectra data of catechin metabolites Purified from EGC

	BM3	BM4	BM5	BM6	BM7	BM8	BM9	BM10	BM11	BM12	BM13
H-1a	2.601 dd (13.7, 7.6)	2.942 dd (13.8, 6.5)	—	—	—	—	—	—	—	—	—
H-1b	2.432 dd (13.7, 8.3)	2.719 dd (13.8, 6.9)	—	—	—	—	—	—	—	—	—
H-2 (or 2a)	3.938 dddd (8.3, 7.6, 4.3, 4.0)	4.898 dddd (8.3, 7.5, 6.9, 6.5)	2.329 ddd (7.5, 7.4, 7.3)	2.532 ddd (17.9, 9.4, 9.0)	2.510 t (6.6)	4.620 d (6.8)	2.441 ddd (15.7, 10.6, 7.4)	2.485 ddd (17.9, 10.3, 8.2)	2.286 m	2.301 t (6.8)	2.286 t (7.0)
H-2b	—	—	2.256 ddd (7.4, 7.4, 7.2)	2.408 ddd (17.9, 8.9, 4.7)	—	—	2.326 ddd (15.7, 8.8, 6.8)	2.341 ddd (17.9, 11.3, 4.9)	—	—	—
H-3 (or 3a)	2.849 dd (13.8, 4.3)	3.010 dd (13.1, 8.3)	1.657 dddd (14.3, 7.5, 7.4, 7.2)	2.262 dddd (12.2, 9.4, 6.9, 4.7)	2.743 t (7.6)	4.000 m	1.805 dddd (13.5, 10.6, 6.8, 3.3)	1.945 dddd (15.0, 11.8.2, 7.0)	1.609 m	1.620 m	1.586 m
H-3b	2.646 dd (13.8, 4.0)	2.737 dd (13.1, 7.5)	1.810 ddd (14.3, 7.3, 7.2, 3.7)	1.964 dddd (12.2, 9.0, 8.9, 7.2)	—	—	1.588 dddd (13.5, 8.8, 7.4, 4.4)	2.243 dddd (15.0, 10.3, 7.3, 4.9)	—	—	—
H-4 (or 4a)	—	—	3.784 m	4.744 dddd (6.9, 7.2, 6.5, 6.4)	—	2.522 dd (16.2, 7.4)	3.708 dddd (9.4, 6.3, 4.4, 3.3)	4.709 dddd (7.3, 7.0, 6.4, 6.3)	1.609 m	1.620 m	1.586 m
H-4b	—	—	—	—	—	2.761 dd (16.2, 5.0)	—	—	—	—	—
H-5a	—	—	2.623 dd (13.5, 6.8)	2.870 dd (13.9, 6.5)	—	—	—	2.715 dd (14.0, 6.0)	2.464 m	2.545 t (6.8)	2.408 t (6.8)
H-5b	—	—	2.562 dd (13.5, 6.2)	2.771 dd (13.9, 6.4)	—	—	—	2.816 dd (14.0, 6.0)	—	—	—
H-6	—	—	—	—	—	5.883 or 5.926 d (2.1)	—	—	—	—	—
H-8	—	—	—	—	—	5.883 or 5.926 d (2.1)	—	—	—	—	—
H-2'	6.220 s	6.240 d (2.1)	6.195 d (2.4)	6.193 d (2.1)	6.165 d (1.9)	6.333 d (2.1)	6.217 s	6.244 s	6.133 d (2.0)	6.637 t (2.4)	6.180 s
H-4'	—	6.151 t (2.1)	6.109 t (2.2)	6.141 t (2.1)	6.085 d (1.9)	6.202 t (2.1)	—	—	6.078 t (2.0)	6.597 dd (7.9, 2.0)	—
H-5'	—	—	—	—	—	—	—	—	—	7.064 dd (7.9, 8.1)	—
H-6'	6.220 s	6.240 d (2.1)	6.195 d (2.4)	6.193 d (2.1)	6.165 d (1.9)	6.333 d (2.1)	6.217 s	6.244 s	6.133 d (2.0)	6.650 d (8.1)	6.180 s
H-3''	5.863 s	5.806 d (2.0)	—	—	—	—	—	—	—	—	—
H-5''	5.863 s	5.773 d (2.0)	—	—	—	—	—	—	—	—	—
[M-H]⁻	307	291	225	207	181	289	241	223	209	193	225
temp	25°C	25°C	40°C	25°C	25°C	25°C	25°C	25°C	25°C	25°C	25°C

Chemical shifts are expressed in ppm downfield from the signal of TMS in CD₃OD. Coupling constants in Hz are in parentheses.

Table 2-2 ^{13}C-NMR spectra data of catechin metabolites purified from EGC

	BM3	BM4	BM5	BM6	BM7	BM8	BM9	BM10	BM11	BM12	BM13
C-1	44.19	43.17	182.97	178.03	144.84		178.4	180.42	178.19	177.56	177.83
C-2	75.38	85.73	34.24	28.11	37.838	82.73	32.03	29.56	35.25	34.92	34.91
C-3	31.64	32.76	35.91	29.53	32.63	68.7	32.87	27.93	25.89	25.70	25.68
C-4	–	–	74.09	83.00	–	27.82	73.26	83.31	31.91	31.95	32.17
C-4a	–	–		–		100.65	–		–	–	–
C-5	–	–	45.13	42.25	–	157.68	44.75	41.78	36.66	36.47	36.16
C-6	–	–		–	–	96.37	–	–	–	–	–
C-7	–	–		–	–	157.91	–	–	–	–	–
C-8	–	–		–	–	95.57	–	–	–	–	–
C-8a	–	–		–	–	156.71	–	–	–	–	–
C-1"	105.75	104.52		–	–	–	–	–	–	–	–
C-2"	158.29	159.55		–	–	–	–	–	–	–	–
C-3"	95.92	96.06		–	–	–	–	–	–	–	–
C-4"	157.76	162.87		–	–	–	–	–	–	–	–
C-5"	95.92	90.56		–	–	–	–	–	–	–	–
C-6"	158.29	159.55		–	–	–	–	–	–	–	–
C-1'	132.35	141.29	142.79	139.88		143.17	131.11	128.46	145.88	145.07	134.67
C-2'	109.47	108.92	109.16	108.93	107.78	106.49	109.42	109.55	107.97	116.23	108.36
C-3'	146.74	159.68	159.40	159.49	159.52	159.55	146.9	147.11	159.38	158.23	146.87
C-4'	132.01	101.78	101.65	102.10	101.44	103.13	132.55	133.11	101.13	113.69	132.03
C-5'	146.74	155.38	159.40	159.49	159.52	159.55	146.9	147.11	159.38	130.29	146.87
C-6'	109.47	108.92	109.16	108.93	107.78	106.49	109.42	109.55	107.97	120.81	108.36
[M-H]-	307	291	225	207	181	289	241	223	209	193	225
temp	25℃	25℃	40℃	25℃	25℃	25℃	25℃	25℃	25℃	25℃	25℃

Chemical shifts are expressed in ppm downfield from the signal of TMS in CD$_3$OD.

Metabolism of EGCG *in vivo*

In order to gain further understanding of EGCG metabolism in the intestinal tract, the author examined metabolites of EGC after direct injection into rat cecum. The metabolites produced in the cecum 5 hours after dosing of EGC (3 mg, 9.8 μmol) were detected by LC-MS system. As indicated in Figure 2-4, the amounts of each metabolite found in the cecum were 0.026, 0.028, 0.857, 1.701 and 0.618 μmol in the cecal contents for metabolite **BM1**, **BM3**, **BM4**, **BM5** and **BM6** respectively. These results demonstrated that EGC was transformed *in vivo* through the metabolic pathway of Route I as revealed in the *in vitro* experiments as described above. In addition, as in previous *in vitro* experiments metabolite **BM5** was also the most dominant metabolite in rat cecum.
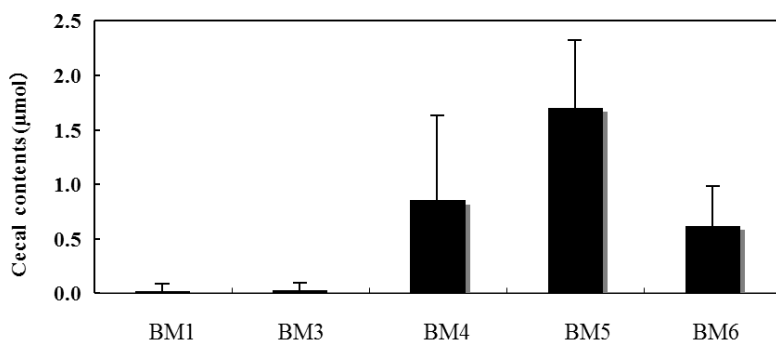
28

Figure 2-4 Cecal metabolites after direct injection of EGC into rat cecum.
3mg EGC was incubated in cecum content for 5 hours under anaerobic condition at 37 °C.
Maeatbolites were analized with LC-MS system. Data expressed as mean ± SD values in μmoles
of six rats, after five hours injected

Further, fecal metabolites after oral administration of EGCG (25 mg, 54.5 μmol) were determined. Six metabolites, **BM3**, **BM4**, **BM5**, **BM6**, **BM11** and **BM12** were detected in feces, but no EGCG or EGC were found. The amounts of the metabolites found are given in Table 2-3. The metabolites were not detected at 0-8 hours post dose and came out mainly at 8-24 hour and 24-31 hour. In the feces, **BM5** (6.16 μmol/feces) was abundant, followed by **BM4** (3.45 μmol) and **BM6** (3.27 μmol). In this experiment, it was considered EGCG converted via the mixed metabolic pathways of Routes I and II found in the *in vitro* experiments.These above *in vivo* experiments suggested that the metabolic pathway of EGCG found in the *in vitro* experiments likely reflected the pathway *in vivo*.

As indicated in Figure 2-4 and Table 2-3, **BM5** was considered as the major metabolite of EGCG produced by rat intestinal bacteria. However, there have been only a few reports that 5-hydroxyphenyl-4-hydroxyvaleric acids were identified as the metabolites produced from catechins such as C (56) and ECG (54). While, phenyl-γ-valerolactone were reported as the urinary majour metabolites in human after green tea catechin comsumption as described in General Introduction (Chapter 1). Thus, there seems to be some discrepancy between the results and those obtained in previous reports. Lactonization reactions such as this are well-known, with γ-hydroxycarboxylic acid being converted rapidly to the corresponding γ-lactone under acidic condition. Therefore, inter conversion of **BM5** and **BM6** by effect of pH, and extraction process with ethyl acetate was examined, next.

Interconversion between BM5 and BM6

As shown in Figure 2-5, **BM5** could not be extracted from the incubation mixture with ethyl acetate until the pH of the mixture was adjusted to less than pH 4.0. Furthermore, under acidic conditions in particular **BM5** tended to be spontaneously converted into **BM6** during

the concentration process. Accordingly, purification of the compound was undertaken with care. The isolation process of **BM9** showed similar tendencies and hence this compound was also purified with care.

Figure 2-6 shows the interconversion ratio of **BM 5** and **BM6** in the pH range of 1.0 to 10.0. **BM5** was foumd to be stable under alkaline conditions, but the conversion into **BM6** occurred under acidic conditions below pH 4. In particular, 90 % or more of **BM5** was spontaneously converted to **BM6** in conditions of pH 2 or below. On the contrary, **BM6** was stable under acidic conditions and began to turn into **BM5** at pH 7 or above. Similar conversions also occurred between **BM9** and **BM10**. Accordingly, much care should be taken when handling these metabolites **BM5, BM6**, **BM9** and **BM10**, especially in the purification process of these compounds.

Table 2-3 Quantification of fecal metabolites after oral administration of 25 mg EGCG.

time (h)	EGCG	BM3	BM4	BM5	BM6	BM11	BM12
0-8	0	0	0	0	0	0	0
8-24	0	0.38± 0.31	3.44±3.25	3.00 ±1.47	1.60 ±1.57	0.06 ±0.09	0
24-31	0	0.07± 0.05	0.01±0.01	2.52 ±1.66	1.37 ±0.87	0.40 ±0.22	0.02 ±0.03
31-48	0	0.05± 0.02	0	0.64 ±0.29	0.30 ±0.13	0.45 ±0.26	0.07 ±0.03
Total	0	0.16± 0.38	3.45± 0.22	6.16± 3.26	3.27 ±3.41	0.09 ±0.57	0.09 ±0.06

Data expressed as mean ± SD values in μmoles of four rats.
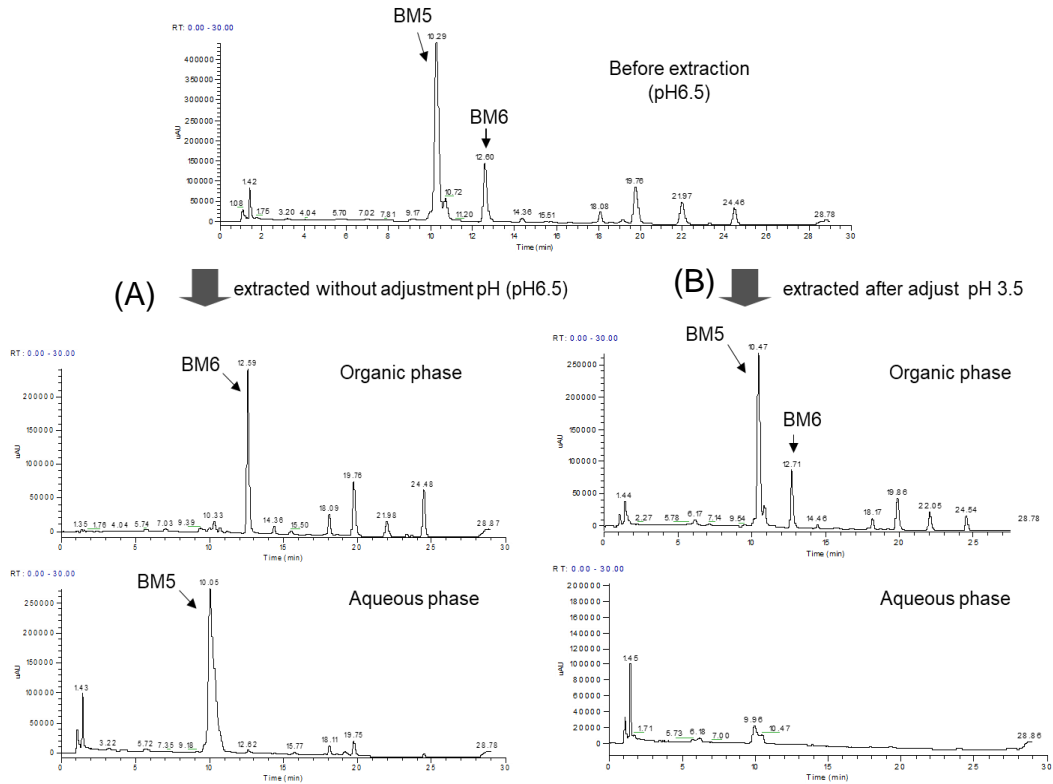
Figure 2-5 Effect of pH range on ethyl acetate extraction process of **BM5** from culture suspension.
(A) Extracted without adjustment pH. (B) extracted after adjastiment pH at 3.5
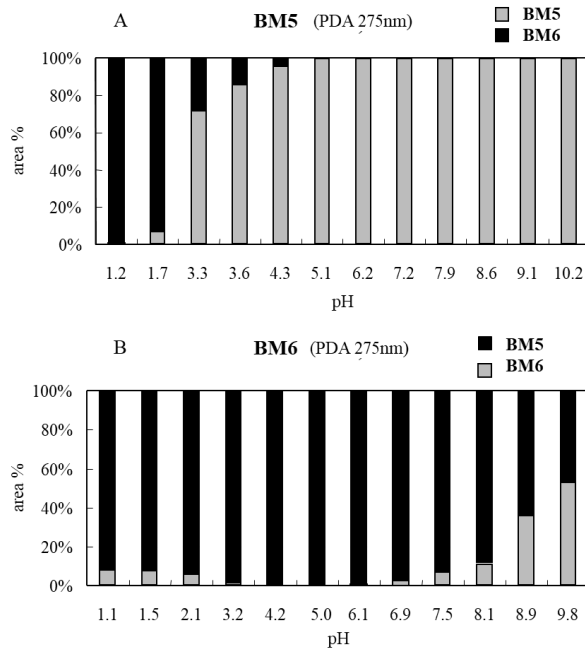

Figure 2-6 Interconversion of in the pH range (1.1 to 10.2)
(A): BM5 to BM6, (B): BM6 to BM5. Incubation of BM5 or BM6 under each pH range buffer under anaerobic condition at 37°C for 24 hours.

DISCUSSION

In this Chapter, metabolic pathways of EGCG by rat intestinal bacteria (Route I to III) were proposed by the time-course analysis and identification of derived metabolites by LC-MS and NMR analysis. As illustrated in Figure 2-3, EGCG is hydrolyzed to EGC and gallic acid at the initial step of metabolism. All of the three pathways had this step in common. In the most dominant metabolic pathway (Route I) in this study, the EGC which is formed from EGCG is converted to **BM3** by reductive opening between the 1 and 2 positions of EGC. The resulting **BM3** is converted to **BM4** by dehydroxylation at 4' position of **BM3**. Then **BM4** further undergoes ring-fission of the phloroglucinol moiety to yield **BM5**, the major metabolite of Route I. At the same time, **BM6** may be formed by lactonization of **BM5** immediately following the ring-fission. Metabolite **BM5** is converted into **BM7**, but its transformation is only very slight. In addition, while the dominant pathway is **BM1** to **BM3**, there is a very small amount of **BM1** converted to **BM8** by dehydroxylation at the 4′ position. This metabolite appeared not to be metabolized any further by the intestinal bacteria in this study. Wang *et al* (52) have discussed the possibility that the reductive opening of EGC's heterocyclic ring, which is essential for its further degradation, may be dependent on the presence of the 4′-hydroxyl. This assumption seemed to be the case for **BM8**. In Route II, one of the two minor pathways, **BM3** formed from EGC undergoes degradation of the phloroglucinol ring producing **BM9**. This compound is transformed into **BM5** by dehydroxylation at the 4′ position. Furthermore, **BM5** is dehydroxylated at the 4 position to form **BM11**, followed by conversion to **BM12** by elimination of the 5′-hydroxyl group in **BM11** of Route II. Metabolite **BM3** is converted to **BM13** via **BM9** in Route III. Finally, **BM13** is converted to **BM11** through dehydroxylation at the 4′ position of **BM13**. Metabolite **BM10** is also produced immediately following ring-fission of the phloroglucinol moiety of **BM3** in addition to **BM9** in Routes II and III, as well as the formation of **BM5** and **BM6** in Route I.

Thus, it was identified the three possible metabolic route of EGCG by rat intestinal flora. The differences in the metabolic pattern of EGCG are considered to be a reflection of differences of the intestinal microflora of rats used. The author further examined whether or not the metabolic pathways proposed in the *in vitro* experiments could reflect the EGCG metabolism in gut tract *in vivo*. The metabolites were determined 5 hour after with direct injection of EGC (**BM1**) into the cecum of the operating rats. As a result, metabolites **EGC**, **BM3**, **BM4**, **BM5**, and **BM6** were detected in the cecal contents, and **BM5** was found to be the most abundant metabolite. The author also investigated the metabolites in rat feces after oral administration of EGCG. Metabolites **BM4**, **BM5**, and **BM6** were found as the major metabolites and **BM5** was found as the dominant in the feces. Therefore, it is likely that the

metabolic pathway proposed *in vitro* experiments in this study reflects the *in vivo* metabolism of EGCG in the rats.

In conclusion in this Chapter, **BM5** was considered as the most dominant metabolite of EGCG produced by rat intestinal bacteria from results both *in vitro* and *in vivo* experiments Finally, wholly metabolic pathway of EGCG by rat intestinal bacteria was revealed through both *in vitro* and *in vivo* experiments. It was also supposed that the metabolic pathway changed somewhat with differences in the composition of rat intestinal bacteria. Since intact EGCG is reported to be poorly absorbed in the body (15, 48) it is thought that substantial amounts of EGCG metabolites are produced in the gut tract. Therefore, the importance of examining the biological activities of the metabolites and their metabolic fate in the body is recognized.

Chapter 3

Examinations on the Major Metabolites of EGCG in the Rat Body

INTRODUCTION

In Chapter 2, **BM5** was found as the major metabolite of EGCG produced by rat intestinal bacteria. On the other hund, lactonization products of 5-hydroxyphenyl-4-hydroxyvaleric acids, 5-hydroxyphenyl-γ-valerolactones such as 5-(3′, 4′-dihydroxyphenyl)-γ-valerolactone, 5-(3′, 4′, 5′-triihydroxyphenyl)-γ-valerolactone, and 5-(3′,5′-dihydroxyphenyl)-γ-valerolactone have been reported to be the major metabolites of C (56), ECG (17, 54), and EGCG (14, 15) as described in General Introduction (Chapter 1). Then, there seems to be some discrepancy between human urinary metabolites and obtained in this study described in **Chapter 2**. Then, to clarify the inconsistency between the results, examinations have conducted to determine whether or not **BM5** is converted to **BM6** in body by conducting intravenous administration of **BM5**. Additionally, the author examined the absorption profiles of **BM5** and **BM6** using in vitro everted sac method with rat large intestine.

MATERIAL AND METHODS

Chemicals and Reagents

Two EGCG metabolites, **BM5** and **BM6** were prepared according to the method described in Chapter 2. β-Glucronidase (type H-1) and Sulfatase (type VIII) was purchased from Sigma-Aldrich Co. (St.Louis, MO). All other chemicals were available products of analytical grade or HPLC grade.

Animal Treatments

Male Wistar rats were purchased from Charles Liver Laboratories Inc. (Yokohama, Japan). Animals were raised under the same conditions as Chapter 2.In this Chapter, 13-21 weeks of age of rats were used. All experimental procedures were in accordance with the guidelines for animal experiments of Food Research Laboratories, Mitsui Norin Co., Ltd.

Analysis of Urinary Metabolites Excreted after Intravenous Administration of BM5 and Oral Dosage of EGCG

The rats were maintained on a special diet free from natural occurring polyphenols for a week. First, intravenous administration of **BM5** was carried out. **BM5** (5 mg) was dissolved in 1 mL of saline and administrated intravenously to rat (12 weeks of age, $n=1$, 28 weeks of age, $n=2$). Urinary samples were separately collected for 12 hours after dosing.

Secondly, oral administration of EGCG was performed. Rats (28 weeks of age, $n=3$) were orally administered EGCG solution (25 mg/ 1 mL saline) and were then placed in stainless steel metabolic cages. Urinary samples were separately collected for 24 hours after dosing. As a control sample, urine was collected for 16 h before dosing

Uurine samples (each of 0.4 mL) were incubated with β-glucronidase Type H-1 which is a mixture of *β*-glucronidase (539 units) and sulfatase Type VIII from abalone entrails (2.3 units) at 37° C for 6 hours. After incubation, the reaction mixtures were centrifuged at 12000 × g for 10 min. The supernatants were analyzed by LC-MS/MS analysis using MRM mode described in Chapter 4. After *β*-glucronidase hydrolysis, total amounts of metabolites (free plus conjugated forms) were quantified. The amount of unconjugated form was determined by preparing samples without enzyme hydrolysis.

Absorption Experiments using in vitro Everted Gut Sac Method with Rat Large Intestine

In vitro everted gut sac method was conducting referring the methods of Mohd A *et al* (59). Male Wistar rats (6 weeks of age) were anesthetized with diethyl ether and then sacrificed. The large intestine (17 cm) was carefully removed from the rats and was rapidly preserved in Krebs buffer (pH 7.4) after washing with the same buffer. Clamp one end of the everted intestine and tie and then put 2 mL of Klebs-ringer buffer without substrate in the internal solution. Seal the filled intestine segment and transfer into 50 mL of Krebs buffer containing 0.61 μM of **BM6** or **BM5.** Incubate at 37°C with bubbling oxygen gently. Every hour, the inner solution was completely taken out, and 2 mL of fresh Klebs-ringer buffer was changed and sampling was continuously performed up to 4 hours. The analysis carried out qualitative analysis by LC-MS/MS (3200 Qtrap).

Preparation of mono-Glucuronide of BM6 (BM6-GlcUA) as Standard sample for Quantitative Analysis

Male Wistar rats (36 weeks, $n=6$, body weight average is 446.3 g), were fasted overnight, and then orally administered **BM6** (16.4 mg /1 mL saline / rat). A urine sample (95.2 mL) was taken 0-24 hours following ingestion and put into a chilled vessel on ice. After centrifugation at 10,000 × g for 15 min at 10°C to eliminate debris, 100 mL of methanol was added to the

urine sample and the resulting suspension was mixed well with a Vortex mixer. After the denatured proteins had been removed by centrifugation (10,000 × g, 10 min), the supernatant was evaporated to dryness, and the residue was dissolved in 3 % aqueous acetonitrile. Preparative HPLC was performed with a Mightysil RP-18GP column (250 mm × 20 mm i.d., 5 μm, Kanto Chemical Co. Ltd., Tokyo, Japan) in a Preparative HPLC system PLC791 (GL Sciences Inc., Tokyo, Japan). The column was eluted with a linear gradient, starting with 3 % (v/v) acetonitrile aqueous solution containing 1 % (v/v) acetic acid and finishing with 40 % (v/v) aqueous acetonitrile containing 1 % (v/v) acetic acid at a flow rate of 15 mL/min at 40°C. The elution pattern was monitored by measuring the absorbance at 270 nm. Ten fractions each containing multiple peaks were collected and a portion of each fraction was analyzed using the LC-MS system described above. The fraction having the mono-glucuronide of **BM6** (m/z 383 [M-H]–) was selected with reference to the MS data reported by Sang *et al* (51) The chosen fraction was evaporated to dryness and the residue was dissolved in 30 mL of 3% aqueous methanol for further purification on the same preparative HPLC system using an isocratic elution with 5 % aqueous acetonitrile containing 1 % acetic acid.

The purified **BM6**-GlcUA exhibited a deprotonated molecular ion peak at m/z 383 [M-H]$^-$ (207+176) in negative ESI-MS and its MS^2 spectrum was similar to that of the glucuronide conjugate of dihydroxyphenyl-γ-valerolactone (15, 51). The 1H-NMR spectrum of **BM6**-GlcUA was very like that of 5-(5'-hydroxyphenyl)- γ-valerolactone-3'-*O*-*β*-glucuronide (15). Accordingly, the compound was identified as 5-(5'-hydroxyphenyl)-γ-valerolactone -3'-*O*-*β*-glucuronide.

Preparation of mono-Sulfate of BM6 (BM6-Sul) as Standard sample for Quantitative Analysis

A mixture of dried pyridine (10 mL, Wako Pure Chemical Industries Ltd., Osaka, Japan), sodium sulfate (5 mg, Tokyo Chemical Industry Co. Ltd., Tokyo, Japan) and **BM6** (163.1 mg) was stirred for 10 min at room temperature. Then, pyridine sulfur trioxide (790.4 mg) was added to the mixture which was agitated for 1 hour at room temperature. After the reaction was stopped by adding 10 mL of 0.2 M sodium phosphate buffer (pH 7.2), the resulting solution was evaporated to dryness and the residue was dissolved in 3 mL of distilled water in order to subject it to preparative HPLC. Preparative HPLC was carried out using a CAPCELL PAK MG column (150 mm × 20 mm i.d., 5 μm, Shiseido Co. Ltd.) in a Preparative HPLC system PLC 791 (GL Sciences Inc., Tokyo, Japan). The column was eluted with mobile phase A (200 mM sodium perchlorate (Kanto Chemical Co., Inc., Tokyo, Japan) in distilled water) and mobile phase B (200 mM sodium perchlorate in acetonitrile) at a flow rate of 19 mL/min at 40 °C. Firstly, the column was eluted with 100 % A for 3 min, followed by linear increases to 100 % B from 3 to 15 min, then with 100 % A from 15 to 16 min, and lastly equilibrated

with 100 % A for 4 min.   The elution pattern was monitored by measuring the absorbance at 280 nm. The fraction containing the mono-sulfate of **BM6** (*m/z* 287 [M-H]–) was then vaporized to dryness. The resulting residue was dissolved in 3 mL of distilled water and was applied to a column of a Supelco Discovery DSC-18 cartridge (20 mL, Sigma-Aldrich Co. LLC., USA) topped with 10 mL of a Chromatorex ODS DU1530MT silica gel (15-30 μm, Fuji Silica Chemical Ltd., Aichi, Japan) which had been washed with 90 mL of acetonitrile and conditioned with 150 mL of distilled water. The column was then washed with 180 mL of distilled water and eluted with 180 mL of acetonitrile. Following evaporation of the eluate to dryness, the resulting residue was dissolved in 3 mL of distilled water and lyophilized.

The compound exhibited a deprotonated molecular ion peak at m/z 287[M-H]– (207+80) and its MS^2 spectrum was in agreement with that of the sulfate conjugate of dihydroxyphenyl-γ-valerolactone (51). ^{1}H-NMR spectra of **BM6**-Sul were similar to those of 5-(3', 5'-dihydroxyphenyl)-γ-valerolactone (4) except for the chemical shifts of the three protons in the hydroxyphenyl moiety. The chemical shifts, 6.56 ppm (1H, dd, J=1.6, 2.0 Hz, H-6'), 6.71 ppm (1H, dd, J=2.0, 2.0 Hz, H-4'), and 6.74 ppm (1H, dd, J=1.6, 2.0 Hz, H-2'), were very similar with those of 5-(5'-hydroxyphenyl)-γ-valerolactone-3'-O-sulfate (60). Accordingly, **BM6**-Sul was identified as 5-(5'-hydroxyphenyl)- γ-valerolactone-3'-O-sulfate.

Quantification Analysis Method of LC-MS/MS

LC-MS/MS analysis was conducted using a model Agilent 1100 series LC system (Agilent Technologies, Tokyo, Japan) coupled with a 3200 QTRAP LC-MS/MS system (AB SCIEX, MA, USA) as described in Chapter 4. Each urine samples and everted gut sac samples were filtered with a 0.45 μm hydrophilic PTFE filter (DISMIC-13HP, ADVANTEC Toyo) , and then subjected to LC-MS/MS analysis. The standard prepared solutions of **BM6**-GluUA and **BM6**-Sul were analyzed same system, and the calibration curves were obtained by plotting the MS intensity of each reference standard against the concentration. Each metabolite was measured using the multiple-reaction monitoring (MRM) mode (Q1/Q3; EGC-M5-GlucUA: 382.95/207.30, EGC-M5-Sul: 286.93/207.20).

RESULTS

Urinary Metabolites after Intravenously Administrated BM5, and Orally Administrated EGCG

The quantitative analyses of rat urinary metabolites after intravenous administration of **BM5,** are shown in Figure 3-1A. A large amount of **BM5** aglycones and conjugates were mainly detected in urine, while only a small amount of conjugate was detected in **BM6.** This result suggests that even if **BM5** is absorbed from the intestine into the body, it is unlikely to undergo lactonization and be converted to **BM6** in the blood circulation. Further, in the same way as previous study, urinary metabolites were abundantly detected as the conjugated form of **BM6** after oral administration of EGCG (15), These results considered, it was suggested that **BM5** produced mainly in the intestinal tract is unlikely to be lactonized after body absorption, and is likely to be lactonized through the absorption process from the intestinal gut tract into the blood circulation.
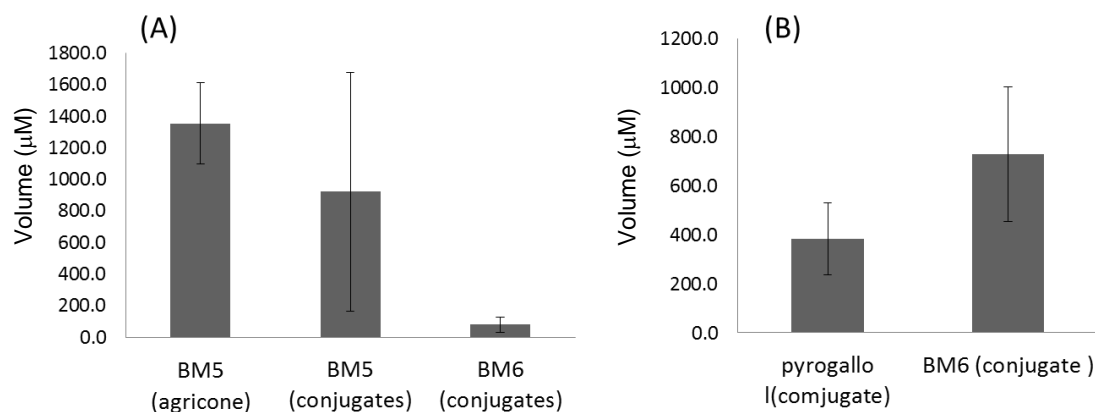
Figure 3-1 Urinary metabolites after intravenous dosage of **BM5** (A) and oral administration of EGCG (B)

(A) Average values of urinary metabolites after 32h of i.v. dosage of 5mg **BM5** (*n*=3; 12weeks=1, 28weeks *n*=2). (B) Average volumes of urinary metabolites after 48h of oral administration of 25mg EGCG (*n*=3: 28weeks *n*=3). The amount of unconjugated form was determined by preparing samples without enzyme hydrolysis.

Examination of Absorption of BM5 and BM6 using in vitro Everted Gut Sac Model

The author examined intestinal absorption of **BM6** using in vitro everted sac method with rat large intestine. Figure 3-2A shows absorption of **BM6** with time. Absorption of the metabolite through large intestine increased in almost direct proportion to the incubation time. However, almost **BM6** absorbed was found to be glucuronide conjugate. These results suggested that **BM6** mainly underwent glucuronidation during the absorption process through rat large intestinal epithelial cells.   In the same method, absorption of **BM5** was examined. As shown in Figure 3-2B, the compound was transported through the large intestine and its absorption curve was lowerd as compared to that of **BM6**. In the case of **BM5** its conjugated form of metabolite was found to be hardly detected and hence **BM5** was absorbed without any conjugation. In consideration of the above results, it is supposed that **BM6** may pass through the large intestine more easily than **BM5**. In addition, **BM6** was also shown to be likely to undergo glucuronidation during passage process through the large intestine.
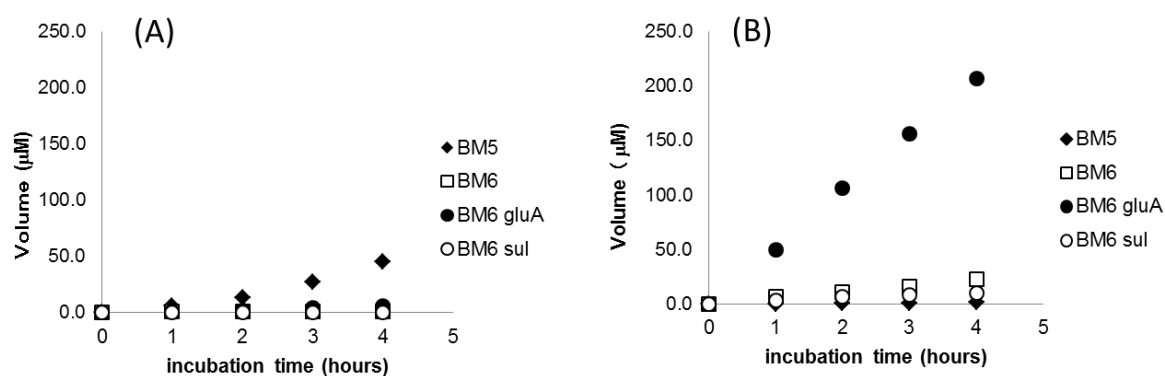

Figure 3-2   Accumulated values of metabolites passed through large intestine by everted gut Sac method
(A) Concentration of internal solution of everted sac in Klebs-ringer buffer containing **BM5** (*n*=2).
(B) Concentration of internal solution of everted sac in Klebs-ringer buffer containing **BM6** (*n*=2).

DISUCUSSION

As described in Chapter 2, EGCG was found to undergo degradation by rat intestinal flora and to produce **BM5** as one of the major products in the gut tract. However, **BM5** is rarely reported as a urinary metabolite after EGCG administration. Instead, **BM6** which is the lactonization products of **BM5**, have been detected abundantly in rat urine after EGCG consumption. Thus, there is an apparent discrepancy that the metabolite found in rat intestinal tract is different from that in the urine. In this Chapter, the author examined the possibility of conversion of **BM5** to **BM6** in the body during absorption process from gut tract, and during blood circulation in the body and excretion into urine.

From results, it was found that **BM5**, which is major degraded product of EGCG, was absorbed almost as aglycone. And **BM5** was likely not as well absorbed from the digestive tract membrane compared with **BM6**. Thus, **BM5** was thought to be easily excreted into feces without being absorbed as shown in the Figure 2-5 (Chapter 2).

On the other hand, **BM6** has been shown to undergo glucuronidation during colonic membrane passage and it is predicted to pass more easily through the gut membrane rather than **BM5.** In general, glucuronidation is known to be catalyzed by UDP-glucuronyltransferase (UGT) (60). UGT displays broad substrate-specificity, and is distributed in many parts of body such as small intestine, kidney, liver, brain. It is reported that, glucuronidated compounds by UGT present in epithelial cells are excreted by any transporter. For estradiol known to be contained in wine, it has been reported that the glucuronaide estradiol is transported through into luminal side by oatp (organic anion transporter) from proximal tubular of epithelial cells (60). Therefore, it is assumed that **BM6** produced in the large intestine is glucuronised in epithelial cells of digestive tract and transferred to the blood by any transporter, and excreted in urine after circulated around the body in blood circulation. According to ECG, studies on absorption using Caco-2 cells have already been reported, (61) and it is also reported that four kinds of transporters such monocarboxylic acid transporter (MCT), multidrug resistance-associated protein 1 (MRP1), multidrug resistance-associated protein 2 (MRP2) and *p*-pglycoprotein, may be involved in absorption process. Konishi *et al* (62, 63) reported the intestinal absorption process of coumaric acid, caffeic acid, 3-(3′-hydroxyphenyl)-propionic acid, gallic acid etc. It is suggested that these phenolic acids, except gallic acid. are absorbed via MCT. Therefore, it was considered that **BM5** having a phenolic acid structure may also be absorbed via MCT. However, since there is no study report on absorption of catechin metabolites, further study is needed for detailed examination on absorption process using such Caco2 cells for clarify detail absorption mechanisms.

Together with the previous results of Kohiri *et al* (15) and the results of in this study, Fig. 2-3 shows the putative metabolic pathway of EGCG in rats. After orally administrated to rat, EGCG have underwent degradation to produce mainly **BM**5 and **BM6** in gut tract. It was considered that **BM5** is unlikely to be easily absorbed into the body, while **BM6** is likely more absorbed undergoing glucuronised mainly into the bloodcirculation. These results are consistent with the other reports in which γ-phenyl-valerolactone compounds were detected as the main urinary metabolites after the oral administration of green tea catechins. From the results, it was concluded that the main metabolite in the body after oral administration of EGCG in rats is **BM6** rather than **BM5**. For this reason, next, it is investigated whether **BM6** which is a main metabolite contributes to functionality in the body after EGCG oral administration.
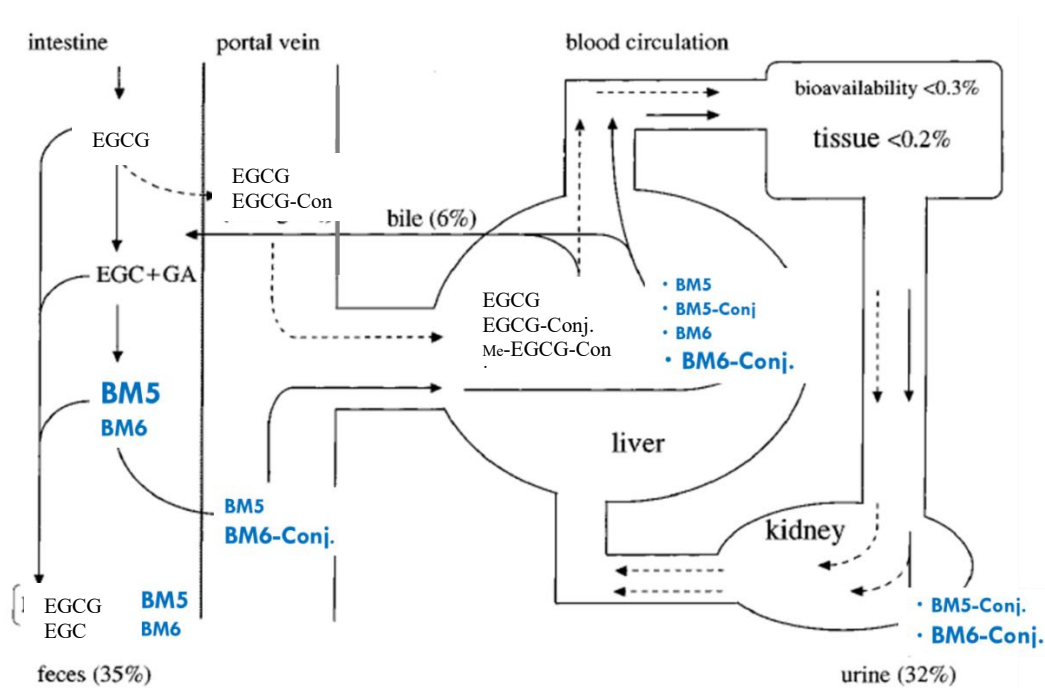

Figure 3-3 Putative metabolic fate of EGCG in rat taking account of results obtained from examination in Chapter 2 and Chapter 3.

41

Chapter 4

Isolation and Characterization of Rat Intestinal Bacteria Involved in Biotransformation of EGC, and Examination of EGC Metabolism by Four Isoflavone-Metabolizing Bacteria

INTRODUCTION

Information available on identification of intestinal bacteria directly involved in the degradation of catechins is limited. It has already reported that *Enterobacter aerogenes*, *Raoultella planticola*, *Klebsiella pneumoniae* subsp. *pneumoniae* and *Bifidobacterium longum* subsp. *infantis* were capable of hydrolyzing EGCG to EGC and gallic acid, as described in Chapter 2 (64, 65). As the next step of catabolize of EGC, Wang *et al* have reported that *Eggerthella* sp. SDG-2 (66) could catalyze the C ring-cleaving and 4'-dehydroxylation of EC and EGC subsequently. Jin and Hattori (67) have reported that *Eggerthella* sp. CAT-1, which is closely similar to strain SDG-2 (99.8 % 16S rRNA gene sequence similarity), was able to catalyze the ring cleavage and subsequent dehydroxylation of 4'-OH of EC and C. Furthermore, Kutschera *et al* (68) have reported that *Eggerthella lenta* rK3 catalyzed the ring-opening of EC and C with the resulting 1-(3′, 4′-dihydroxyphenyl)-3-(2, 4, 6-trihydroxyphenyl)propan-2-ols being degraded to 4-hydroxy-5-(3′, 4′-dihydroxyphenyl)valeric acids, and its corresponding γ-valerolactones by *Flavonifractor plautii* aK2. These studies have demonstrated the platform of the metabolic pathways of tea catechins by intestinal bacteria.

In this Chapter 4, the author examined the biotransformation of EGC by intestinal bacteria (strains MT4s-5 and MT42) isolated from rat feces and their related bacterial strains. The author already isolated and identified these bacteria to be *Adlercreutzia equolifaciens* MT4s-5 (69) and *Flavonifractor plautii* (formerly *Eubacterium plautii*) MT42 (69). In addition, it was found that some bacterial strains were responsible for catabolism of EGC as symbiotic bacteria, the author refers to the role of these bacteria. Furthermore, the author has investigated the abilities of several commercially available isoflavone-metabolizing bacteria (67-72) to degrade EGC, and the *p*-dehydroxylation abilities of EGC metabolites, **BM9** and **BM10** by these isoflavone-metabolising bacteria.

MATERIALS AND METHODS

Commercially Availabl Bacteria

Eggerthella lenta JCM 9979 and *Escherichia coli* K-12 were purchased from Riken Bioresource Center (Ibaragi, Japan). *Flavonifractor plautii* ATCC 29863 (formerly *Eubacterium plautii*) and *Flavonifractor plautii* ATCC 49531 (formerly *Clostridium orbisciendens*) were obtained from American Type Culture Collection (ATCC, Manassas, VA, USA). *Adlercreutzia equolifaciens* JCM 14793 (70), *Asaccharobacter celatus* JCM 148113 (71,72), *Slackia equolifaciens* JCM 16059 (73,74), and *Slackia isoflavoniconvertens* JCM 16137 (75) were purchased from Riken Bioresource Center (Ibaragi, Japan).

Isolation of EGC-Converting Bacterium

Fresh fecal sample (2 g) was collected from male Wistar rats (13-20 weeks age), and homogenized in 5 mL of GAM broth and loopfuls of the resulting homogenate were streaked on plates of GAM broth with 0.5 % agar. Incubation of the plates was done at 37°C for 72 hours. Anaerobic bacterial populations found on several parts of the GAM agar plate were each transferred to fresh GAM broth (3 mL) containing 1 mM EGC which was prepared by adding EGC solution previously filtrated with a sterilized membrane filter (DISMIC-25cs, cellulose acetate, 0.2 μm, ADVANTEC Toyo, Tokyo, Japan). After incubation for 48 hours at 37°C, in order to select the bacterial mixtures capable of cleaving EGC a portion of each culture was centrifuged at $1,2000 \times g$ for 10 min and the resulting supernatants were analyzed by an LCQ Deca XPplus LC-MS system as described later in this chapter. The selected bacterial mixtures were separately re-streaked on the 0.5 % GAM agar plates which were incubated at 37°C for 72 hours. Several of the bacterial populations grown on each of the agar plates were picked up and then transferred separately to GAM broth containing 1 mM EGC. After incubation for 48 hours at 37 ℃ and then centrifugation to remove bacterial cells, the supernatants were analyzed using the LC-MS system. The bacterial cultures which could degrade EGC were selected. After repetition of the above procedures five to six times, the selected bacterial cultures with EGC-degrading ability were diluted by factors of 10^{-2} to 10^{-7} with sterile water and then each of the diluted cultures was spread onto the GAM agar plates. After incubation for 48 hours at 37°C, two bacterial strains (MT4s-3 and MT4s-5) which had formed a single colony were selected. Then, these two strains were separately cultured in GAM broth containing 1 mM EGC for 48 hours at 37°C. After centrifugation, the metabolites in each supernatant were analyzed by LC-MS system.

Isolation of Intestinal Bacterium with EGC cleaving ability

Fresh fecal sample (2 g) was suspended in 5 mL of distilled water and 0.1 mL each of the suspension was placed in 10 or more test tubes containing GAM broth (2 mL) and 1 mM **BM3.** After incubation at 37°C for 48 hours, 1 mL each of the cultures was taken and centrifuged at $1,2000 \times g$ for 10 min. The supernatants were applied to the LC-MS system to examine the converting ability of **BM3**. The cultures showing conversion abilities were selected and 0.1 mL each of the selected cultures was further subcultured in two fresh GAM broths (2 mL) containing **BM3** and then cultures showing the conversion abilities were again selected by LC-MS analysis. After repetition of the above procedure five to six times, a bacterial culture in which the converting ability of **BM3** could be maintained was finally selected. Then, 0.1ml each of 10^{-1} to 10^{-7} dilute solutions of the culture were spread onto GAM agar plates and the plates were incubated at 37°C for 48 hours. More than 100 individual colonies were isolated and examined for the degradation ability of **BM3** by LC-MS analysis.

Isolation of Symbiotic Bacteria Working with Strain MT4s-5

Fresh rat fecal sample (2 g) was homogenized in 5 mL of GAM broth, and the resulting homogenate was diluted serially from 10^{-1} to 10^{-9} using the same medium. Suspensions (50 μL) from the 10^{-5} to the 10^{-9} dilutions were put onto petri dishes respectively. GAM agar, which had been previously autoclaved and cooled to achieve a temperature of around 40°C, was poured into the dishes and mixed gently. All dishes were anaerobically incubated at 37 °C for 72 hours. Single colonies in the dishes were separately transferred to 3 mL of GAM broth containing 1mM EGC and then the preculture (50 μL) of isolate MT4s-5 in GAM broth was added to the medium. After incubation at 37°C for 48 hours, cultures were centrifuged at $1,2000 \times g$ for 10 min and the supernatants were analyzed by LC-MS system to observe the conversion of EGC to metabolite **BM4**.

Determination of 16S rRNA Gene Sequences of Isolates and Phylogenetic Analysis

16S rRNA gene sequences were determined using a MicroSEQ 16S rRNA Full Gene PCR and Sequencing Kit according to the protocol of the manufacturer (Life Technologies, Carlsbad, CA USA). PCR products were purified using a QuickStep 2 PCR Purification Kit (Edge BioSystems, MD USA) and AutoSeq G-50 (GE Healthcare UK Ltd.). 16S rRNA sequences of the PCR products were analyzed using an ABI PRISM 3100 Genetic Analyzer with Sequencing Analysis Software v.5.1.1 (Life Technologies). Primer sequences were removed from the target nucleotide sequences and the trimmed sequences were subjected to similarity searches. Closest relatives were identified using a BLASTN search algorithm of the GenBank database (67) or a MicroSEQ ID Software v.2.1.1. (Life Technologies).

Sequences of isolates and their related species were aligned with a CLUSTAL W program (77), and gaps and unidentified base positions were removed using a BioEdit (78) software package. Phylogenetic trees were reconstructed using the neighbour-joining method with a MEGA software version 4 (79). Bootstrap values were based on 1000 replications. Evolutionary distances were calculated using a Kimura two parameter model (80).

Degradation of EGC by Isolate MT4s-5 and *Eggerthella lenta* JCM 9979

Strain MT4s-5 and strain *Eg.lenta* JCM 9979 were separately precultured in GAM broth (5 mL) at 37ºC for 48 hours. Then each pre-culture (0.5 mL) was inoculated into 5 mL of fresh GAM broth containing 1 mM EGC and incubated at 37ºC. As a control, GAM broth containing EGC was also incubated under the same condition without bacterium. After incubation for 24, 48, and 72 hours, aliquots (0.5 mL) of the incubation mixture were taken out, inside an anaerobic glovebox under CO_2 atmosphere. After the addition of 50 μL of 2 M HCl to each sample, bacterial cells were removed by centrifugation at $1,2000 \times g$ for 10 min at 4ºC. A portion (0.2 mL) of each resulting supernatant was then diluted with 0.8 mL of 0.5 % aqueous acetic acid, and the samples were analyzed using a 3200QTRAP LC-MS/MS system. This quantitative analysis of metabolites is described later.

Degradation of EGC and Metabolites BM3 and BM4 by Isolate MT42 and Its Closely Related Bacterial Strains

After incubation of strain MT42 in GAM broth (5 mL) at 37ºC for 24 hours, aliquots (0.5 mL) of the culture were inoculated into 5 mL of fresh GAM broth containing 1 mM metabolite **BM3,** then the culture was incubated at 37ºC. After every 24 hours of incubation, a portion (0.5 mL) of the culture was removed inside an anaerobic glovebox under CO_2 atmosphere and 50 μL of 2 M HCl was added. Centrifugation ($1,200 \times g$ for 10 min) was performed to remove bacterial cells, then a portion (0.2 mL) of each resulting supernatant was diluted with 0.8 mL of 0.5% aqueous acetic acid. The samples were analyzed using the 3200QTRAP LC-MS/MS system for quantitative analysis of metabolites. Degradation experiments for EGC and metabolite **BM4** were performed as in the experiment for metabolite **BM3**. In the case of *Flavonifractor plautii* strains ATCC 29863 and ATCC 49531, degradation experiments for EGC, **BM3**, and **BM4** were also carried out according to the same procedure as described above.

Degradation of EGC by Isolate MT4s-5 and *Eggerthella lenta* JCM 9979 in the Presence of Symbiotic Bacteria

Isolates MT4s-3, MT01 and MT12, and *Escherichia coli* K-12 were the symbiotic bacteria used in this study. Strains MT4s-5 and MT4s-3 were separately precultured with GAM broth

(5 mL) at 37ºC for 48 hours. The precultures (0.5 mL each) of both strains were inoculated into GAM broth (5 mL) containing 1 mM EGC and then the mixed culture was incubated at 37ºC. After incubation for 24, 48, and 72 hours, aliquots (0.5 mL) of the incubation mixture were removed, inside an anaerobic glovebox under CO_2 atmosphere. The culture was centrifuged (1,200 × g for 10min) after adding 50 μL of 2 M HCl to acidify pH 3.0-4.0. The supernatant (0.2 mL) was diluted with 0.8 mL of 0.5 % acetic acid and the sample was analyzed under the LC-MS/MS system for quantitative analysis of metabolites. Strains were co-cultured as follows: MT4s-5 with K-12, MT4s-5 with MT01, MT4s-5 with MT12, *Eg.lenta* JCM 9979 with MT4s-3, JCM 9979 with K-12, JCM 9979 with MT01, and JCM 9979 with MT12; in the same way as above. The sample preparation from each co-cultivation mixture and quantitative analysis by LC-MS/MS were also performed by the same method as described above.

Cultivation of Isolate MT4s-5 and *Eggerthella lenta* JCM 9979 in a Culture Vessel Physically Separated from Symbiotic Bacteria with Membrane Filter

In order to examine the conditions produced by symbiotic bacteria which are required for 4'-dehydroxylation of EGC by strains MT4s-5 and JCM 9979, a culture vessel (PAL Corporation, Tokyo, Japan) separated into two partitions A and B by a membrane filter was used. This method, designed by Ohno *et al* (81) uses a vessel consisting of two parts, each of which has a cotton-plugged inlet and the assembled vessel can contain 114 mL of media in total. Between the two partitions A and B there is a membrane filter (Supor 200, PES, 0.2 μm, PAL Corporation, Tokyo, Japan) with a diameter of 47 mm. GAM broth (50 mL) was poured in each partition of the vessel, and then, EGC solution sterilized by membrane filter was aseptically added to the GAM broth in both partitions to make up a medium containing 1 mM EGC. Preculture (15 mL) of strain MT4s-5 in GAM broth was inoculated into the medium in partition A and preculture (1 mL) of strain MT4s-3 into the medium in partition B. The vessel was anaerobically incubated at 37º for 24 hours with gentle shaking. Aliquots (1 mL) of the culture in partition A were taken and then centrifuged at 1,200 × g for 10 min. The resulting supernatant (0.2 mL) was diluted with 0.5% acetic acid (0.8 mL) and the sample was quantitatively analyzed under the 3200QTRAP LC-MS/MS system. The same method of analysis was conducted with the strain pairs MT4s-5 and *Escherichia coli* K-12, JCM 9979 and MT4s-3, and JCM 9979 and K-12, respectively.

Screening Assay of factor (s) Required for Dehydroxylation Reaction by Isolate MT4s-5 and *Eggerthella lenta* JCM 9979

Preculture (0.5 mL) of strain MT4s-5 in GAM broth that had been kept at 37ºC for 24 hours, was inoculated into GAM broth (5 mL) containing 1 mM EGC and 3 mM sodium

formate, and then it was incubated anaerobically at 37ºC. After the 24 and 48 hours incubation, aliquots (0.5 mL) of the incubation mixture were taken, inside an anaerobic glovebox under CO_2 atmosphere and 50 μL of 2M HCl were then added. After centrifugation (1,200 × g, 10 min) to remove bacterial cells, the supernatants were analyzed by LC-MS. Similar methods were performed using lactic acid, butyric acid, methanol, ethanol, 2-propanol, 2-butanol, sodium acetate, sodium fumarate, disodium succinate, sodium propionate, sodium nitrate, sodium carbonate, and sodium sulfate, respectively. The method for strain JCM 9979 was also conducted in the same way as above. In the case of the hydrogen test, each preculture (1 mL) of strains MT4s-5 and JCM 9979 was inoculated into GAM broth (5 mL) containing 1 mM EGC and then hydrogen gas was aseptically bubbled into the incubation mixture for 10 sec at a flow rate of about 800 mL/min. The resultant culture in test tube was packed in an Anaero Pouch (800 mL) with AnaeroPack system. Air in the pouch was roughly removed by hand and hydrogen gas was injected into the pouch for 30 sec at the same flow rate as above. Cultivation, sampling, and the LC-MS/MS analysis were performed in the same manner as above.

Dehydroxylation of Metabolites BM3, BM9, and BM10 by Isolate MT4s-5 and *Eggerthella lenta* JCM 9979

Preculture of strains MT4s-5 and JCM9979 was inoculated in GAM broth (5 mL) containing 1 mM each of metabolites **BM3**, **BM9**, and **BM10** and incubated anaerobically at 37ºC. At intervals of every 24 hours intervals a portion (0.5 mL) of each incubation mixture was removed, inside an anaerobic glovebox under CO_2 atmosphere, and 50 μl of 2 M HCl was added. After centrifugation (1,200 × g for 10min), the supernatant (0.2 mL) was diluted with 0.5% acetic acid (0.8 mL) and was analyzed using the LC-MS/MS system. The same experiments were also carried out in the presence of symbiotic bacteria, hydrogen, and formate, respectively.

Formate and Hydrogen Analysis

Commensal bacteria were inoculated individually into 5 mL of GAM broth and cultured under anaerobic condition for 24 hours at 37°C. After centrifugation (1,200 × g for 5 min) for removal of the bacterial cells, the supernatants were applied to a G1600A Capillary electrophoresis (CE) system (Agilent Technologies Japan, Ltd, Tokyo, Japan). Separation of organic acids was done using a fused silica capillary tube (i.d.75 μm, effective length = 72 cm, total length = 80.5 cm, Agilent Technologies) at a constant temperature (20 °C). The electrode was calibrated using an Organic acids buffer (pH5.6) for CE (Aglent Technologies). Sample solutions were injected at 50 mbar for 2.0 sec. The electrophoretic separation process was

conducted under -25 kV and monitored by photodiode array (PDA) detector at signal = 350 nm / Bandwidth = 20 nm and reference = 270 nm / bandwidth = 10 nm.

GEach preculture of the commensal bacteria was inoculated into GAM broth (10 mL) in sterilized glass vessel (25 mL capacity) as described above. After incubation at 37°C for 2 hours, each vessel was sealed up inside a glovebox filled with CO_2 atmosphere and was further incubated anaerobically for 24 h. Headspace gas (2 mL) in each vessel was analyzed with a GC-14B system (Shimadzu corporation, Kyoto, Japan) at SEIKAN Co., Ltd. (Shizuoka, Japan) to determine the level of hydrogen generated.

Degradation of EGC by Isoflavone-Metabolizing Bacteria

Four bacterial strains, *Ad. equolifaciens* JCM 14793, *As. celatus* JCM 14811, *S. equolifaciens* JCM 16059 and *S. isoflavoniconvertens* JCM 16137, were individually pre-cultured in GAM broth (5 mL) at 37ºC for 48 hours. Each preculture (0.5 mL) was then inoculated into 5 mL of fresh GAM broth containing 1mM EGC or GC and was cultured at 37 ºC. As the control, GAM broth containing EGC was also cultured without bacterium under the same condition. After incubation for 24, 48, and 72 hours, aliquots (0.5 mL) of the incubation mixture were removed inside an anaerobic glovebox under CO_2 atmosphere. After the addition of 50 μL of 2 M HCl to each sample, bacterial cells were removed by centrifugation at 12,000 × *g* for 10 min at 4ºC. A portion (0.2 mL) of each resulting supernatant was then diluted with 0.8 mL of 0.5 % aqueous acetic acid, and the sample was analyzed under the LC-MS system for identification of metabolites and the LC-MS/MS system for quantitation of metabolites.

Degradation of EGC by Isoflavone-Metabolizing Bacteria in the Presence of Hydrogen

Each preculture (0.5 mL) of the four strains was inoculated into GAM broth (5 mL) containing 1 mM EGC and the hydrogen gas was then aseptically bubbled into the incubation mixture for 10 sec at a flow rate of about 50 mL/min. The resultant culture contained in a test tube was packed in an Anaero Pouch (800 mL) with AnaeroPack system (Mitsubishi Gas Company, Inc.). Removal of the air in the pouch was done roughly by hand and hydrogen gas was injected into the pouch for 30 s at a flow rate of 800 mL/min. Each of the resultant cultures was incubated anaerobically at 37ºC. The cultures were sampled as described above, then hydrogen gas was injected into the pouch again and the culture was continued. Samples for LC-MS and LC-MS/MS analyses were taken in the same way as described above.

Dehydroxylation of BM3, BM9, and BM10 by Isoflavone-Metabolizing Bacteria

The respective aqueous solutions of **BM3**, **BM9**, and **BM10** were aseptically added to GAM broth (5 mL) to make up mediums containing 1 mM of each of the metabolites. Each

medium was separately inoculated with the preculture of each of the four strains and was incubated anaerobically at 37℃. Samples for LC-MS and LC-MS/MS analyses were taken in the same way as described before. And, the above four strains were incubated in GAM broth each containing **BM3**, **BM9**, and **BM10** in the presence of hydrogen under the same conditions as described above.

LC-MS Analysis for Screening and Structural Analysis

LC-MS analysis and NMR analysis were performed using a Surveyor HPLC and an LCQ Deca XPplus system as described in Materals and Method in Chapter 2.

LC-MS/MS Analysis for Quantitation of Metabolites

LC-MS/MS analysis was conducted using a model Agilent 1100 series LC system (Agilent Technologies, Tokyo, Japan) coupled with a 3200QTRAP LC-MS/MS system (AB SCIEX, MA, USA). HPLC was performed using a 100 mm × 2 mm (i.d.) , 3μm, CAPCELLPAK MG column (Shiseido Co., Ltd, Tokyo, Japan), with a gradient solvent system consisting of solvent A (water/ acetonitrile/ acetic acid 500/12.5/0.5 v/v/v) and solvent B (water/ acetonitrile/ methanol/ acetic acid 100/100/100/0.3, v/v/v/v). Gradient elution was performed at 0.2 mL/min with the following elution conditions; 4 min hold at 100% solvent A, 5 min linear gradient in solvent B from 0 to 10 %, 9 min hold at 10 % B, 3 min linear gradient from 10 to 25 % B, 3 min linear gradient from 25 to 100 % B, 0.1 min linear gradient in solvent A from 0 to 100 %, and 6 min hold at 100 % A. The mass detector was fitted with turbo-ion spray (electrospray ionization, ESI) source and operated in multiple reactions monitoring (MRM) under negative ion mode. For all the mass scan modes, ion spray voltage was kept at -4000 V, curtain gas was set to 10 (arbitrary units), the collision gas was 5 (arbitrary units), and capillary temperature was set at 550°C. The optimized instrument setting for each metabolite is listed in Table 4-1. The LC-MS/MS system was controlled with an Analyte version 1.6.1 software. The data were acquired and processed using the same software.

Standard solutions were prepared by accurately weighing each reference standard (metabolites **BM3**, **BM4**, **BM9**, **BM10**, **BM5**, **BM6**, and **BM8**) and dissolving in 0.1 % aqueous acetic acid containing 3 % methanol, then each solution was diluted with 0.5 % aqueous acetic acid at five concentration levels in the range from 50 to 500 μM. To 0.2 mL of the respective solutions, 0.2 mL of GAM broth and 0.6 mL of 0.5 % aqueous acetic acid were added. The standard solutions thus prepared were analyzed with the LC-MS/MS system and the calibration curve of each standard compound was obtained by plotting MS intensity of each reference standard against the concentration.

Other Analytical Methods

NMR analysis was done on a Bruker Ultrashield 400 plus system (^{1}H, 400 MHz; ^{13}C, 100 MHz: Bruker BioSpin K. K., Yokohama, Japan). Samples were dissolved in methanol-d_4 (Kanto Chemical, Tokyo, Japan). Chemical shifts were referenced against tetramethylsilane (TMS) at 0 ppm. Specific rotations ($[\alpha]_D^{20}$) of metabolites were measured using a P-1020 Polarimeter (JASCO Corporation, Tokyo, Japan), and the solvents and sample concentrations used were as described in the text.

Table 4-1 Molecular weight (MW) and optimized instrument settings for LC-MS/MS

Compounds	MW	Transitions(m/z)		DP	CE	CXP
		Precursor	Product			
EGC	306	305.1	161.1	-45.0	-18.0	-4.0
BM3	308	307.1	151.0	-50.0	-12.0	-18.0
BM4	292	291.3	125.0	-55.0	-50.0	-3.0
BM9	242	241.0	101.0	-20.0	-20.0	-2.0
BM10	224	223.1	125.0	-65.0	-22.0	0.0
BM5	226	225.0	101.0	-20.0	-20.0	-2.0
BM6	208	207.1	145.1	-65.0	-22.0	0.0
BM8	290	289.0	271.0	-45.0	-18.0	-4.0

CE; collision energy, DP; declustering potential, CXP; collision cell exit potential

RESULTS

Isolation and Identification of EGC-Degrading Bacterium

In order to confirm the intestinal bacteria responsible for the catabolism of EGCG and EGC, the author attempted to isolate bacteria from rat feces, that were capable of degrading EGC. The bacterial strain MT4s-5 was isolated as an EGC-degrading bacterium. This isolate was found to catalyze the conversion of EGC into **BM3**, **BM4**, and **BM8**. The 16S rRNA gene sequence of the strain was determined and then it was compared with corresponding bacterial sequences in databases. The sequence of strain MT4s-5 (1460 bp, accession number AB693938) was highly-homologous not only to *Adlercreutzia equolifaciens* strains FJC-B9 (AB306661, 99.9 % similarity) and FJC-A10 (AB306660, 99.8 % similarity) (70) but also *Asaccharobacter celatus* do03 (AB266102, 99.9 % similarity) (72) and a human intestinal bacterium SNU Julong 732 (AY310748, 99.8 % similarity). Reports showed these above bacteria, which were highly-homologous to strain MT4s-5, could convert daidzein to equol (72). Strain MT4s-5 was also shown to have the ability to convert daidzein to equol via dihydrodaidzein (82). Further, the 16S rRNA gene sequence of *Ad.equolifaciens* FJC-B9 was found to be also highly-homologous (99.9 % similarity) to that of *As. celatus* do03 and therefore isolate MT4s-5 was determined to be either *Adlercreutzia equolifaciens* or *Asaccharobacter celatus*. Although the author could not give a single name to isolate MT4s-5, since *Adlercreutzia equolifaciens* gen. *nov*., sp. *nov*., (70) had been proposed a little bit earlier than *Asaccharobacter celatus* gen. *nov*. sp. *nov*., (72), this author tentatively named strain MT4s-5, *Adlercreutzia equolifaciens*. Figure 3-1 illustrates the phylogenetic tree giving the relationships between strain MT4s-5 and some related taxa, based on 16S rRNA gene sequences. It was already reported that *Eggerthella* sp. SDG-2 (52), *Eggerthella* sp. CAT-1 (67), and *Eg.lenta* rK3 (68) had similar conversion ability to strain MT4s-5, but the 16S rRNA gene sequence of strain MT4s-5 showed only 91.8 %, 92.3 %, and 91.3 % similarities to those of strains SDG-2 (66), CAT-1 (67), and rK3 (68), respectively.
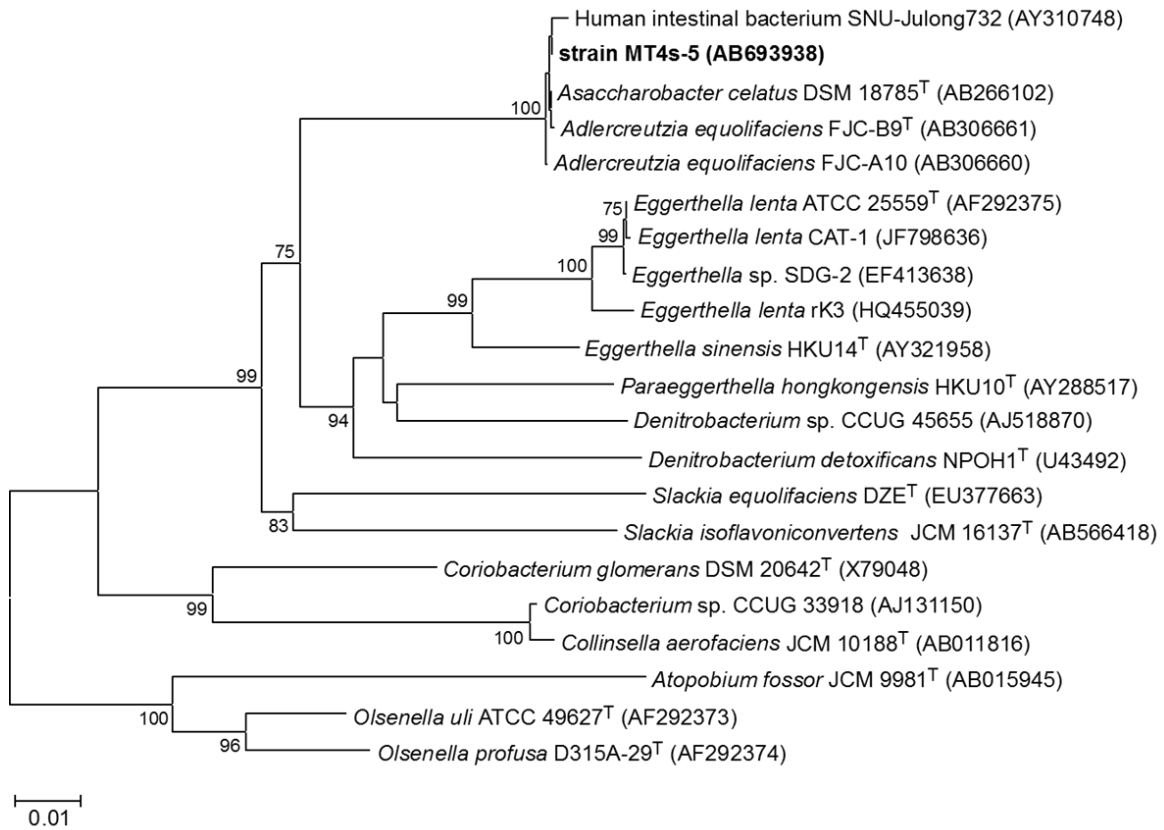
Figure 4-1 Phylogenetic tree showing the relationship between strain MT4s-5 and some related taxa. The tree was constructed by using neighbour-joining method based on 16S rRNA gene sequences. For the phylogenetic analysis, 1250 bp of each sequence were used. Bootstrap values (>70 %) based on 1000 replications are listed as percentages at branching points. Bar 0.01 substitutions per nucleotide position. Numbers in parentheses are GeneBank accession numbers
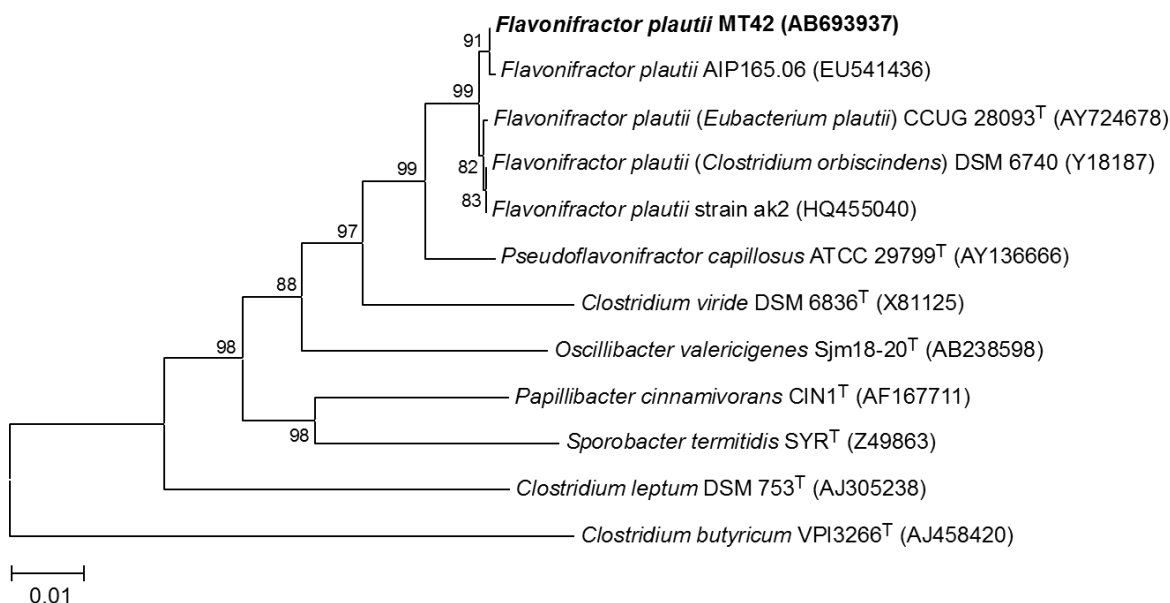
52

Figure 4-2   Phylogenetic tree showing relationships between strain MT42 and some related taxa. The tree was constructed by using neighbour-joining method based on 16S rRNA gene sequences. For the phylogenetic analysis, 1386 bp of each sequence were used. Bootstrap values (> 70 %) based on 1000 replications are listed as percentages at branching points. Bar 0.01 substitutions per nucleotide position. Numbers in parentheses are GeneBank accession numbers

Isolation and Identification of a Bacterium Capable of Degrading BM3

Adlercreutzia equolifaciens MT4s-5 have found capable of opening between the 1 and 2 position of C ring of EGC to yield metabolite **BM3**, but there was no further degradation of **BM3**. Then next screening of enteric bacteria was targeted to the bacterium which is capable of degrading **BM3** from rat feces, and finally the author was successed isolation a strain MT42. The 16S rRNA gene sequence of strain MT42 was shown to be almost identical to that of *Flavonifractor plautii* strains such as AIP 165.06 (EU541436, 99.9 % similarity), CCUG 28093 (AY724678, 99.7 % similarity), aK2 (HQ455040, 99.5 % similarity) and DSM 6740 (Y18187, 99.5 % similarity). Therefore, strain MT42 was identified as *Flavonifractor plautii* (AB693937). Figure 3-2 illustrates the phylogenetic tree showing relationships between strain MT42 and some related taxa, based on 16S rRNA gene sequences. Among *F. plautii* strains, strains aK2 and DSM 6740 have been reported to have similar degrading ability to strain MT42 (65).

Biotransformation of EGC by Isolate MT4s-5 strain and *Eggerthella lenta* JCM 9979

Strain MT4s-5 was incubated in GAM broth at 37ºC anaerobically containing 1mM EGC. One mL of the GAM broth culture was taken every 24 hours and applied for centrifugation to

remove the bacterial cells. The resulting supernatant was applied for LC-MS analysis for structural identification, and for LC-MS/MS was conducted to quantification as indicated in "Materials and Methods" section in Chapter 3. Metabolites **BM3**, **BM4**, and **BM8** were detected and their formations along with incubation time and MS and MS/MS data are shown in Figure 4-3. The major **BM3** had almost the same HPLC retention time, UV spectra, and MS and MS/MS data as those of the reference standard 1-(3, 4, 5-trihydroxyphenyl)-3-(2, 4, 6-trihydroxyphenyl)propan-2-ol, and ^{1}H- and ^{13}C-NMR spectra of **BM3** were superimposable to those of the reference standard (data not shown). Metabolite **BM3** was therefore confirmed to be the same compound as the reference standard. In the same way, other metabolites **BM4** and **BM7** as shown in Figure 4-3 were also isolated and their structures were determined by comparing HPLC retention time, UV spectra, and MS, MS/MS and NMR data of the two metabolites with those of reference standards. Finally, **BM4** and **BM7** were identified as 1-(3, 5-dihydroxyphenyl)-3-(2, 4, 6-trihydroxyphenyl)propan-2-ol and 4'-dehydroxylated EGC [(2S, 3S)-flavan-3, 3', 5, 5', 7-pentol], respectively. Optical rotation value of the latter was observed to be $[\alpha]^D_{20}$ -51.4° (c 0.49, methanol). With regard to the formation of the above metabolites, strain MT4s-5 was observed to produce **BM3** as a major metabolite decreasing with EGC and also after prolonged incubation, to form a small amount of **BM4** (Figure 4-3). Further, this strain could also catalyze 4'-dehydroxylation of EGC and produced some quantity of **7**.

Wang *et al* (52) have reported that *Eggerthella* sp. SDG-2, which was identified by Jin *et al* (66), catalyzed the ring-opening reaction of EGC, followed by 4'-dehydroxylation to yield **BM3**. The enterobacteria *Eggerthella lenta* JCM 9979 (=ATCC 25559) was purchased, a closely related bacterial strain to strain SDG-2 (99.9 % 16S rRNA gene sequence similarity), and examined its ring-opening ability on EGC. Strain JCM 9979 was shown to transform EGC to **BM3** (Figure 4-4) as well as the isolate MT4s-5 and *Eggerthella* sp. SDG-2 (52). However, while strains MT4s-5 and SDG-2 could catalyze the 4'-dehydroxylation to form metabolite **BM4,** strain JCM 9979 could not. (Figure 4-2, 4-3, 4- 4).
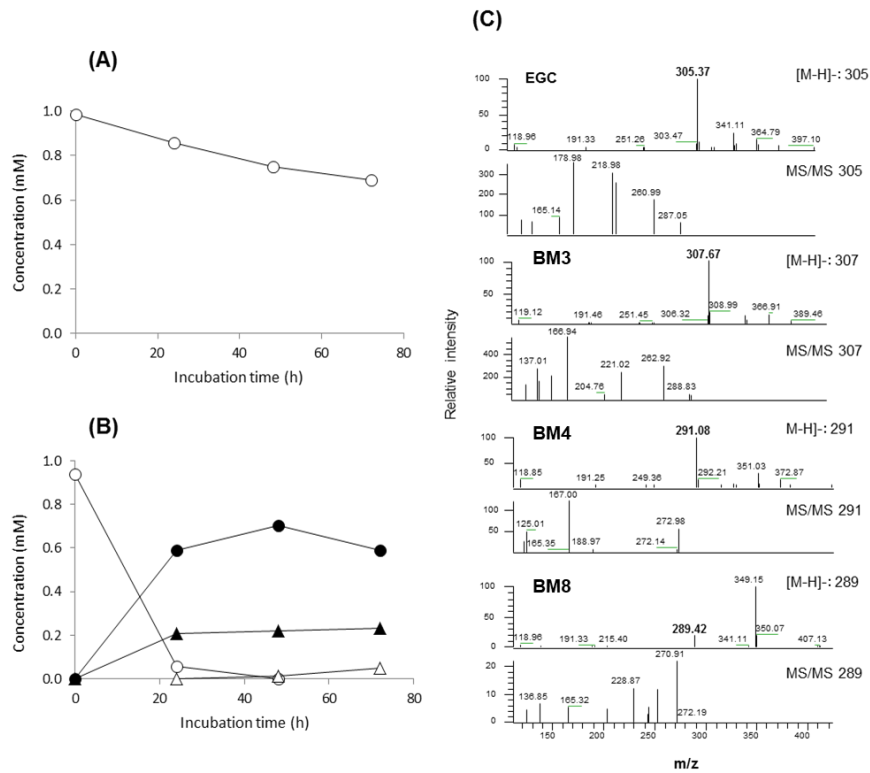
Figure 4-3 Biotransformation of EGC (○) to **BM3** (●), **BM4** (△), and **BM8** (▲) by strain MT4s-5 and their MS and MS/MS spectra.

　(A) without the bacterium (control), (B) in the presence of the bacterium, (C) MS and MS/MS spectra of EGC and its metabolites
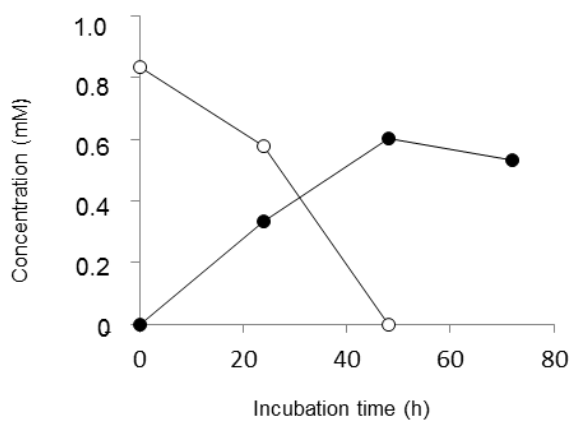

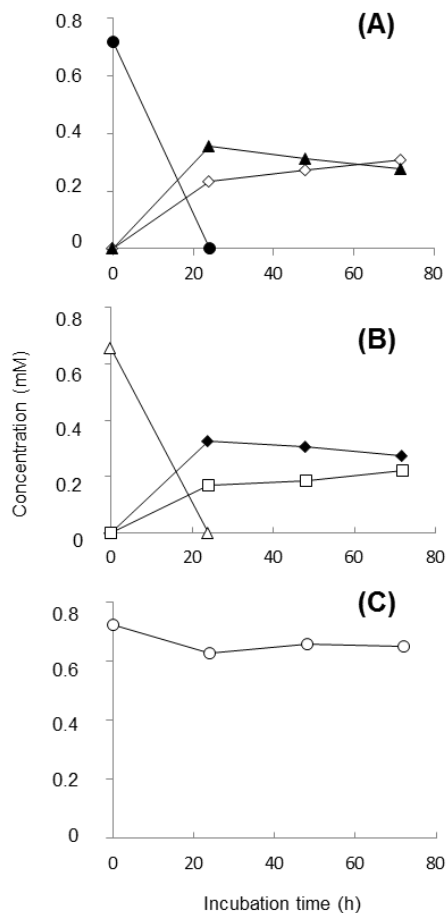**Figure 4-4**　Biotransformation of EGC by *Eggerthella lenta* JCM 9979. EGC (○), **BM3** (●)

Figure 4-5. Degradation of BM3 (A) and BM4 (B), and EGC (C) by strain MT42. EGC (○), BM3(●), BM4 (△), BM9 (▲), BM10(◇), BM5 (◆), BM6 (□)

Biotransformation of BM3 and BM4 by Isolate MT42 and Its Closely Related Bacteria and Identification of their Products

Flavonifractor plautii MT42 was separately incubated with **BM3, BM4**, and EGC, and then each culture filtrate was analyzed under the LC-MS system. From strain MT42 metabolites **BM9** and **BM10** from **BM3** were produced. Similarly, this strain transformed **BM4** into metabolites **BM5** and **BM6**. This author isolated the above metabolites produced from **BM3** and **BM4** at first and determined their structural features based on HPLC retention times, and UV spectra, MS, MS/MS and NMR data. These data of metabolites **BM9** and **BM10** were superimposable to those of the respective reference standards, 4-hydroxy-5-(3′, 4′, 5′-trihydroxyphenyl)valeric acid and 5-(3′, 4′, 5′-trihydroxyphenyl)-γ-valerolactone (data not shown). Structures of **BM5** and **BM6** were determined in the same way as described for **BM9** and **BM10**. Finally, the metabolites **BM9**, **BM10**, **BM5**, and **BM6** were identified as 4-hydroxy-5-(3′,   4′,   5′-trihydroxyphenyl)valeric   acid,   5-(3′,   4′,

5′-trihydroxyphenyl)-γ-valerolactone, 4-hydroxy-5-(3′, 5′-dihydroxyphenyl)valeric acid and 5-(3′, 5′-dihydroxyphenyl)- γ-valerolactone, respectively. Furthermore, metabolite formation from **BM3**, **BM4**, and EGC was quantitatively determined using the LC-MS/MS system. The results are shown in Figure 4-5. It was thought that strain MT42 simultaneously produced **BM9** and **BM10** from **BM3**, and **BM5** and **BM6** from **BM4**. However, strain MT42 could not convert EGC and **BM8** (data not shown). These results implied that *F. plautii* MT42 had the ability to decompose the compounds having phloroglucinol moiety.

The author further investigated whether or not other bacterial strains closely related to *F. plautii* MT42 had similar phloroglucinol-decomposing ability. On the basis of the similarity of 16S rRNA gene sequence to strain MT42, *F. plautii* strains ATCC 29863 (formerly *Eubacterium plautii*) and ATCC 49531 (formerly *Clostridium orbisciendens*) were obtained as commercially available strains and the ability of the two strains to degrade metabolites **BM3** and **BM4** was tested. As shown in Figure 4-6, the two strains were found to transform **BM3** into **BM9** and **BM10**, and **BM4** into **BM5** and **BM6** in a similar way as strain MT42. Kutschera *et al* (68) have reported that *F. plautii* strains aK2 and DSM 6740 (same strain as ATCC 49531 used in this study) catalyzed the conversion of 1-(3, 4-dihydroxyphenyl)-3-(2, 4, 6-trihydoxyphenyl)propan-2-ol to 4-hydroxy-5-(3′, 4′-dihydroxyphenyl)valeric acid and 5-(3′, 4′-dihydroxyphenyl)- γ-valerolactone. Therefore, it seems likely that *F. plautii* strains generally have the decomposing ability of phloroglucinol moiety regardless of the difference in the number of hydroxyl group in the aromatic B ring of 1-hydroxyphenyl-3-(2, 4, 6-trihydoroxyphenyl)propan-2-ols.
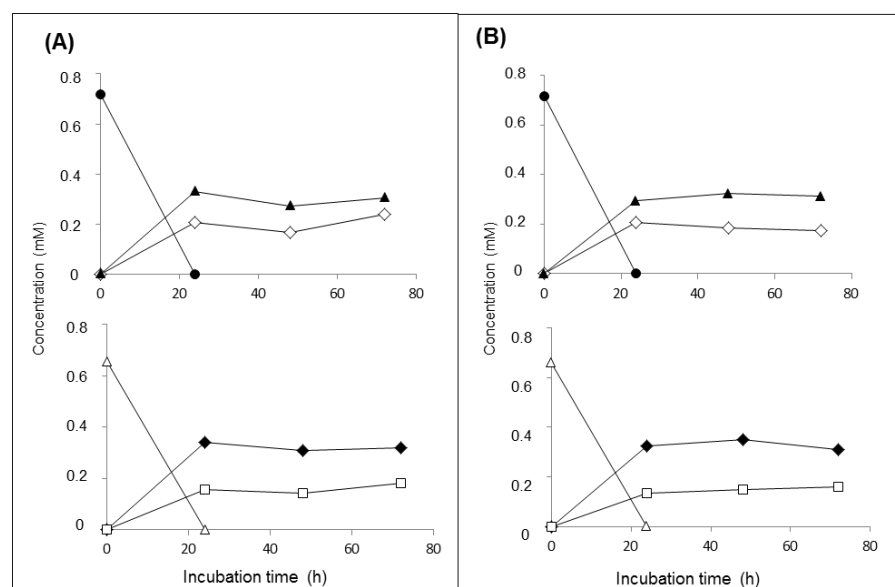

Figure 4-6. Degradation of BM3 and BM4 by *F. plautii* strains ATCC 29863 (A) and ATCC 49531 (B). **BM3 (●), BM4 (△), BM10(▲), BM9(◇), BM5 (◆), BM6 (□)**

Biotransformation of EGC by Strain MT4s-5 and *Eggerthella lenta* JCM 9979 in the Presence of Symbiotic Bacteria

During the process of isolating EGC-degrading bacteria from rat feces, the bacterial mixture containing isolate MT4s-5 was observed to quickly convert EGC into metabolite **BM4**. Two different bacteria were eventually isolated from the above bacterial mixture. One was tentatively identified as *Ad.equolifaciens* MT4s-5, as described above, and another one as *Escherichia coli* MT4s-3 due to 16S rRNA gene sequence of strain MT4s-3 exhibiting 99.8 % similarity to that of *E. coli* ATCC 11775 (type strain). Of the two isolates, only strain MT4s-5 could biotransform EGC to yield **BM3**, **BM4**, and **BM8** (Fig. 4-3). However, the formation of **BM4** by this strain was observed to be much lower than that formed by the bacterial mixture containing at least strains MT4s-5 and MT4s-3 (data not shown). From these observations, it was predicted that the full potential ability of strain MT4s-5 to convert EGC to **BM4** could be achieved when in coexistence with isolate MT4s-3. To clarify this supposition, co-cultivation of strain MT4s-5 with *E.coli* MT4s-3 was performed in GAM broth containing **BM3** 1 mM EGC and metabolite formation was examined. Strain MT4s-3 was found to make the formation of **BM4** by strain MT4s-5 proceed more easily as shown in Figure 4-7A. In addition to strain MT4s-3, formation of **BM4** was also facilitated by *E.coli* K-12 (Figure 4-7A). The results revealed that *E.coli* strains stimulated the 4'-dehydroxylation reaction catalyzed by strain MT4s-5, to produce **BM4** from **BM3,** and therefore they functioned as symbiotic bacteria.

Even though *Eg.lenta* JCM 9979 was found to catalyze only the transformation of EGC to **BM3** (Figure 4-4), the formation of **BM4** by this strain was examined in co-cultivation of strain JCM9979 with *E.coli* strains K-12 or MT4s-3. Interestingly, it was discovered that strain JCM 9979 had the ability to catalyze the conversion of EGC into **BM4** in the presence of *E. coli* strains (Figure 4-7B). These results indicated that strain JCM 9977 had the potential ability to catalyze 4'-dehydroxylation of **BM3** and this ability could be achieved in coexistence with symbiotic bacteria. Thus, symbiotic bacteria are considered to play an important role in the catabolism of EGC and EGCG.

Further screening of symbiotic bacteria involved in the conversion of EGC to **BM4** was conducted by the author. Finally, two bacterial strains were isolated from rat feces and identified as *Butyricimonas synergistica* MT01 (= JCM 15148 = CCUG 56610) and *Butyricimonas viosa* MT12 (= JCM 15149 = CCUG 56611) (53). Strains MT4s-5 and JCM 9979 were cocultured with each strain of MT01 and MT12 in GAM broth containing EGC to examine the formation of **BM4** from EGC. Similar results as shown in Figure 4-7 were observed in the experiments (data not shown) and hence strains MT01 and MT12 were confirmed to act as symbiotic bacteria.
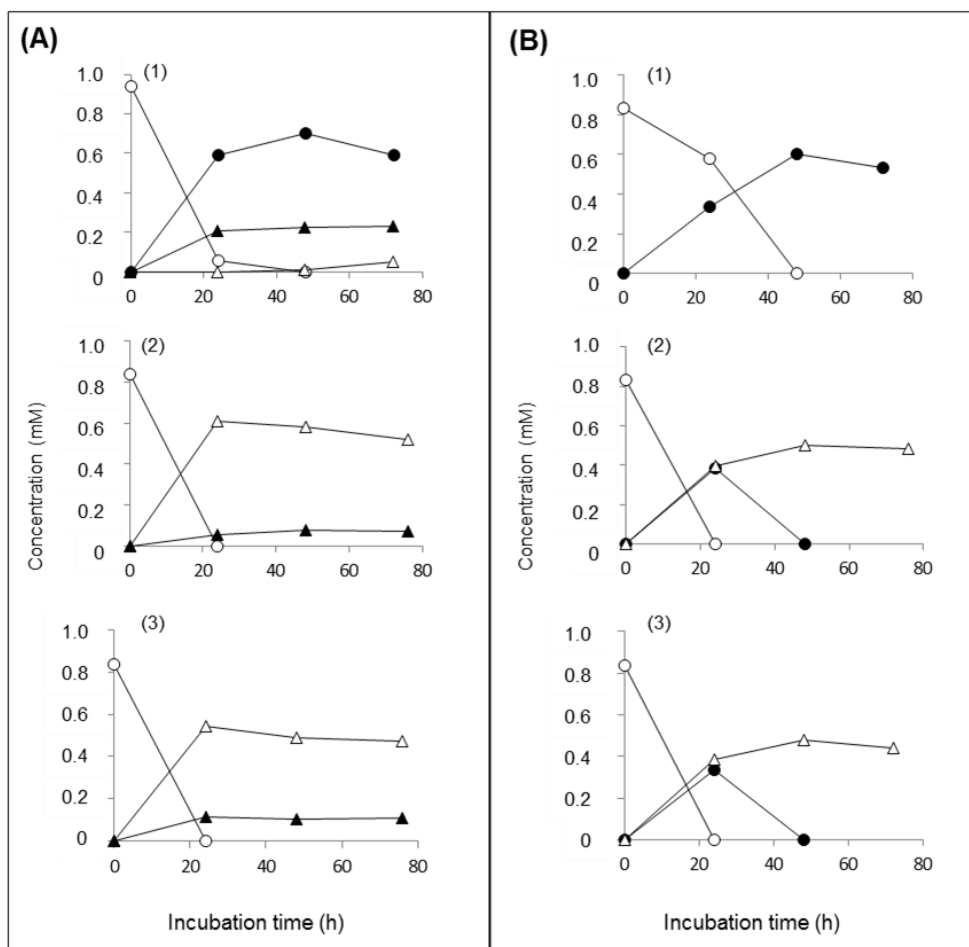
Figure 4-7 Conversion of EGC to BM4 by strains MT4s-5 (A) and JCM 9979 (B) in the presence of symbiotic bacteria, *E. coli* strains MT4s-3 and K-12. (1) without symbiotic bacteria, (2) in coculture with E. coli MT4s-3, (3) in coculture with *E. coli* K-12. EGC (○), BM3 (●), BM4 (△) BM8 (▲)

Biotransformation of EGC to BM4 by strain MT4s-5 and *Eggerthella lenta* JCM 9979 in the Presence of Hydrogen or Formate

Furthermore, the author examined the condition(s) which strains MT4s-5 and JCM 9979 require for converting metabolite **BM3** into **BM4**. Strain MT4s-5 and the symbiotic bacterial strains (MT01, MT02 and MT4s-3) were incubated with a culture vessel physically, which is separated into two partitions A and B by a membrane filter (0.2 μm). The strains MT4s-5 and either one of the symbiotic bacteria were inoculated separately into the partitions A and B, and were cultured under anaerobic condition. The same method was also used with strain JCM 9979. After centrifugation of the culture, the resulting supernatant was analyzed using LC-MS/MS system. While both strains rapidly produced **BM4** from EGC, they did not produce **BM3** (data not shown), suggesting that the two strains require some substance(s)

which is produced by the symbiotic bacteria. The author further attempted to determine the condition(s) which is produced by the symbiotic bacteria. Experiments by Krumholz and Bryant (83) have already reported that *Eubacterium oxidoreducens* G41 could degrade pyrogallol in the presence of supernatant fluids of either anaerobically grown G44 strain or *E. coli*, and that H_2 or formate could replace the supernatant fluids of the strain G44 or *E. coli*. It was also demonstrated that the strain G41 catabolized gallate and phloroglucinol in the presence of formate or hydrogen. Exocellular electron transfer is well known to play an important role in anaerobic microbial communication and interspecies hydrogen transfe among anaerobic microorganisms is one of the driving effector for degradation of organic compounds (84). Accordingly, strains MT4s-5 and JCM 9979 were separately cultured in GAM broth containing 1mM EGC in the presence of either one of electron donor candidates as written in "Materials and Methods" section. As a result, it was found that strain MT4s-5 could transform EGC into metabolite **BM4** rapidly in the presence of hydrogen and strain JCM 9979 could catalyze the transformation in the presence of either hydrogen or formate. These results were in agreement with those obtained in co-culture with symbiotic bacteria as shown in Figure 4-7. Yet, other electron donor candidates showed no effects. These observations indicated that symbiotic bacteria supplied hydrogen and/or formate to the EGC-degrading bacteria. The author further looked at whether or not symbiotic bacterial isolates, *B. synergistica* MT01, *B. viosa* MT12, and *E.coli* strains MT4s-3 and K-12, actually produced hydrogen and/or formate. These bacteria individually incubated in GAM broth at 37 ºC for 24 h, were analyzed by GC and CE systems, respectively, for the presence of hydrogen and formate in the culture fluid. The experimental results showed that hydrogen was produced by all of the four symbiotic bacteria and formate by *E. coli* strains (Table 4-2). Therefore, it was determined that strains MT4s-5 and JCM 9979 converted EGC into **BM3** and subsequently metabolite **BM3** into **BM4** by utilizing hydrogen and/or formate.

Dehydroxylation of Metabolites BM3, BM9, and BM10 by Strain MT4s-5 and *Eggerthella lenta* JCM 9979

Further examination whether or not strains MT4s-5 and JCM 9979 could cause *p*-dehydroxylation of pyrogallol moiety of **BM3**, **BM9** and **BM10** was investigated. It was determined that strain MT4s-5 catalyzed the *p*-dehydroxylation of **BM3**, **BM9**, and **BM10** to produce **BM4**, **BM5**, and **BM6**, respectively (Fig. 4-8A). The dehydroxylation reaction by the strain was also observed to be stimulated by the presence of symbiotic bacterial strain MT01 (Fig. 4-8 B) or hydrogen (Fig. 4-8C). Similar results were obtained with other symbiotic bacteria (data not shown), but formate did not exhibit acceleration effects (Fig. 4-8D). These results showed that strain MT4s-5 had the ability to catalyze the *p*-dehydroxylation reaction of the metabolites and required the hydrogen supplied by symbiotic bacteria for stimulation of

the reaction. On the other hand, while strain JCM 9979 alone could not catalyze the *p*-dehydroxylation of **BM3**, **BM9**, and **BM10** (Fig. 4-9A), in the presence of strain MT12 it rapidly catalyzed the *p*-dehydroxylation of these metabolites (Fig. 4-9B). Similar results were also observed with other symbiotic bacteria (data not shown). The dehydroxylation process readily progressed in the presence of either hydrogen or formate (Figs. 4-9C and 4-9D). From these results it is clear that strain JCM 9979 required at least either hydrogen or formate as an electron donor in order to catalyze the dehydroxylation reaction of metabolites **BM3**, **BM9**, and **BM10**.

Table 4-2 Concentrations of formate and hydrogen produced by symbiotic bacteria

Bacterial strains	Formate (mM) [a]	Hydrogen (%) [b]
E. coli MT4s-3	18.0	9.4
E. coli NBRC 3301	23.0	8.1
B. synergistica MT01	ND [c]	4.2
B. virosa MT12	ND [c]	3.9

a Formate concentrations in the incubation mixtures 24 h after cultivation were quantitated. *b* Hydrogen gas concentrations (%) of headspace gasses in the culture tubes were determined after an incubation time of 24 h. *c* ND; not detected

Table 4-3   Isoflavone-metabolizing bacteria used in this study

bacterium	No. of JCM	Refferences	
S. equolifaciens DZE	JCM 16059	*Int J Syst Evol Microbiol* 58,1721-	(2010)
S. isoflavoniconvertens HE8	JCM 16137	*Appl Environ Microbiol* 75, 1740-	(2009)
Ad. equolifaciens FJC-B9	JCM 14793	*Int J Syst Evol Microbiol* 58,1228-	(2008)
As. celatus do3	JCM 14811	*Int J Syst Evol Microbiol* 58, 1238-	(2008)

All listed bacteria are commercially available. The supplier is listed in Material & Method.
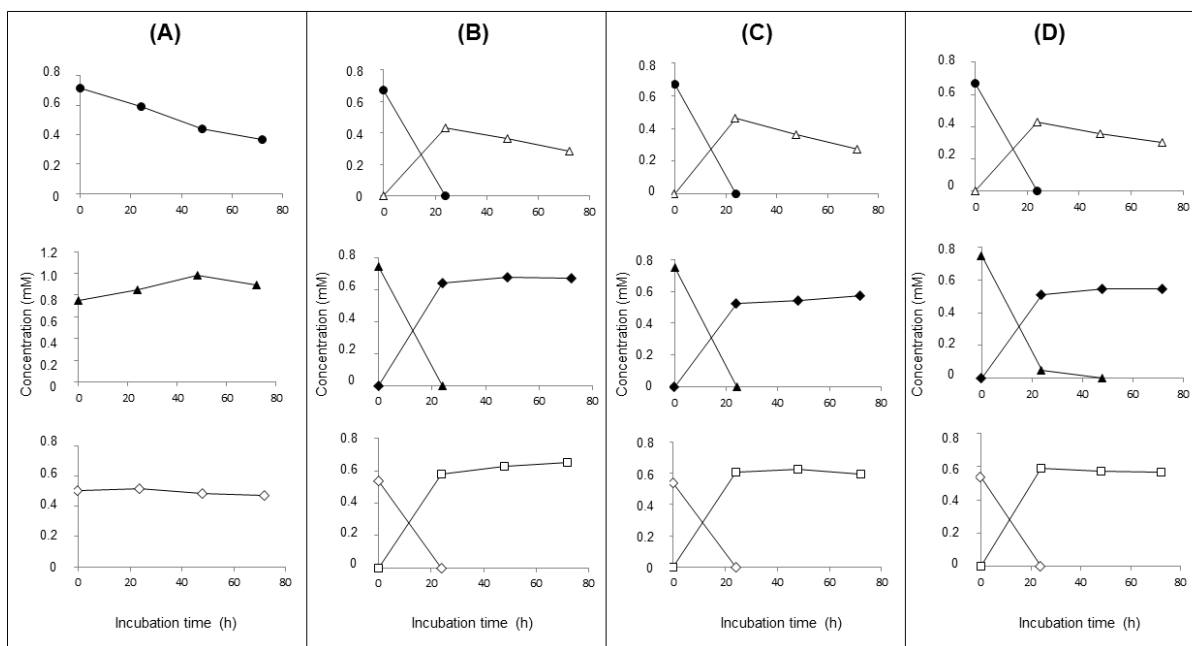
Figure 4-8. p-Dehydroxylation of **BM3**, **BM10**, and **BM9** by *Ad.equolifaciens* MT4s-5. (A) strain MT4S-5 alone (B) in coculture with *B. synergistica* MT01, (C) addition of hydrogen, (D) addition of formate. **BM3** (●), **BM4** (△), **BM10** (▲), **BM9** (◇), **BM5** (◆), **BM6** (□)
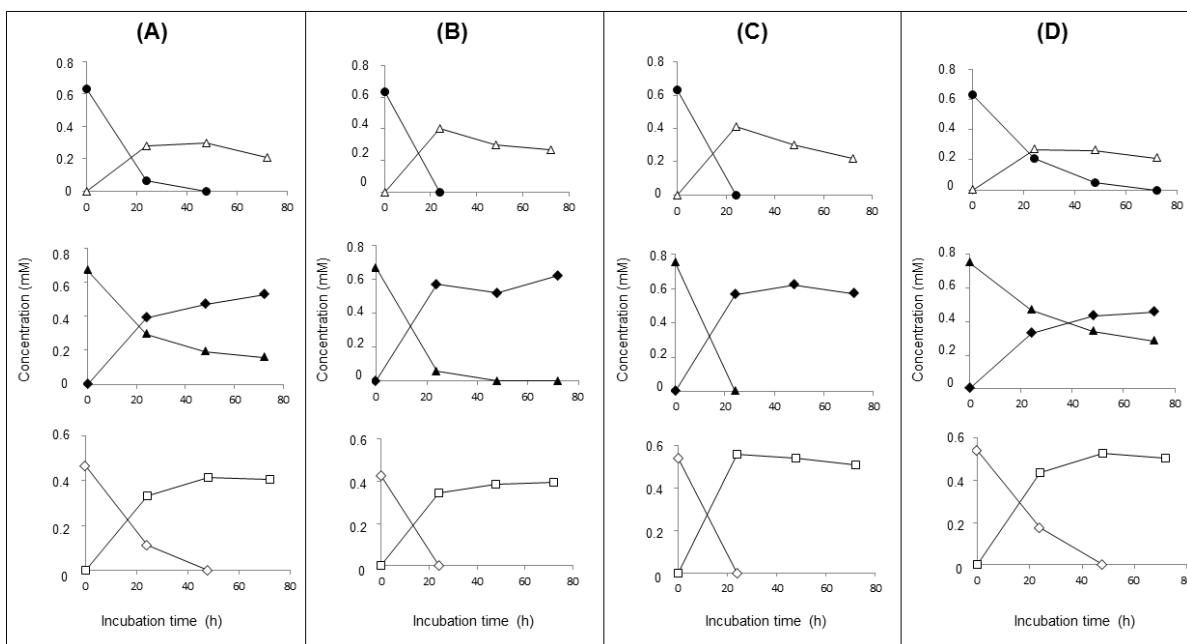

Figure 4-9. p-Dehydroxylation of **BM3**, **BM9**, and **BM10** by *Eg.lenta* JCM 9979. (A) strain JCM 9979 alone (B) in coculture with *B. virosa* MT12, (C) addition of hydrogen, (D) addition of formate. **BM3** (●), **BM4** (△), **BM9** (▲), **BM10** (◇), **BM5** (◆), **BM6** (□)

Biotransformation of EGC and GC by Isoflavone-metabolizing Bacteria

This author examined whether or not four isoflavone-metabolizing bacterial strains possessed the ability to degrade EGC. Isoflavone-metabolizing bacteria used in this Chpter are listed in Table 4-3. *Adlercreutzia equolifaciens* JCM 14793, *Asaccharobacter celatus* JCM 14811, and *Slackia equolifaciens* JCM 16059 were shown to have catalyzed the biotransformation of EGC, but *Slackia isoflavoniconvertens* JCM 16137 could not (Figure 4-10).

In *Ad. equolifaciens* JCM 14793, EGC was transformed into **BM8** and there was strong stimulation of this conversion in the presence of hydrogen (Fig. 4-10A). *As. celatus* JCM 14811 mainly produced **BM8** from EGC, along with a minor amount of **BM3** (Fig. 4-10B). In the presence of hydrogen, strain JCM 14811 could convert **BM3** into **BM4** and the increase in the C ring-cleaving product was proportionally higher as compared with that produced without hydrogen (Fig. 4-10B). *S. equolifaciens* JCM 16059 catalyzed only the C ring-cleaving reaction of EGC forming **BM3,** regardless of whether or not hydrogen was present (Figs. 4-10C), and the reaction was found to be very slow but was stimulated to some degree by hydrogen (Fig. 4-10C). On the other hand, unlike strains JCM 14793 and JCM 14811, strain JCM 16059 did not show any ability to catalyze 4'-dehydroxylation of **BM3**.

Dehydroxylation of BM3, BM9, and BM10 by Isoflavone-Metabolizing Bacteria

TThe dehydroxylation reaction of **BM3**, **BM9**, and **BM10** by the four isoflavone-metabolizing bacteria was examined further by the author. From results it was determined that *Ad. equolifaciens* JCM 14793 and *As. celatus* JCM 14811 could catalyze *p*-dehydroxylation of the pyrogallol moiety in **BM3**, **BM10**, and **BM9**, but *S. equolifaciens* JCM 16059 and *S. isoflavoniconvertens* JCM 16135 could not.

Ad. equolifaciens JCM 14793 converted **BM3** to **BM4** very slowly but this transformation was stimulated by hydrogen (Fig. 4-11B). Strain JCM 14793 also facilitated *p*-dehydroxylation of **BM9** and **BM10** to produce **BM5** and **BM6**, respectively, and the dehydroxylation was stimulated in the presence of hydrogen (Fig. 4-11B).

As. celatus JCM 14811 could catalyze the dehydroxylation of **BM3** to form **BM4** and the dehydroxylation was accelerated to some degree by hydrogen (Fig. 4-11C). Strain JCM 14811 also transformed **BM9** and **BM10** into BM**5** and BM**6,** respectively, and these conversions were enhanced in the presence of hydrogen, as they were too in the case of *Ad. equolifaciens* JCM 14793.
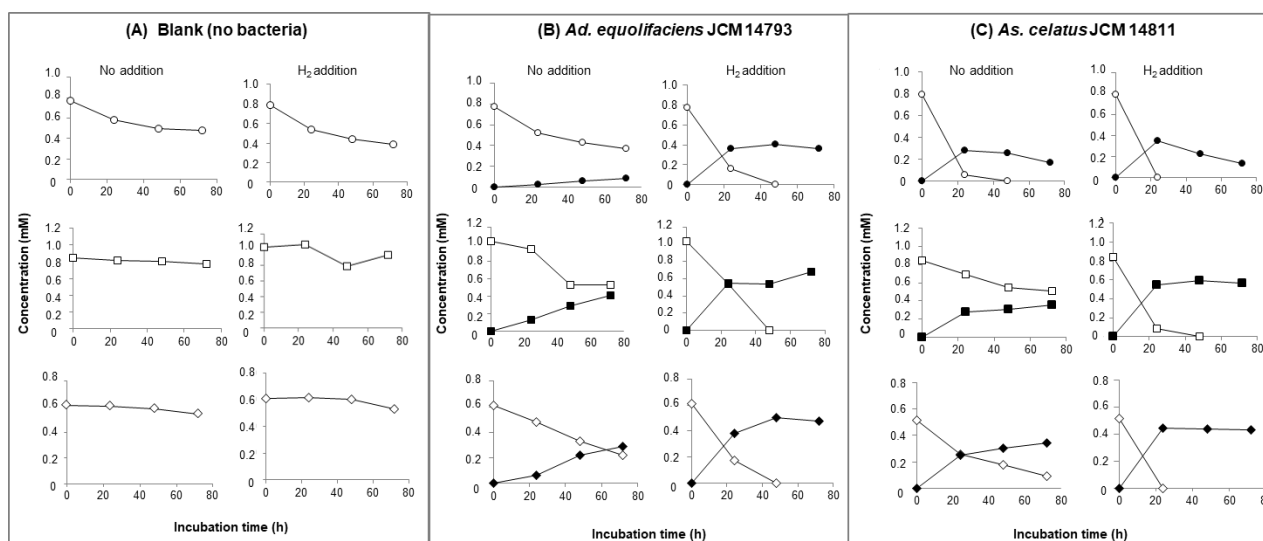
Figure 4-10 Conversion of EGC by *Ad. equolifaciens* JCM 14793, As. celatus JCM 14811, and *S. equolifaciens* JCM 16059EGC (○), **BM3**(□), **BM4** (■), and **BM8** (◊).
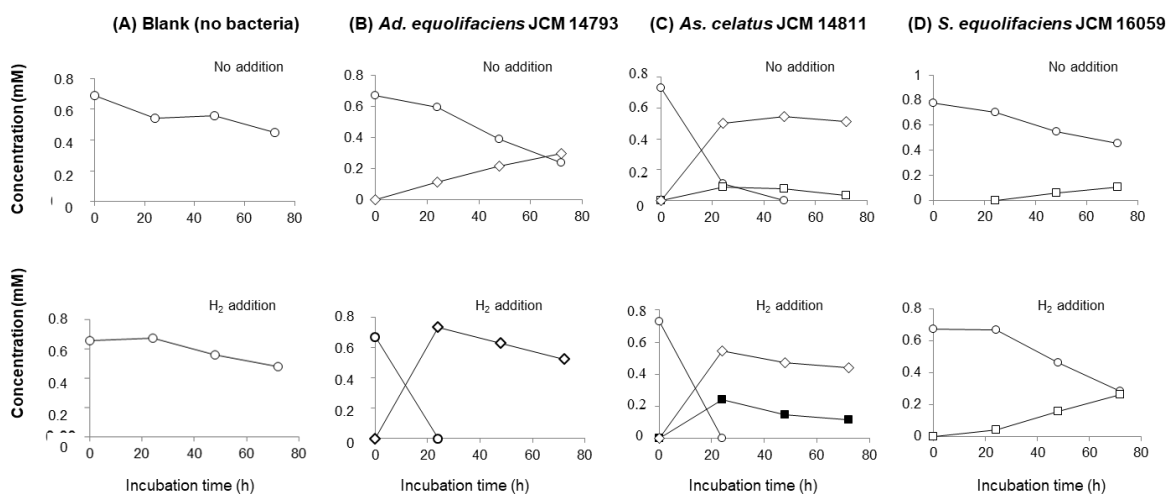

Figure 4-11. Dehydroxylation of **BM3**, **BM4**, and **BM10** by *Ad. equolifaciens* JCM 14793 and *As. celatus* JCM 14811, **BM3** (○), **BM4** (●), **BM9** (□), **BM10** (◊), **BM5** (■), and **BM6** (♦).

64
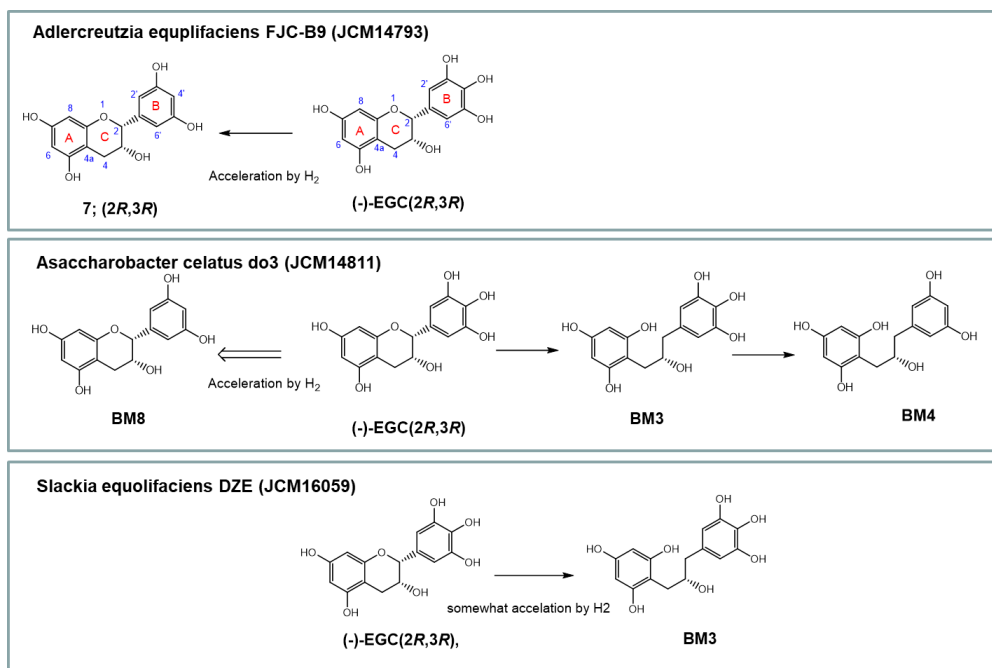
Figure 4-12 EGC metabolism by isoflavone-metabolizing bacteria.

DISCUSSION

Wang *et al* (52) first reported that *Eggerthella* (formally *Eubacterium*) sp. SDG-2 transformed EGC and EC into their corresponding 1, 3-diphenylpropan-2-ols, and the propan-2-ols formed underwent 4'-dehydroxylation of the B ring. Jin and Hattori (67) further reported that *Eggerthella* sp. CAT-1, which is very similar in 16S rRNA gene sequence to strain SDG-2, biotransformed EC and C, producing their corresponding 1, 3-diphenylpropan-2-ols, and had the ability to catalyze continuously 4'-dehydroxylation of the propan-2-ols. Kutschera *et al* (68) have recently shown that *Eggerthella lenta* rK3 is capable of catalyzing the ring-cleaving of EC and C, producing their corresponding 1, 3-diphenylpropan-2-ols, and further that *Flavonifractor plautii* strains aK2 and DSM 6740 are capable of simultaneously producing 4-hydroxy-5-(3′, 4′-dihydroxyphenyl)valeric acids and 5-(3′, 4′-dihydroxyphenyl)-γ-valerolactones from the above propan-2-ols. In this study, the author isolated two bacterial strains, *Ad.equolifaciens* MT4s-5 and *F. plautii* MT42, from rat feces. Strain MT4s-5, as well as *Eggerthella* sp. SDG-2, catalyzed the ring-opening reaction of EGC, producing its corresponding metabolite **BM3** (Figure 4-3) (52). This ring-opening reaction was also found to be catalyzed by *Eg.lenta* JCM 9979 which is commercially available (Figure 4-4). However, in addition to the production of metabolite **BM3,** strain MT4s-5 was also capable of catalyzing the conversion of EGC into **BM8**. Eamination

65

whether or not **BM8** as a substrate further underwent ring cleavage by strains MT4s-5 and JCM 9979 was conducted, and found these two strains could not catalyze ring-cleaving reaction of **BM8** (data not shown), suggesting that for the ring cleavage of ECC by these strains, it is the 4'-hydroxyl group that is important. Wang *et al* (52) already observed that since 4'-methylated EGC was not biotransformed by *Eggerthella* sp. SDG-2, the presence of free 4'-hydroxyl group of catechins appears to be necessary for ring cleavage of EGC. Accordingly, it was assumed that the presence of 4'-hydroxyl group at the B ring of catechins is essential for their ring cleavage by catechin-degrading bacteria. Furthermore, we have discovered that *Ad.equolifaciens* MT4s-5 has the ability of transforming daidzein into equol (82) as do some *Ad.equolifaciens* strains which were reported to show isoflavone metabolizing ability (70). These observations led us to speculate that *Ad.equolifaciens* strains which possess the ability to metabolize isoflavones, also show catechin-metabolizing capability.

Metabolite **BM3** was further transformed into its corresponding **BM9** and **BM10** by *F. plautii* MT42 (Figure 4-5) as well as with *F. plautii* strains aK2 and DSM 6740 (68). Commercially available *F. plautii* strains ATCC 29863 and ATCC 49531 also degraded the phloroglucinol moiety of **BM3** (Figure 4-6). Furthermore, these three strains can convert **BM4** into its corresponding **BM5** and **BM6** simultaneously. Actually, *F. plautii* ATCC 49631 could be expected to be capable of degrading the phloroglucinol moiety of 1-(3, 4-dihydroxyphenyl)-3-(2, 4, 6-trihydroxyphenyl)propan-2-ol derived from EC and C because strain ATCC 49631 is the same strain as DMS 6740 reported by Kutschera *et al* (68). These observations possibly suggest that *F. plautii* strains have the ability of degrading the phloroglucinol moiety regardless of the number and positions of hydroxyl groups in B ring of the 1, 3-diphenylpropan-2-ols. Therefore, it is thought to be most likely that *F. plautii* ak2 degrades metabolites **BM3** and **BM4** as well as 1-(3, 4-dihydroxyphenyl)-3-(2, 4, 6-trihydroxyphenyl)propan-2-ol from EC and C. All considered, it can be expected that *F. plautii* strains generally have the ability capable of degrading compounds which possess phloroglucinol moiety.

The author was the first to reveal that the 4'-dehydroxylation following the ring cleavage of EGC by strains MT4s-5 was accelerated remarkably by co-cultivation with symbiotic bacteria such as *Butyricimonas synergistica* MT01 (JCM 15148), *B. virosa* MT12 (JCM 15149), and *E.coli* MT4s-3 and K-12; and that dehydroxylation by strain JCM 9979 occurred only in a mixed culture of the symbiotic bacteria (Figure 4-7). The author further confirmed that the dehydroxylation by strain MT4s-5 was stimulated in the presence of hydrogen and the reaction by strain JCM 9979 proceeded only in the presence of either hydrogen or formate. It was also determined that hydrogen was produced by all the symbiotic bacteria, while two of them also produced formate (Table 4-2). From these findings it is clear that the

EGC-degrading bacteria caused reductive degradation of EGC by utilizing the hydrogen and/or formate supplied by the symbiotic bacteria. Such symbiotic relationships are commonly known of in anaerobic microbial communities and the transfer of hydrogen is termed interspecies hydrogen/formate transfer. An example representative of this is the interspecies hydrogen transfer between methanogens and hydrogen-producing bacteria where the hydrogen transfer is a key process for methanogenesis. This study also revealed the important role interspecies hydrogen/formate transfer may play in the catabolic processes of EGC, where EGC-degrading bacteria are working in partnership with hydrogen/formate-producing bacteria. In relation to this, Decroos *et al* (85) reported that equol production from isoflavone daidzein by an equol-producing bacterial consortium (EPC4 containing at least 4 different bacteria) was induced to a large extent by hydrogen. Recently, Bolca and Verstraete (86) reported that in the co-culture of EPC4 and a methanogenic or a sulfate-reducing bacterium, EPC4 significantly suppressed methane or hydrogen sulphide production in the presence of soy germ powder, a source of daidzein. In their results, they discussed how the beneficial health effects of soy consumption seem to be mainly attributable to equol production which reduces methane and hydrogen sulphide that are negatively associated with health. In this study, the author has determined that hydrogen was utilized by the EGC-degrading bacteria, strains MT4s-5 and JCM 9979. From such observations, it may be expected that the EGC-degrading bacteria reduce methanogenesis and sulphidogenesis in the presence of catechins as does ECP4 (the equol-producing bacterial consortium). In fact, there have been reports that human fecal sulfide significantly decreased 21 days following administration of catechin mixture in elderly residents under enteral feeding (87).

Additionally, the author investigated whether or not strain MT4s-5 had the capability of catalyzing 4'-dehydroxylation in the B ring of metabolites **BM3**. Unexpectedly, strain MT4s-5 easily catalyzed the dehydroxylation of **BM3** to form **BM4** (Fig. 4-8A) while on the other hand there was little production of **BM4** via **BM3** from EGC (Fig. 4-3). However, strain MT4s-5 catalyzed smoothly both the ring cleavage of EGC and subsequent dehydroxylation of **BM3** to yield **BM4** in the presence of symbiotic bacteria or hydrogen (Fig. 4-7A). The author cannot clearly explain the reason for the above phenomena, but the following is a possible explanation. The same cofactor, e.g., NADH, NADPH, FADH$_2$, and coenzyme F420 etc., is used by strain MT4s-5 to catalyze both the ring cleavage of EGC and the dehydroxylation of **BM3.** There is a certain amount of this cofactor stored in the strain's grown cells, however, since the cofactor is consumed for the ring cleavage in the first step when EGC is used as a substrate, the dehydroxylation at the next step is strongly suppressed or ceased due to a lack of the cofactor. Then, on the other hand, in the presence of symbiotic bacteria or hydrogen the ring-cleaving of EGC and subsequent dehydroxylation by strain MT4s-5 progressed smoothly due to the strain regenerating the consumed cofactor by

67

utilizing hydrogen supplied by symbiotic bacteria. When metabolite **BM3** which already underwent the ring cleavage is used as a starting material, the strain easily catalyzes the conversion of **BM3** into **BM4**. This is because it still has a sufficient store of the cofactor in its cell. The above explanation can also be applied to the dehydroxylation by strain MT4s-5 of **BM9** and **BM10** to yield **BM5** and **BM6** (Fig. 4-8A).

Recently, Thawornkuno *et al* (88) reported that a crude enzyme preparation (culture supernatant) from *Asaccharobacter celatus* do03 (JCM 14811), with close similarity (99.9 %) of 16S rRNA gene sequence to strain MT4s-5, catalyzed the reduction of daidzein to dihydrodaidzein in the presence of the coenzyme NADPH, while another crude enzyme preparation (cell debris) caused reductive conversion of dihydrodaidzein into equol by utilizing this same coenzyme. These findings which show that two different enzymes are required the same coenzyme (NADPH) in their reactions, seem to concur with our explanation as discussed above. In the case of strain JCM 9979, it catalyzed the ring cleavage of EGC but there was no subsequent dehydroxylation of **BM3** at all (Fig. 4-4). Dehydroxylation by strain JCM 9979 did not occur at all even when metabolite **BM3** was used as starting material (Fig. 4-9A). It was only in the presence of either hydrogen or formate supplied by symbiotic bacteria, that the dehydroxylation took place (Figs. 4-9 B-D). The reason only strain JCM 9979 showed no progression to the dehydroxylation reaction may be that this strain catalyzes the ring cleavage of EGC with a cofactor existing in its grown cell but the subsequent dehydroxylation does not proceed because there is no availability of the cofactor in the cell for the dehydroxylation. An explanation for the rapid progress of the ring cleavage and subsequent dehydroxylation by strain JCM 9979 in the presence of the hydrogen or the formate, may be that the strain generates another cofactor which is available for the dehydroxylation by using either the hydrogen or the formate. This hypothesis could explain well enough the fact that dehydroxylation of **BM9** and **BM10** by strain JCM 9979 took place only in the presence of symbiotic bacteria or hydrogen and/or formate (Fig. 4-9). However, further study on other enzymes which catalyze the ring cleavage and dehydroxylation are needed to clarify the above phenomena.

Further, the author has demonstrated here that several isoflavone-metabolizing bacteria have the ability to biotransform EGC. Based on these results, the behavior of the isoflavone-metabolizing bacteria on bioconversion of EGC is shown in Figure 4-10. In *Ad. equolifaciens* JCM 14793, EGC underwent 4'-dehydroxylation to form **BM8**. *As. celatus* JCM 14811 catalyzed both 4'-dehydroxylation and C ring cleavage of EGC. It was found that the reaction site specificity of *Ad. equolifaciens* JCM 14793 and *As. celatus* JCM 14811 varied to some extent in the presence of hydrogen. However, *S. equolifaciens* JCM 16059 and *Ad. equolifaciens* MT4s-5 showed no reaction site specificity differences in the bioconversion of EGC, either with or without hydrogen. Thus the above observations indicated differences

exist in reaction site specificities among the microbial strains. Similar phenomena have been seen in the biotransformation of (+)-catechin and (-)-epicatechin by *Eggerthella* sp. strains SDG-2 and CAT-1 (67).

Ad. equolifaciens JCM 14793 and *As. celatus* JCM 14811 were determined to have the ability to catalyze *p*-dehydroxylation of **BM3**, **BM9**, and **BM10**, as was *Ad. equolifaciens* MT4s-5 (89) (Figure 4-11). The presence of hydrogen clearly stimulated the *p*-dehydroxylation reaction. While it was expected from the above observations that *Ad. equolifaciens* JCM 14793, *Ad. equolifaciens* MT4s-5, and *As. celatus* JCM 14811 would have the potential to catalyze *p*-dehydroxylation of gallic acid and pyrogallol which are produced from galloylated catechins (EGCG, GCG etc.) and from gallic acid, respectively, by intestinal bacteria (17, 54, 65), this was not the case (data not shown). Results showed that several isoflavone-metabolizing bacteria had the ability to transform not only EGC and GC but also their metabolites (**BM3**, **BM9** and **BM10**), and therefore may contribute to the metabolism of catechins in the intestinal tract.

Based on the findings here along with previous reports, a major metabolic pathway of EGC and EGCG by catechin-degrading bacteria including isoflavone-metabolizing bacteria is proposed as shown in Figure 4-12. First EGCG is hydrolyzed to EGC and gallic acid by enteric bacteria such as *Enterobacter aerogenes*, *Raoultella planticola*, *Klebsiella pneumoniae* subsp. *pneumoniae*, and *Bifidobacterium longum* subsp. *Infantis,* as reported in Chapter 2 (65). Following hydrolization, EGC undergoes ring cleavage to produce **BM3** by *Adlercreutzia equolifaciens* MT4s-5, *Eg.lenta* JCM 9979, *As. celatus* JCM 14811, *S. equolifaciens* JCM 16059, *Eggerthella* sp. SDG-2 (52), and probably *Eg.lenta* rK3 (67) and *Eggerthella* sp. CAT-1 (67). Strain SDG-2 is capable of transforming EGC into **BM4** via **BM3**. Strains MT4s-5, JCM 9979 and JCM 14811 can also catalyze the above transformation more rapidly in the presence of hydrogen and/or formate produced by symbiotic bacteria such as *Escherichia coli* strains MT4s-3 and K-12, *Butyricimonas synergistica* MT01, and *Butyricimonas virosa* MT12. In this acceleration of the conversion, interspecies hydrogen/formate transfer between the EGC-degrading bacteria and symbiotic bacteria plays an important role. Later, the phloroglucinol moiety of metabolite **BM3** which has formed is degraded, yielding metabolites **BM9** and **BM10** simultaneously by *Flavonifractor plautii* strains MT42, ATCC 29863, ATCC 49531, and most probably aK2 (68). Similarly, metabolite **BM4** is transformed simultaneously into **BM5** and **BM6** by the *F. plautii* strains. Furthermore, both in the presence and absence of hydrogen released by symbiotic bacteria, metabolites **BM3**, **BM9**, and **BM10** undergo *p*-dehydroxylation of pyrogallol moiety in their structure by strain MT4s-5, forming **BM4**, **BM5**, and **BM6**, respectively, although dehydroxylation by this strain is facilitated in the presence of the hydrogen. However, for the dehydroxylation of **BM3**, **BM9**, and **BM10** by strain JCM 9979 the presence of the hydrogen

and/or formate is required. And strain MT4s-5 also has the ability to catalyze 4'-dehydroxylation in the B ring of EGC to produce **BM8**. In addition to isoflavone-metabolizing bacteria, *Ad. equolifaciens* JCM 14793 and *As. celatus* JCM 14811 were found to have the ability to catalyze *p*-dehydroxylation of **BM3**, **BM9**, and **BM10**. The *p*-dehydroxylation reaction was clearly activated in the presence of hydrogen in the case of both of isoflavone-metabolizing bacteria. From the above observations *Ad. equolifaciens* JCM 14793, *Ad. equolifaciens* MT4s-5, and *As. celatus* JCM 14811 were expected to have the potential ability to catalyze *p*-dehydroxylation.

In this Chapter, it was demonstrated that EGC, resulting from hydrolysis of EGCG by enteric bacteria (64, 65), was catabolized by both bacteria which had ring-cleaving ability combined with other bacteria possessing phloroglucinol-decomposing ability. Further, the author found that the ring-cleaving bacteria facilitated or initiated *p*-dehydroxylation of EGC metabolites possessing the pyrogallol moiety through the utilization of hydrogen/formate obtained by interspecies hydrogen/formate transfer between the ring-cleaving and the symbiotic bacteria. Thus, this is the first to determine the important role that symbiotic bacteria play on the catabolic processes of EGC, especially dehydroxylation processes. These findings explain to some extent the reason why a variety of metabolites are produced from EGC. However, further research based on this enzymological approach will be needed in order to better understand the degradation mechanisms of catechins by intestinal bacteria.
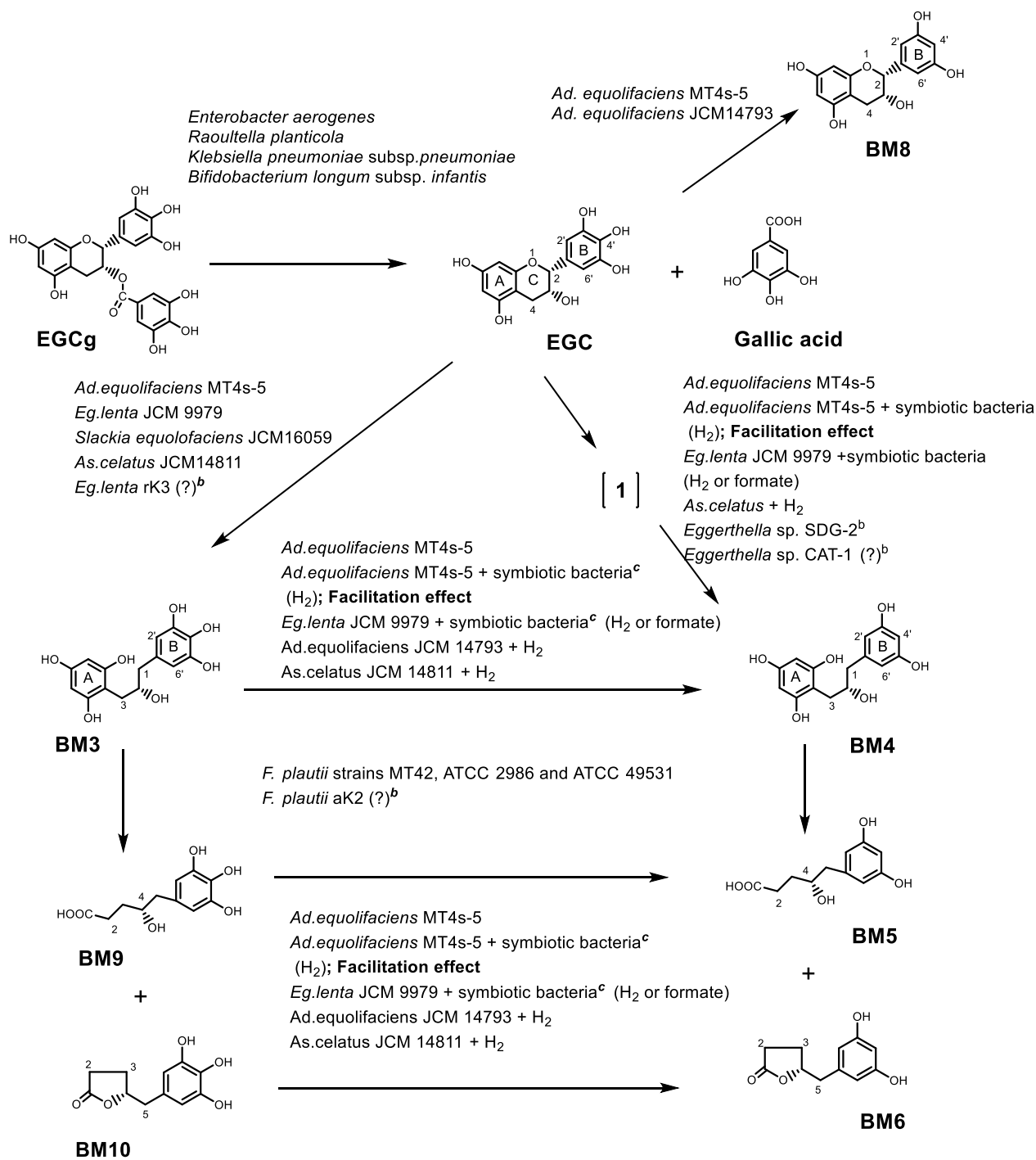
Figure 4-13 Putative metabolic pathway of EGCG by rat intestinal flora

a quotation from Takagaki and Nanjo 2010 (65), *b* quotation from Kutschera et al. 2011(68), *c* E. coli MT4s-3, E. coli K-12, B. synergistica MT01, and B. virosa MT12(64), *d* quotation from Wang et al. 2001 (52), *e* quotation from Jin and Hattori 2012 (67)

Chapter 5

Effects of BM6 on Glucose Uptake in L6 Skeletal Muscle Cell and Glucose Tolerance in ICR Mice

INTRODUCTION

Through described in Chapter 2, 3 and 4, EGCG metabolic pathway and EGC degradation bacteria wew identified. As described in Chepter 1, EGCG is reported to be slightly absorbed in the body, but various physiological functions following EGCG comsumptions have much reported. In order to further understanding of EGCG in vivo functions, mainly focusing on **BM6** as the main metabolite in the rat body, were examined with the aime to study whether the metabolite contributes to the function in the body after administration of EGCG.

With the aging of the population in the world, the increase of health care cost has become a global issue. Especially the number of patient with Lifestyle-related disease continues to increase in many countries. Hyperglycemia has become a serious health problem in dayly life. Due to the rapidly increasing number of people with diabetes and type 2 diabetes, many studies have been conducted to prevent and improve hyperglycemia in daitary foods, including green tea catechins (22, 90, 91). Igarashi *et al* have reported that long-term oral dosage of green tea catechins to Goto–Kakizaki (GK) rats with type 2 diabetes, it have lowered blood glucose levels as shown by the oral glucose tolerance test (92). It has been reported that EGCG improves glucose tolerance level and increases glucose-stimulated insulin secretion after 10 weeks of dietary treatment with AIN-93 diet containing EGCG 1 % (w/w) in genetically diabetic db/db mice (93).

As one of the mechanisms that regulate blood sugar levels, glucose uptake into skeletal muscle has been studied as the effective target to glucose tolerance. This is because skeletal muscle is the largest organ in the human body, accounting for about half of the body weight, and is known to uptake about 80% of blood glucose under insulin stimulation. Skeletal muscle have been considered as the largest tissue that plays important role in maintaining glucose homeostasis in body (32), and insulin resistance in skeletal muscle is considered as the major leading cause of diabetes. Reduced insulin-regulated glucose uptake in skeletal muscle has been reported primarily in patients with type 2 diabetes (94). Therefore, investigating effective dietary components that can improve glucose uptake in skeletal muscle to improve glucose tolerance and alleviate hyperglycemia is a focus of research interest. Glucose transporter 4 (GLUT4) is a major glucose transporter that is specifically expressed in skeletal and cardiac muscle, and is known to play significant role in maintain glucose

homeostasis by regulating cellular glucose uptaking. Insulin stimulation or stimulation by muscle contraction can promote the transfer of GLUT4 from intracellular to the cell membrane, result promoting glucose uptake into skeletal muscle cells. Thus, the evaluation of expression of GLUT4 activation on the plasma membrane of skeletal muscle is considered to be the effective target for improving glucose tolerance in body. Glucose uptake ability of green tea catechins was already studied and catechins, particulary EGCG could found to increase glucose uptake to muscle cells and enhance GLUT4 translocation in L6 myotubes. However, the effect of green tea catechin metabolites on hyperglycemia still remains unknown.

In this Chapter, the author attempted to evaluate of physiological functions of EGCG metabolites with aim to investigate contribution in vivo function following green tea consumption. As the first step, glucose uptake ability and antioxidant ability were examined in vitro examination. Next, this author focused evaluation of the improvement of glucose tolerance by microbial metabolites of green tea catechins produced from EGCG or EGC. The aime of this Chapter was to evaluate the effect of ring fission metabolites to improve glycemic control in skeletal muscle, and to discuss the possibility of these metabolites could be the contributor of hyperglycemic effect in vivo following EGCG consumption. In particular **BM6** which is degraded from EGCG (15, 59) and would bet the main metabolite in body, was investigated for the facilitation effect of GLUT4 translocation. Furthermore, effects of **BM6** to reduce hyperglycemia were conducted by performing an oral glucose tolerance test in ICR mice.

MATERIALS AND METHODS

Chemicals and Reagents

Glucose-6-phosphate dehydrogenase (G6PDH), 2-deoxyglucose (2-DG) and insulin were obtained from Sigma-Aldrich Japan Co. LLC. Resazurin sodium salt, 5-Amino-4-imidazolecarboxamide-1-β-D-ribofuranoside (AICAR), insulin receptor β-subunit (IR), and triethanolamine hydrochloride (TEA) were purchased from Wako Pure Chemical Industries, Ltd. (Osaka, Japan). Diaphorase, ATP and nicotinamide adenine dinucleotide phosphate (NADP) were purchased from Oriental Yeast Co. Ltd. (Tokyo, Japan). For Western blot analysis, anti-IRβ was obtained from Santa Cruz Biotechnology Inc. (Santa Cruz, CA, U.S.A.). Anti-GLUT1, anti-AMPKα, anti-GLUT4, anti-phospho-AMPKα at Thr 172, anti-phospho-PI3K at Tyr 199 and Tyr 458, anti-Akt, anti-phospho-Akt at Thr 308 and Ser 473, anti-phospho-PKCζ/λ at Thr 403 and Thr 410, horseradish peroxidase (HRP)-conjugated anti-mouse immunoglobulin G (IgG) and HRP-conjugated anti-rabbit IgG antibodies were

obtained from Cell Signaling Technology Inc. (Danvers, MA, U.S.A.). Anti-PKCλ antibodies and anti-PI3K were purchased from Becton, Dickinson and Company (Franklin Lakes, NJ, U.S.A.).

Cell Culture of Rat L6 myoblast

Rat L6 myoblast cells were obtained from Sumitomo Dainippon Pharma Co., Ltd. (Osaka, Japan). L6 myoblast cells were cultured with Eagle's minimum essential medium (MEM; Nissui Pharma Co., Ltd., Japan) containing 10 % heat-inactivated fetal bovine serum (FBS; Sigma-Aldrich Japan Co. LLC.) under 5 % CO_2 atmosphere at 37°C. The cells were grown in a 96-well plate for 2-DG uptake assay and 35-mm diameter dish for Western blot analysis. The differentiation of L6 myoblasts to myotubes (4.0×10^3 cells) was performed according to the described Yamamoto *et al.* method (95). The cells were maintained with MEM containing 10% FBS for two days and incubated with MEM containing 2 % FBS. Differentiated L6 myotubes were serum starved in MEM containing 0.2 % BSA for 18 hours. Serum-starved L6 myotubes were treated with 0.1, 1, and 3 µM **BM6** for 15 min and subjected for Western blotting analysis.

Glucose Uptake Ability of BM6

Glucose uptake was determined by enzymatic fluorescence assay for 2-DG uptake in myotubes (95). Serum-starved L6 myotubes in a 96-well plate were treated with **BM6** dissolved with DMSO at a final concentration ranged 1 nM to 10 µM for 4 hours in 0.2 % (w/v) BSA/MEM. DMSO was used as a vehicle control, and insulin at 100 nM was used as a positive control. The treated cells were further incubated with 1 mM of 2-DG for 20 min in Krebs–Ringer-Phosphate–N-(2-hydroxyethyl)piperazine-N′-2-ethanesulfonic acid (HEPES) buffer (KRPH; 50 mM HEPES, pH 7.4, 137 mM NaCl, 1.85 mM CaCl2, 4.8 mM KCl, and 1.3 mM $MgSO_4$) containing 0.1 % BSA. Then the cells were washed twice with KRPH buffer containing 0.1% BSA, lysed with 0.1 M NaOH, and dried for 50 min at 85°C. The dried cell lysates were solubilized and neutralized in 0.1 M HCl and 150 mM TEA buffer pH 8.1. The solubilized lysates were incubated with assay cocktail (50 mM TEA, pH 8.1, 0.02 % BSA, 50 mM KCl, 0.1 mM NADP, 0.2 units/mL diaphorase, 15 units/mL G6PDH and 2 mM resazurin sodium). The fluorescence of the resorufin produced from resazurin was measured at emission and excitation wavelengths of 530 and 570 nm, respectively, using plate reader Wallac 1420 ARVOsx of Perkin-Elmer, Boston, MA, U.S.A.

Preparation of Plasma Membrane Fraction

Protein in the whole lysates and the plasma membrane fraction from cultured cells and muscle tissues were prepared according to Ashida and Nishiumi's methods (84, 85). For the

plasma membrane fraction, L6 myotubes or muscle tissue were collected with 50 mM Tris buffer, pH 8.0, containing 1 mM Na_3VO_4, 0.1% Nonidet P-40® (NP-40), 0.5 mM dithiothreitol (DTT), 10 mM NaF and protease inhibitor cocktail and homogenized by pestle homogenizer and 25-gauge needle. The lysates were centrifuged at $200 \times g$ for 1 min and the supernatant was collected. The supernatant was centrifuged at $750 \times g$, for 10 min and the pellet was re-suspended with 50 mM Tris buffer containing 10 mM NaF, 0.5 mM DTT, 1 % NP-40, 1 mM Na_3VO_4 and protease inhibitor cocktail at 4°C for 60 min with occasional mixing. The suspension was centrifuged at $12000 \times g$ for 20 min and the supernatant was collected as the plasma membrane fraction. For the whole lysate fraction, L6 myotubes or muscle tissues were lysed with 20 mM Tris buffer at pH 8.0, containing 1 % sodium deoxycholate, 300 mM NaCl, 1 mM DTT, 20 mM NaF, 0.2 % Sodium dodecyl sulfate (SDS), 2 mM Na_3VO_4, 2 % NP-40, and protease inhibitor cocktail; and homogenized by 25-gauge needle and pestle homogenizer. The lysates were centrifuged at $12000 \times g$ for 20 min and the supernatant was collected as a whole lysate fraction.

Western Blotting Analysis

Proteins of myotubes and muscle tissues were separated with SDS-polyacrylamide gels and transferred electrophoretically to the polyvinylidene fluoride (PVDF) membranes. After blocking with Blocking-one™ solution (Nacalai Tesque, Kyoto, Japan), the membranes were washed with TBST (10 mM Tris–HCl, 150 mM NaCl, 0.06 % Tween 20, pH 8.0). The antibodies were diluted in Can Get Signal Immunoreaction Enhancer Solution (TOYOBO CO., LTD., Osaka, Japan) and incubated at 4°C for overnight. The membranes were incubated with the corresponding horseradish peroxidase-conjugated secondary antibody at room temperature for 1 hour. The proteins were visualized using ImmunoStar LD (Wako Pure Chemical Industries, Ltd.) and detected with Light-Capture II (ATTO Corp., Tokyo, Japan).

Preparation of Purified BM6 for Animal Treatment (80)

Metabolite **BM6** used for animal treatment in this study were prepared with isolated bacterium described in Chapter 4. For the production of metabolites **BM6**, a mixed culture of the strains *Eggerthella lenta* JCM 9979 (100 mL of preculture), *Flavonifractor plautii* MT42 (20 mL of preculture) and *Escherichia coli* K-12 (20 mL of preculture) in 500 mL of GAM broth containing 500mg EGC was incubated at 37 ºC were performed under anaerobic condition with an Anaero Pack system. Anaerobic incubation was continued until complete conversion of EGC into **BM5** and **BM 6**. The culture was centrifuged to remove bacterial cells by centrifugation at $8000 \times g$ at room temperature for 10 min. The supernatant was adjusted the pH range to around 2.0 with 5 M HCl and incubated at 37ºC to convert of **BM5** to **BM6**. The culture was extracted three times with 400 mL of ethyl acetate, after pH

adjustment of the culture to about 4.0 with 2 M NaOH. The ethyl acetate fraction containing **BM6** was then evaporated to dryness. The residue was dissolved in small amount of 5 % aqueous methanol. The sample solutions were applied to preparative HPLC. Preparative HPLC was conducted with a 250 mm × 20 mm (i.d.), 5 μm, Mightysil RP-18GP column in an LC-908-G30 recycling preparative HPLC system (Japan Analytical Industry Co. Ltd., Tokyo, Japan). The column was eluted with a linear gradient of solvent, starting with 1 0% (v/v) aqueous methanol containing 0.5 % (v/v) acetic acid and ending with 60 % (v/v) aqueous methanol containing 0.5 % (v/v) acetic acid at the flow rate of 15 mL/min. The elution patterns were monitored with absorbance at 230 nm. The effluent containing **BM6** was collected and evaporated to dryness. The residues were each dissolved in a small amount of distilled water and freeze-dried to obtain **BM6** (215 mg).

Animal Treatment

Male ICR mice were obtained from SLC Japan, Inc. and maintained at 23 ± 2°C with a 12-hours light-dark cycle. The mice were fed with a pelleted diet (Research Diets, Tokyo, Japan) for a week. All experimental procedures in Chapter 5 and Chapter 6 were in accordance with the guidelines for animal experiments of Kobe University Animal Experimentation Regulation with the permission of Kobe University Institutional Animal Care and Use Committee (Chapter 5 : Permission #1-27-05-09). Mice were subjected to an oral glucose tolerance test (OGTT) for the detection of GLUT4 translocation and its related signaling pathways. For OGTT, the mice aged 6 weeks were divided into five groups (n = 4– 5) with similar average weights (weight av. 16.5 g). After a 16 hours fast, 0.32, 3.2, 32 or 64 mg/kg/10 mL of **BM6** dissolved in saline was dosed orally to mice with a gastric metal probe. Only saline (10 mL/kg) was administered as the vehicle control group. After 1 hour of **BM6** administration, 1.0 g/kg/10 mL of glucose aqueous solution was orally administrated to all mice. Blood samples were collected from the tail vein at 0 (before administration), 15, 30, 60 and 120 min after an oral administration of glucose with heparinized tubes. Blood samples (25 μL) were centrifuged at $9600 \times g$ at 4°C for 10 min. Resultant plasma sample (2 μL) was measured for glucose levels using Labassay1 Glucose Wako kit (Wako Pure Chemical Industries, Ltd.).

Measurement of GLUT4 translocation and its related signal pathways were conducted as below. Mice aged 8 weeks were divided into four groups ($n = 5$) with similar average weights (weight av. 41.8 g). After a 16 hours fast, 3.2 mg, 32 mg or 64 mg/kg/10 mL of **BM6** dissolved in saline was administered orally to mice with a gastric metal probe. Only saline (10 mL/kg) was dosed for the vehicle control group. The mice were sacrificed 60 min after the administration of **BM6** under anesthesia using sodium pentobarbital and euthanized by exsanguination from cardiac puncture. Soleus muscle of the hind legs was collected, and its

plasma membrane fraction and tissue lysate were prepared and subjected to Western blot analysis. At the same time, blood samples were collected from the cardiovascular organ, and were used for the quantitative analysis of metabolites of **BM6** as described below.

GLUT4 Translocation and Its Related Signal Pathways in Mice of BM6

Plasma membrane fraction and tissue lysate of soleus muscle were prepared according to Nishiumi and Ashida's protocol (95, 96). Proteins in the plasma membrane fraction and tissue lysate were separated by SDS-polyacrylamide gels and transferred to the PVDF membranes.

Quantitative Analysis of Plasma Metabolites after Oral Administration of BM6

The author performed the quantitative analysis containing plasma metabolites with the intent to confirm **BM6** had been absorbed at the time of the *in vivo* effects of **BM6** on GLUT4 translocation, phosphorylation of the signal pathways and OGTT in mice. Plasma samples were prepared by centrifugation of the blood samples at $3000 \times g$ at 4°C for 10 min (MX-301, TOMY SEIKO CO., LTD., Tokyo, Japan). Aliquots (200 µL) of plasma samples were added to 0.2 M sodium acetate buffer (pH 4.0) and 1 mL of acetonitrile. The solution was mixed well, and centrifuged $10000 \times g$ for 10 min at 10°C. The supernatants were placed in a new vessel, and the pellet was washed twice using 1 mL of 80 % aqueous methanol. After centrifugation $10000 \times g$ for 10min, the supernatant was collected and then evaporated to dryness with Centrifugal Concentrator CC-105 (TOMY SEIKO CO., LTD.). The residue was dissolved in 200 µL of 5% aqueous methanol. The resultant solution was filtrated with DISMIC-13HP (Toyo Roshi Kaisha Ltd., Tokyo, Japan) and subjected to LC- ESI-MSn and LC-MS/MS analysis.

Quantification of plasma metabolites was conducted with LC-MS/MS analysis according to the procedure described in Chapter 4.

Statistical Analysis

All values are expressed as the mean ± standard error of the mean (SEM). Statistically significant differences between control and test substance-treated groups were performed using Dunnett's test. The statistical calculations were done with IBM SPSS Statistics 19 (IBM Japan, Tokyo) (Figs. 5-2 and 5-6) or JMP® (SAS Institute Inc., U.S.A.) (Figs. 5-3 to 5–5, 5-7, and 5-8). Differences are considered significant at $p < 0.05$.

RESULTS

Glucose Uptake Ability of EGCG Metabolites into L6 Skeletal Muscle Cell

Firstly, eleven kinds of EGC metabolites were examined for 2-DG uptake in L6 myotube cells that had been treated with 3 μM concentration of each metabolite for 15 min. As positive and negative controls, L6 myotube cells were also treated with 100 nM insulin or dimethyl sulfoxid (DMSO). Comparative potential of glucose uptake in L6 myotubes is shown in Fig. 5-1. It was found that **BM6**, **BM9**, **BM10**, and **BM12** increased glucose uptake significantly. Glucose uptake enhancement of each metabolite was 164.2 % (**BM6**), 165.2 % (**BM9**), 167.6 % (**BM10**), and 146.3 % (**BM12**) compared with DMSO-treated negative control cells. These results indicate some EGCG metabolites have insulin-like activity. The glucose uptake potency of these metabolites in 3 μM treated cells was found to be slightly lower than that of 100nM Insulin-treated cells (198.6 %), but higher than that of 100 nM EGCG treated cells (132.1 %). Structural relevance among these effective metabolites has not been found.
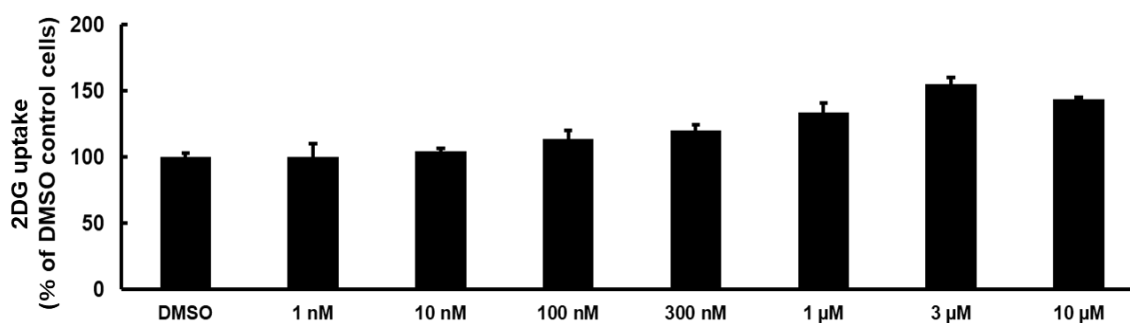
Figure 5 -1   Effect of BM6 on glucose uptake in L6 myotubes.
The results are presented as the mean ± SEM (n = 3−5).
Significantly different from DMSO treated control group (*p <0.05, **p <0.01 Dunnett's test).

Glucose Uptake Ability of BM6

When L6 myotubes were treated with **BM6** in concentrations within the range of 1 nM to 10 μM, the glucose uptake was significantly confirmed at the concentrations of 1, 3, and 10 μM, as shown in Figure 5-1. To my knowledge, this is the first report of the promotive activity of glucose uptake in skeltal muscle cells by EGCG microbial metabolites. This result indicates that EGCG microbial metabolites could be bioactive factor which improve insulin resistance in skeletal muscle.

GLUT 4 Translocation and Phosphorylation of Signal Pathway

To examine the promotive effect of **BM6** on the GLUT4 translocation from intracellular pool to plasma membrane in L6 skeletal muscle, expression of GLUT4 of plasma membrane fraction was evaluated with immunoblot analyses by western blotting. 100 nM insulin and 1nM of 5-Amino-4-imidazolecarboxamide-1-β-D-ribofuranoside (AICAR) were used for positive controls, and DMSO was used for a vehicle control. As shown in Figure 5-2, **BM6** could significantly enhance expression of GLUT4 in L6 myotube cells at the concentrations of 1.0, or 3.0 μM. In particular, L6 myotubes treated with 3.0 μM **BM6** showed strong promotive effect with the same degree of 1 nM AICAR, which is known as an activator of AMPK, suggests that **BM6** can promote GLUT4 translocation effectively in L6 skeletal muscle cell. EGCG showed a significant stimulation of glucose uptake accompanied by GLUT4 translocation in L6 myotubes at 1 nM concentration (36), indicating that the in vitro effect of **BM6** on glucose uptake ability with GLUT4 translocation is lower than that of EGCG.

GLUT4 translocation is known to be induced by phosphorylation of signaling proteins via both insulin-dependent and insulin-independent pathways. Therefore, phosphorylation of protein kinase C (aPKC), protein kinase B (Akt) and PI3K was examined as an insulin-dependent signaling pathway, and phosphrylation of AMPK was examined as insulin-independent pathway by western blot analysis. In this study, phosphorylation of AMPK was significantly increased in L6 myotube cells treated with **BM6** at 1.0 and 3.0 μM concentrations. In particular, the 3.0 μM **BM6**-treated cells showed a relatively strong phosphorylation levels, comparable to the 1 nM positive control AICAR (Figure 5-3). This result indicates that **BM6** can promote GLUT4 translocation throgh activation of the insulin-independent AMPK signaling pathway. On the other hand, there was no significant difference in p-PI3K/PI3K, p-Akt/Akt (Thr 308), p-Akt/Akt (Ser 473) and p-aPKC/aPKC as the insulin-dependent signaling proteins in **BM6**-treated L6 myotube cells under our experimental conditions (Figure 5-4). These findings indicated that **BM6** can promote translocation of GLUT4 to the plasma membrane by activating AMPK signaring pathway, leading to an increasement glucose uptake into skeletal muscles consequentially.
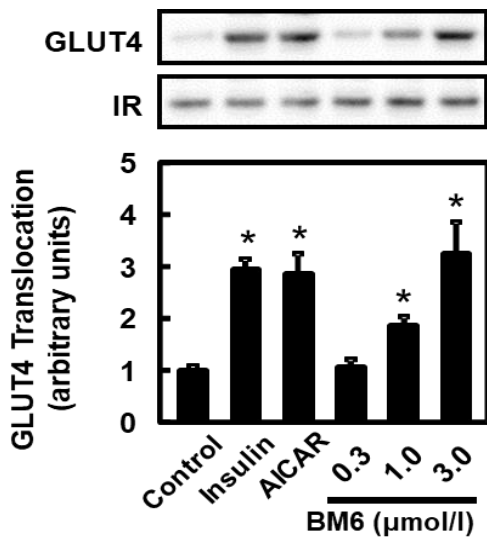
Figure 5-2. Effect of BM6 on GLUT4 translocation in L6 myotubes

The results are presented as the mean $\pm$ SEM (n=3). Significantly different from control group (*p <0.05, Dunnett's test).
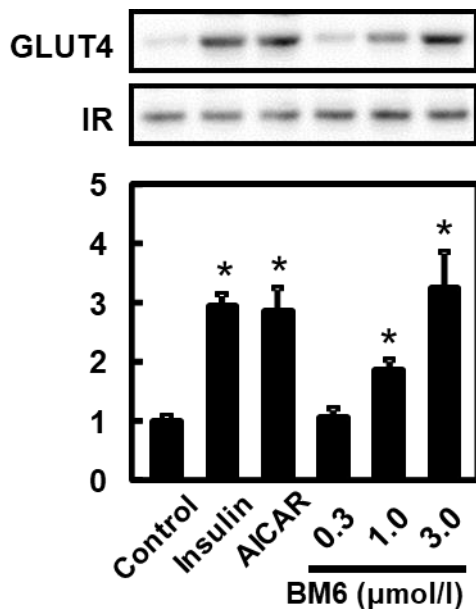

Figure 5-3. Effect of BM6 on Phosphorylation of AMPK in L6 Myotubes

The results are presented as the mean $\pm$ SEM (n=3). Significantly different from control group (*p <0.05, Dunnett's test).

It has been reported that activation of AMPK by adiponectin, which is an adipocyte-derived hormone, could enhance glucose metabolism via the stimulation of glucose uptake in skeletal muscle tissue and also fatty-acid oxidation (97). AMPK activation also inhibited hepatic gluconeogenesis by improving insulin resistance (97). Furthermore, the AMPK activation has been described recent evidence regarding with inhibition mechanism in cancer cell growth (98). Therefore, AMPK activators will be the therapeutic targets because of their applications in the treatment and prevention of metabolic syndrome, hyperglycemia, hypertension and hyperlipidemia, and cancer prevention (99). Procyanidin is one of the plant polyphenol containing dietary polyphenols such as nuts, cacao, berries and red wine, and procyanidin has been reported to be as an AMPK activator. Cacao liquor procyanidin (CLPr) extract has been reported to the promotive effect of AMPK activation and translocation of GLUT4 in the

plasma membrane of skeletal muscle (100). Screening of AMPK activators in dietary polyphenols, including plant polyphenol metabolites such as **BM6**, is great interest in preventing metabolic syndrome and cancer.
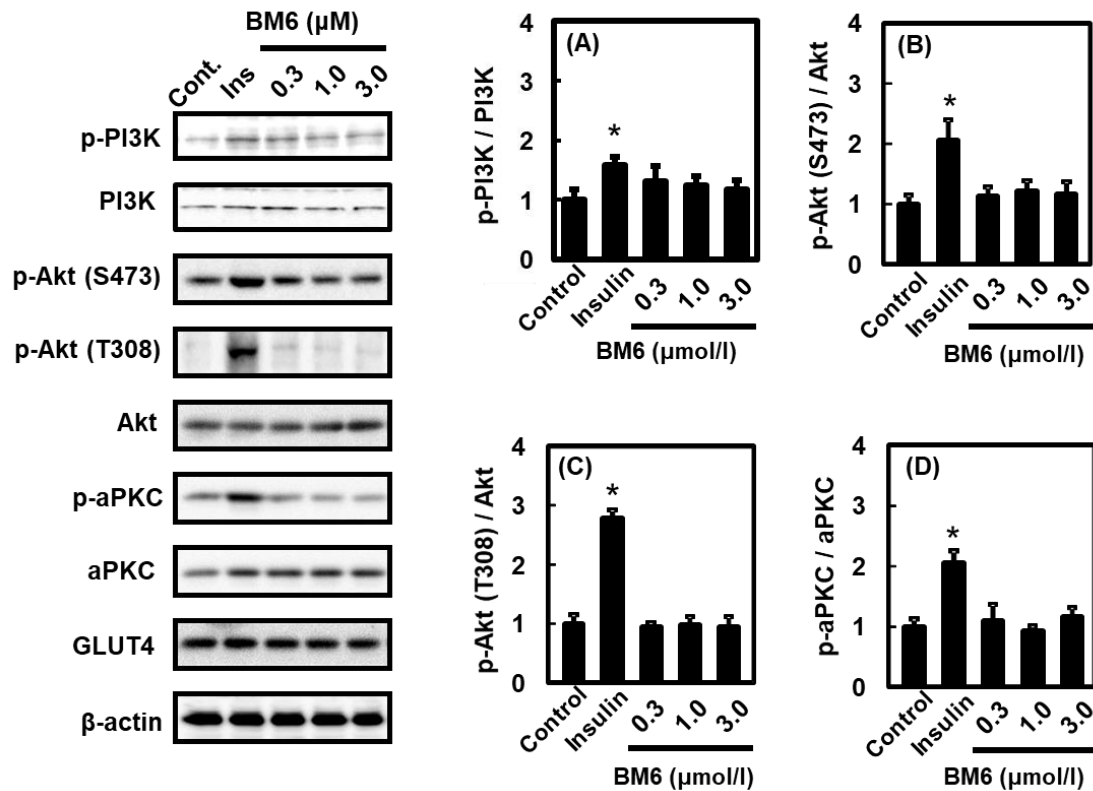

Figure 5-4   Effect of BM6 on phosphorylation on the insulin-signaling pathway in L6 myotubes Immunoblotting analysis to determine (A) p-PI3K and PI3K; and (B) p-Akt serine 473 and Art; (C) p-Akt threonine 308   and Akt; (D) p-aPKC and aPKC were performed by Western blotting. The results are presented as the mean ± SEM (n=3).
Significantly different from control group (*p <0.05, Dunnett's test).

Oral Glucose Tolerance Test (OGTT) of BM6 in ICR Rats.

It is newly discovered that **BM6** has a promotive effect on glucose uptake, GLUT4 translocation, and AMPK phosphorylation in skeletal muscle cells through in this Chapter. These results suggest that **BM6** has the ability to improve glucose tolerance by enhancing skeletal muscle glucose uptake.

We conducted an oral glucose tolerance test (OGTT) in ICR mice to evaluate **BM6** potential for suppression of postprandial hyperglycemia. Figure 5-5 (A) shows the effect of **BM6** single oral dosage on the plasma glucose level to an oral load of glucose. After 15 min in response to oral glucose loading, plasma glucose level was reached the maximum value after 15 min (216.3 ± 21.5 mg/dL), and decreased after 30 min (171.5 ± 27.0 mg/dL), and reached the normal value level by 120 min in the vehicle control group. In the **BM6** (32

mg/kg of body weight) treated group, postprandial hyperglycemia inhibition was observed with plasma glucose concentration at 15min (150.5±13.6mg/dl) and 30 min (108.5 ± 17.2 mg/dl) after oral glucose load being significantly suppressed compared with saline control group. Following the glucose load, the 64 mg/kg body weight **BM6** treated group significantly inhibited postprandial hyperglycemia after only 15 min (133.7±10.1mg/dL), and maximum blood glucose concentration (149±8.1mg/dl) was reached 30 min after glucose loading.

The area under the curve (AUC) values calculated 0 to 120 min after glucose loading are shown in Figure 5-5(B). A significant decrease was seen in the 32mg/kg body weight of **BM6** treated group, while no statistically significant effect was found in the 64mg/kg treated group. From this observation, it may be deduced that there exists an appropriate dose of **BM6** to take for suppression of postprandial hyperglycemia in vivo.
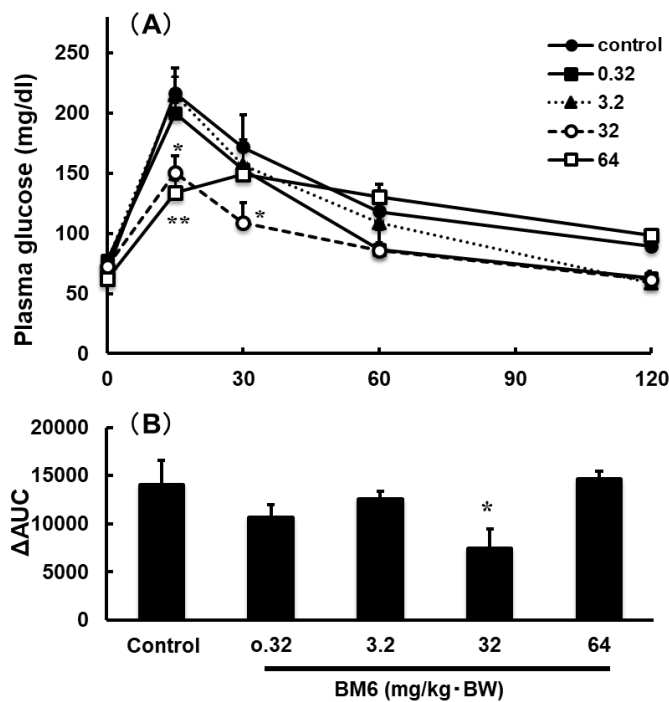

Figure 5-5 Effect of BM6 on plasma glucose level in ICR mice during an oral glucose tolerance test
(A): Oral glucose tolerance tests (OGTT) were carried after the treatment with 0.32 (■), 3.2 (▲), 32 (○), and 64 (□) mg/kg body weight of BM6 or saline (●). Sixty minutes after the administration of BM6, the mice were orally given glucose solution (1 g/kg body weight) followed by plasma glucose measurements at 0, 15, 30, 60 and 120 min.
(B): Values of area under the curve (AUC) calculated from 0 to 120 min after glucose loaded. Values are the means ± S.E.M (n = 4-5). Significantly different from control group (*p <0.05, **p <0.01; Dunnett's test).

GLUT 4 Translocation and Phosphorylation of Signal Pathway in Soleus Muscle of ICR Mice.

The translocation of GLUT4 and phosphorylation of signaling protein induced by **BM6** was also examined in the soleus muscle of ICR mice treated with **BM6** at concentrations of 3.2, 32 or 64 mg/kg of body weight. Dosages of **BM6** to mice were adjusted the same dosages as in the OGTT test.

The results of the western blotting analysis are illustrated as an expression of GLUT4 (Figure 5-6), and phosphorylation of signal pathways (Figure 5-7). Concerning to the translocation of GLUT4 in the soleus muscle of ICR mice treated with **BM6**, it can be stated that only the 32 mg/kg body weight dosed group significantly increased GLUT4 translocation in the plasma membrane as compared with results of control group dosed the saline (Figure 5-6). Whereas in the 64mg/kg body weight treated group, no significant increase was detected by statistical analysis. The dosage which exhibited a significant decrease in GLUT4 expression (32 mg/kg of body weight) is in accord with the dosage which showed significant differences in the glucose tolerance test.

Regarding to the phosphorylation of signal protein following administration of **BM6,** at concentrations 3.2, 32 or 64 mg/kg of body weight, results are indicated in Fig. 5-4 to 5-7. No significant increasement was observed in the phosphorylation level of p-PI3K/PI3K (Figure 5-7 (A)), p-Akt/Akt (Ser 473) (data not shown) and p-Akt/Akt (Thr 308) (data not shown). These results are in accordance with *in vitro* examination of L6 myotubes. While the phosphorylation level of p-AMPK/AMPK was significantly increased in both the 32 and 64 mg/kg body weight **BM6** dosed groups (Fig. 5-7B). The potential of **BM6** for AMPK activation observed *in vitro* examination with L6 myotubes was confirmed in skeletal muscle tissue following **BM6** administration *in vivo*.
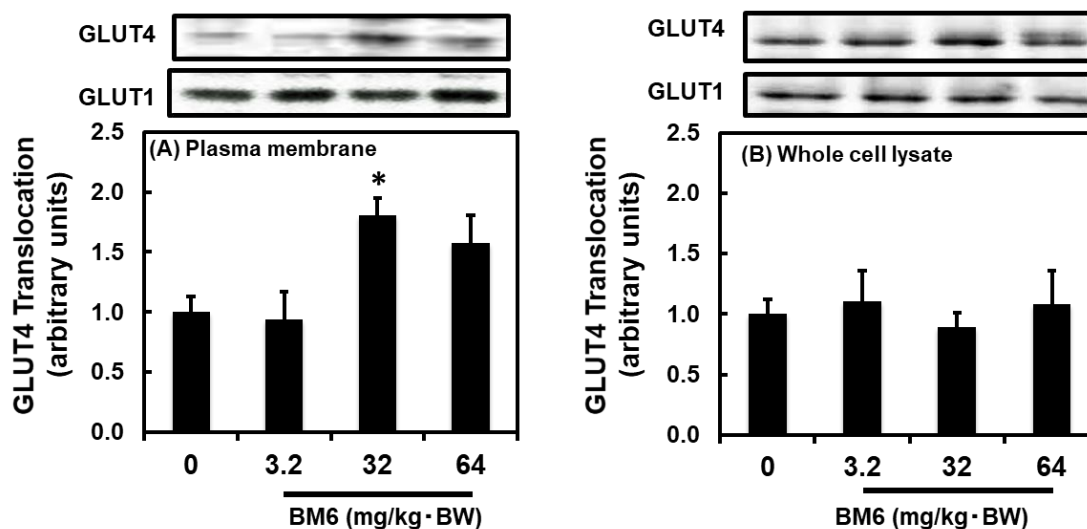

Figure 5-6 Effect of BM6 on GLUT 4 translocation in skeletal muscle of ICR mice
The amounts of GLUT4 and GLUT1 proteins in the plasma membrane (A) and the tissue lysate (B) of the muscle were determined by immunoblotting. The density of each band was analyzed and normalized to that of GLUT1. The results are presented as the mean ± SEM (n=5). Significantly different from control group (*p <0.05, Dunnett's test).
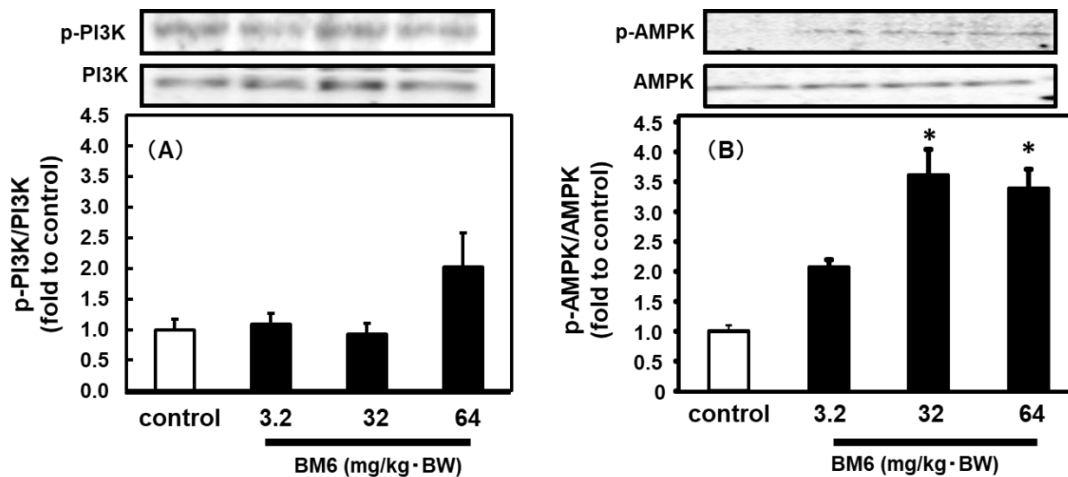
83

Figure 5-7 Effect of **BM6** on GLUT 4 translocation in skeletal muscle of ICR mice. ICR mice were treated with 3.2mg/kg, 32mg/kg or 64mg/kg body weight of **BM6** as described in Material & Method. Skeletal muscle was removed 60 min after administration. The amounts of GLUT4 and GLUT1 proteins in the plasma membrane (A) and the tissue lysate (B) of the muscle were determined by immunoblotting. The density of each band was analyzed and normalized to that of GLUT1. The results are presented as the mean ± SEM (n=5). Significantly different from control group (*$p < 0.05$, Dunnett's test).

From the results indicated Figs.5-5, 5-6, and 5-7, it can be stated that **BM6** is the effective contributor to improve postprandial hyperglycemia and insulin resistance *in vivo*. Then, this author tried to qualitative and quantitative analysis of plasma metabolites at 60 min after oral administration of **BM6** by LC-ESI-MSn and LC-MS/MS analysis with the intent to confirm **BM6** absorption in the body. From the LC-ESI-MSn analysis, **BM6** aglycone, **BM6** monoglucuronide (**BM6**-GlcUA) and **BM6** monosulfate (**BM6**-Sul) were detected. The results of concentrations of **BM6** metabolites detected in the plasma are listed in Table 5-1. The **BM6** aglycone was detected at the concentrations of 0 μmol/mL (3.2 mg/kg dosed group), 5.62 μmol/mL (32 mg/kg dosed group) and 3.15 μmol/mL (64 mg/kg dosed group) in plasma samples 60 min after of oral dosage of **BM6**. As shown in Figs. 5-5(B) and Figure 5-6(A), significant lowering of blood glucose AUC and significant promotion of GLUT4 translocation in soleus muscle were only observed in the 32 mg/kg **BM6** dosed group and not in the 64 mg/kg dosed group. With regard to concentration of **BM6** aglycone, in the 32 mg/kg dosed group this was found to reach the concentration at 5.62 μmol/mL, which is higher than that of the 64 mg/kg dosed group. Thus it speculated that **BM6** could enter into muscle tissue and still retain an effective concentration in the 32 mg/kg dosed mice group. On the basis of these results, the author reached the tentative conclusion that the **BM6** aglycone absorbed in the blood may be contributing to improvement of glucose tolerance in mice.

Majority of the **BM6** was detected as the conjugated form in the blood after oral administration, it appears that conjugation of glucuronide and sulfate occurs during the absorption process through the digestive tract. Relevance of conjugates, such **BM6**-GlcUA and **BM6**-Sul, in the prevention of hyperglycemia in body is the next expanded research agenda.

Table 5-2   Quantitative analysis of plasma metabolites after 60 min oral dosage of BM6 in mice.

	Plasma metabolites (μmol/mL)		
	3.2 mg/kg of dosage	32 mg/kg of dosage	64 mg/kg of dosage
BM6 aglycone	0	5.62 ±1.31	3.15± 2.27
BM6 -GlcUA	1.56 ±0.73	38.5±4.63	57.45 ± 8.91
BM6-Sul	2.62±1.47	24.3±3.31	38.30 ±12.97

Data are expressed as the mean ± S.E.M. (n = 5).

DISSCUSSION

In order to investigate whether intestinal bacterial metabolites contribute to physiological effect in vivo after oral administration of EGCG, we investigated the antidiabetes potential of **BM6**, the main intestinal bacterial metabolite of EGCG. It is the first time to investigate on the antidiabetic effect of EGCG-derived microbial metabolites described in this Chapter. Results showed several EGCG metabolites could promote glucose uptake into L6 myotubets. The major metabolite of EGCG, **BM6** activates insulin-independent AMPK pathway and translocation of GLUT4 to the membrane is induced leading to glucose uptake in skeletal muscle. Further ingested **BM6** was confirmed to induce translocation of GLUT4, while reduction of postprandial hyperglycemia elevated after glucose load was observed.

Furthermore, **BM6** has found to have strong potential for contribution through AMPK activation. These findings indicate that metabolites produced after green tea intake will play an important role in metabolic regulation in the body, since AMPK has been considered as an important therapeutic target (35) to control human diseases including metabolic syndrome and cancer.

On the other hand, there are many research reports on the anti-hyperglycemi effect of EGCG, and the effects of EGCg in several functional mechanisms have already been revealed. The mechanisms for regulating blood glucose concentrations of EGCG were studied from several functional aspects, such as inhibition of α-glucosidase and other carbohydrate

digestive enzymes (101, 102), stimulation of insulin secretion from pancreatic beta cells (103, 104), and inhibition of gluconeogenic enzymes in the liver (19, 105). Recent reports explaining the mechanism of hyperglycemic glycosuria have focused on the insulin-sensitive glucose transporter 4 (GLUT4), expressed in adipose tissue, skeletal muscle, and cardiac muscle, as a novel target for an antidiabetic agent. Regarding the promotive effect of glucose into skeletal muscles, intact EGCG has been already reported to have a promotive effect on GLUT4 translocation in Sprague-Dawley rats and phosphorylation of PI3K/PKC and AMPK signaling pathways with oral dosing of 75mg/kg body weight of EGCG (36). In this Chapter, the improvement effect of glucose tolerance in the body by EGCG microbial metabolites was partly confirmed to promote glucose metabolism by AMPK activation in skeletal muscle. However, antidiabetic effect on other mechanisms has not yet been verified to be attributable to EGCG. It may also be involved in the anti-diabetic effects verified in the body after ingestion of green tea catechin, and how the microbial metabolites are involved in blood glucose control in the body is a topic for future study.

In conclusion, the author suggested that BM6 degraded from EGCG by intestinal flora is the contributing factor which improves glucose tolerance in the body. Although reports on the function of catechin metabolites have been increasing in recent years, there is still a lack of information on those mechanisms involved in beneficial health effects. The author expect these advances in research on EGCG metabolite functionality will lead to more detailed elucidation of the mechanisms of physiological functions following EGCG intake.

We, hereby, report for the first time the in vitro and in vivo ability of microbial metabolites of EGCG to exert an antidiabetic effect for improvement of hyperglycemia. Several EGCG metabolites have been found to promote glucose uptake into L6 myotubes. As the major microbial metabolite of EGCG, **BM6** has the potential to promote activation of AMPK signaling pathway and induce the translocation of GLUT4 to the plasma membrane in skeletal muscle both in vitro and in vivo. In conclusion, we substantiated the functional relevance of EGCG metabolites in the reduction of postprandial blood glucose levels and improvement of glucose tolerance following green tea consumption. Further studies are needed to clarify the role of conjugated metabolites on antidiabetic effects.

Chapter 6 (Appendix)

Effect of BM10 on Improvement of Glucose Tolerance throght Promoting Glucose Uptake in Skeletal Muscle in Mice

INTRODUCTION

Through this doctoral study, **BM6** is considered as the main metabolites of EGCG in rats. Concerning the beneficial effcts of **BM6**, glucose uptake ability into L6 skeletal muscle cells and suppression on postprandial blood glucose was investigated in Chapter 5. As the result, **BM6** was found to have a significant promotive effect on GLUT4 (1.0 to 3.0 μM) to the cell membrane in L6 myotubes. Furthermore, significant suppression on postprandial blood glucose elevation was confirmed in the **BM6** administered group (32 mg / kg of body weight) in the OFTT test. In conclusion, the ability of **BM6** for improvement of glucose metabolism in the living body was confirmed.

In recent years, several studies on the identification and quantification of human urinary metabolites after drinking green tea were reported (60, 106). In these reports, the conjugated form of **BM10**, in addition to **BM6**, were detected as the metabolites present following green tea consumption. Justin JJ van der Hooft *et al* (60) conducted identification of urinary metabolites by HPLC-FTMSn and HPLC-TOFMS-SPE-NMR in four human volunteers after green tea drinking, and identified 138 kinds of metabolites including 48 kinds of γ-valerolactone metabolites. In the urine accumulated over 26 hours after consuming the green tea drink, glucronide form of **BM6** (5-30 μmol/mL) and glucronide of **BM10** (50-150 μmol/mL) were detected in concentrated amounts.   Luca Calani et al. 19) reported on urinary metabolites collected up to 48 hours from 20 healthy volunteers who drank RTD green tea beverages containing mainly EGCG, EGC, ECG. They reported the detection of the conjugate form of **BM6**, **BM10** and 5-(3',4'-dihydroxyphenyl)-γ-valerolactone in the human urine. The 5- (3', 4'-dihydroxyphenyl) γ– valerolactone and 5- (3-hydroxyphenyl) –γ -valerolactone are degradation products from catechol type catechins (for example EC, ECG and C) (107), and , metabolites derived from the pyrogallol-type catechins EGCG and EGC, found in human urine, are regarded as **BM6** and **BM10**.

Furthermore, phenyl-γ-valerolactones and phenylveleric acids have been reported as main colonic metabolites of dietary flavan-3-ol sources (108, 109). The presence or absence of the p-hydroxyl group of the benzene ring of phenyl-γ-valerolactone is reported to differ due to the differences in the intestinal flora as studied in Chapter 4. As the next step, anti-hyperglycemia effect of **BM10** was investigated in order to gain a better understanding of the contribution of

degraded metabolites to the anti-hyperglycemic effect following green tea consumption. The present study was conducted to determine the promotive effect of GLUT4 translocation and increases in glucose uptake in skeletal muscle cells in vivo and in vitro of **BM10** as one of the major metabolite of EGCG in humans.

MATERIALS AND METHODS

Measurement of Glucose Uptake Ability into L6 Myotubets

Evaluation of glucose uptake ability and phosphorylation on its related sygnaring pathway with Western blotting analysis were conducted according to the mathods descrived in **Chapter 5.** Structures of EGCG and **BM6** and **BM10** are illustrated in Figure 6-1.

Preparation of Purified BM10 for Animal Treatment

Metabolite **BM10** used for animal treatment in this Chapter were prepared with isolated bacterium described in Chapter 4. For the production of metabolites **BM6**, a mixed culture of the strains *Eggerthella lenta* JCM 9979 (100 mL of preculture), *Flavonifractor plautii* MT42 (20 mL of preculture) in 500 mL of GAM broth containing 500 mg EGC was incubated at 37 ºC were performed under anaerobic condition with an Anaero Pack (anaerobic cultivation) system (Mitsubishi Gas Chemical Company, Inc., Tokyo, Japan). After anaerobic incubation, purification of **BM10** was performed with same procedure according to the **BM6** preparation method described in Chapter 5. Finally, freeze-dried **BM10** was obtained 148.0 mg.

Animal Treatment

Aninal treatment on the oral glucose tolerance test was performed with same procedure on **BM6** described in Chapter 5. All experimental procedures were in accordance with the guidelines for animal experiments of Kobe University Animal Experimentation Regulation with the permission of Kobe University Institutional Animal Care and Use Committee (Permission #1-27-05-09). For OGTT, the mice aged 8 weeks were divided into five groups (n = 5) with similar average weights (weight av. 24.45 g). For the evaluation of GLUT 4 translocation and activation of its signaling transduction pathway in body, **BM10** was dosed to ICR mice (10weeks old, weight av. 33.80 g), configured as 0.32, 3.2, or 32 mg/kg of mice body weght. Preparation of soleus muscle of the hind legs and evaluation by western blotting were identically treated with **BM6** as described in Chapter 5. Statistical processing was performed in the same way as Chapter 5.
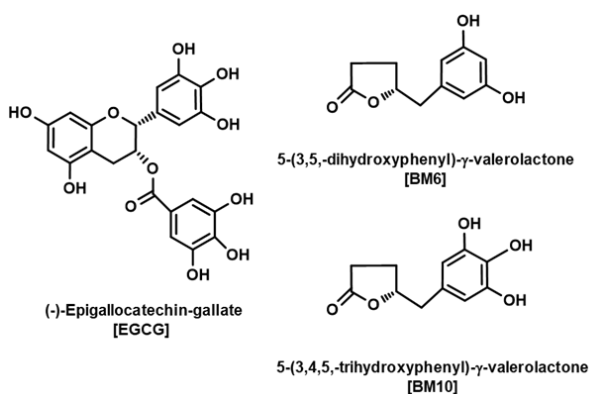
Figure 6-1   Structures of EGCG and γ-valerolactone metabolites (BM6 and BM10)

RESULTS

Effect of BM10 on Glucose Uptake in L6 Myotubes

Structures of EGCG and **BM6** and **BM10** are illustrated in Figure 6-1. To examine the promotive effect of **BM10** on the GLUT4 translocation from intracellular pool to plasma membrane in skeletal muscle, expression of GLUT4 of L6 myotubes plasma membrane fraction was evaluated with immunoblot analyses by Western blotting.

Figure 6-2 shows GLUT4 expression with 0.3, 1.0, or 3.0 μM of **BM10** treated to L6 myotubes compared with **BM6**. For positive controls, the cells were treated with 100 nM insulin and 1μM EGCG. As a negative control, vehicle (final 0.1 % of DMSO) was used. At all concentrations of **BM10** examined treated L6 myotubes, significantly increase of GLUT4 translocation compared with DMSO given controls was detected. The value of GLUT4/IRβ of 1.0 μM **BM10** (174.4 %) treated cells showed a comparatively intense level of phosphorylation and to the same degree as 0.1 μM of insulin (144.4 %). This result suggested that EGC-M7 is effective in promoting GLUT4 translocation to the plasma membrane of skeletal muscle, leading to glucose uptake into cell.
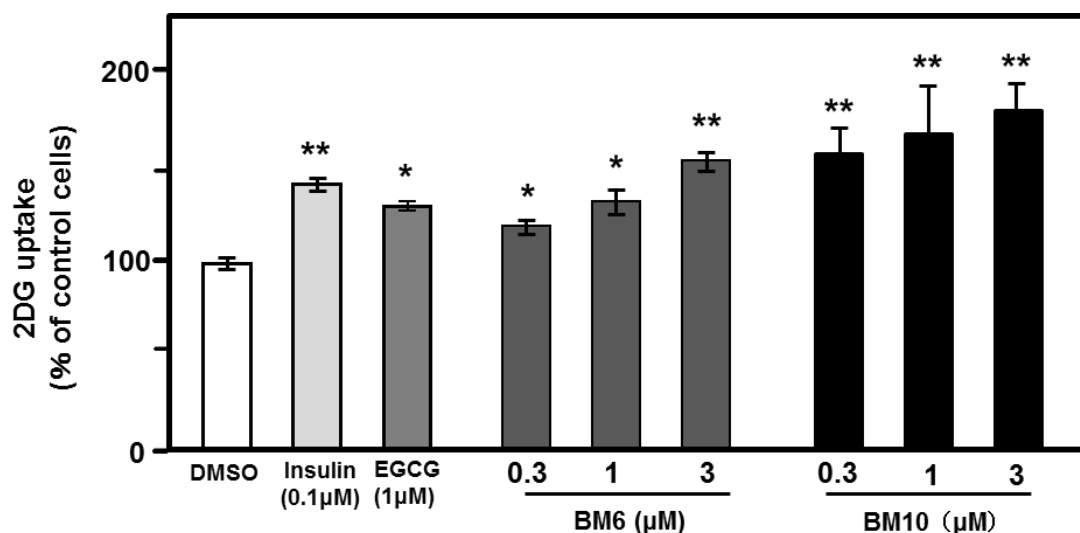
Figure 6-2   Effect of **BM10** and **BM6** on glucose uptake in L6 myotubes

 DMSO was used for a vehicle control, while 100 nM insulin and 1 mM EGCG was used for a positive control. The results are presented as the mean ± SEM ($n = 5$).   Asterisks indicate significantly different from the control group (*p <0.05 Dunnett's test).

Promotive Effect of GLUT 4 Translocation by BM10 and Phosphorylation of Relative Signaling Pathway

The promotive effect of **BM10** for translocation of GLUT 4 from the intracellular pool to the plasma membrane in L6 skeletal muscle was evaluated using immunoblot analyses by western blotting. As shown in Figure 6-3, **BM10** could significantly promote GLUT4 expression in L6 myotube cells at concentrations of 0.3, 1.0, or 3.0 μM (2.08 ± 0.25, 2.68 ± 0.60, 4.48 ± 0.21).

GLUT4 translocation could be induced by phosphorylation of signaling proteins through both insulin-dependent and insulin-independent pathways. In Chapter 5 (110), **BM6** was found to have the potential to promote activation of AMPK signaling pathway and induce the translocation of GLUT4 to the plasma membrane in L6 skeletal muscle cell. Similarly to **BM6**, the expression of signal transduction involved in membrane translocation of GLT4 was also examined by Western blotting for **BM10**. The result of AMPK phosphorylation in L6 myotubes by **BM10** is indicated in Figure 6-4. It was discovered that activation level of p-AMPK/AMPK in L6 myotubes treated with **BM10** was significantly increased at all concentrations of 0.3, 1.0 and 3.0 μM. In regarding to **BM6**, significantly enhanced GLUT 4 translocation and AMPK phosphorylation were induced only at the concentration of 1.0 μM or more, not at 0.3 μM (28). As described above, **BM10** was found to be capable of promoting GLUT 4 translocation from intracellular pool to plasma membrane, and

enhancement of AMPK phosphorylation at a low concentration of 0.3 μM (Fig.6-4). Activation value of p-AMPK/AMPK in L6 myotubes treated with 0.3, 1, and 3 μM **BM10** was indicated at 3.43 ± 0.75, 3.75 ± 0.93 and 3.46 ± 0.70. As the positive control, 0.1μM AICAR treated myotubets   indicated the p-AMPK/AMPK value at 4.15 ± 0.30. This result indicated the high effectivity of **BM10** for GLUT 4 translocation via AMPK activation rather than **BM6**.
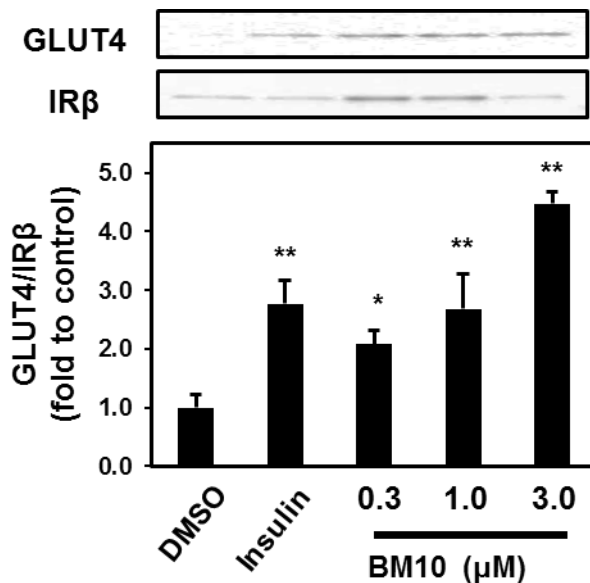

Figure 6-3   Effect of **BM10** on GLUT4 translocation in L6 myotubes.
The results are presented as the mean ± SEM (n=3). Asterisks indicate significantly different from the control group (*p <0.05, **p <0.01, Dunnett's test).

On the other hand, phosphorylation of protein kinase B (Akt) and phosphatidylinositol 3 kinase (PI3K) were examined as an insulin-dependent signaling pathway by Western blot analysis. The effects of **BM10** on activation of these insulin-dependent signaling pathways are illustrated in Figure 6-5. There was no significant difference in p-PI3K/PI3k, p-Akt /Akt (Ser473), p-Akt /Akt (Thr308) as the insulin-dependent signaling proteins in **BM10**-treated L6 myotube cells, compared with the positive control of insulin. (Figure 6-5)   Thus, the phenomenon that **BM10** does not activate the insulin-dependent signaling pathway was in agreement with as **BM6** (110).

To summarize the above results, that **BM10** was found to promote translocation of GLUT4 from intracellular pool to plasma membrane, by accompanying AMPK phosphorylation, leading to an increased glucose uptake into L6 skeletal muscle cells, as same as **BM6**.
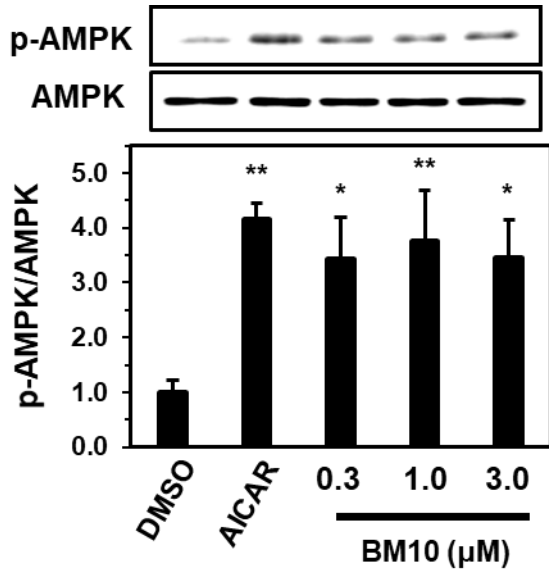
Figure 6-4 Effect of **BM10** on Phosphorylation of AMPK in L6 Myotubes

The results are presented as the mean ± SEM (*n*=3). Asterisks indicate significantly different from the control group (*p* <0.05, Dunnett's test).
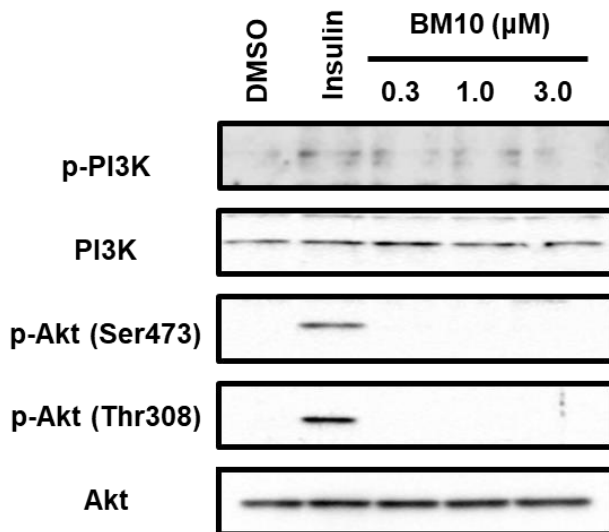

Figure 6-5 Phosphorylation of insulin dependent signal pathway in L6 myotubes by **BM10** treatment

DMSO and 100 nM insulin were used as the negative and positive controls, respectively. Tissue lysate of L6 myotubes were subjected to immunoblotting analysis to determine PI3K and Akt and their phosphorylationforms (p-PI3K, p-Akt at ser473 and thr308). Significant difference from the control cells by Dunnett's test (*p<0.05)

Oral Glucose Tolerance Test in ICR Mice with BM10

Figure 6-6 shows the effect of **BM10** dosage on changes in plasma glucose tolerance. In the saline control group, plasma glucose level increased in response to oral glucose loading and reached maximum after 15 min following (179 ± 9.70 mg/dL), 30 min (161 ± 11.15 mg/dL) and lowered to the normal value level up to 120 min. In the 32 mg/kg body weight **BM10** treated group, plasma glucose levels at 15min (130 ± 12.20 mg/dL) and 30 min (92 ± 17.10 mg/dL) after glucose administration were significantly suppressed as compared with the

postprandial hyperglycemia of control group. On the other hand, plasma glucose levels at 15min (164 ± 13.00 mg/dL) and 30 min (130 ± 14.67 mg/dL) after glucose administration were not suppressed in the 64 mg/kg body weight **BM10** treated group as compared with the postprandial hyperglycemia of control.

A significant hyperglycemic effect was clearly observed only in the 32 mg/kg treated group, while there was no significant effect observed in the 64mg/kg treated group. This result may be deduced that there is an optimum intake dose of **BM10** for suppression of postprandial hyperglycemia. Since same phenomenon was observed in the same way when **BM6** was conducted OGTT (110), thereby ensuring the hypothesis that there is optimal dose concentration of the phenyl-γ-valerolactones to improve glucose tolerance in the body.
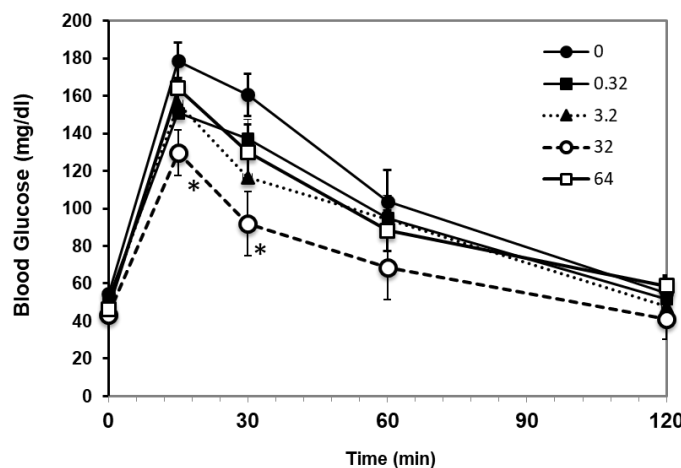

Figure 6-6 Oral glucose tolerance test of **BM10** in ICR mice

Oral glucose tolerance tests (OGTT) were carried after the treatment with **BM10** at 0.32 (■), 3.2 (▲), 32 (○), and 64 (□) mg/kg body weight or saline (●) as a control. Sixty minutes after the administration of BM10, the mice were orally given glucose solution (1 g/kg body weight) followed by plasma glucose measurements at 0, 15, 30, 60 and 120 min. Values are the means ± S.E.M (n = 5). Asterisks indicate significantly different from the control group (*p <0.05, Dunnett's test).

GLUT4 Translocation and Phosphorylation Signaling System in Mice Skeletal Muscle After Oral Administration of BM10.

Finally, *in vivo* enhancement of GLUT 4 translocation and activation of accompanying signaling pathways in soleus muscle of ICR mice treated with **BM10** were measured by western blotting analysis. Because the suppressive effect of **BM10** on postprandial hyperglycemia was found only in the 32 mg/kg administration group in OGTT as described above, the phosphorylation effect on signaling pathway in skeletal muscle tissue was investigated on the mice administered with **BM10** dosed at 0.32, 3.2 and 32 mg/kg.

Expression of GLUT4 in the plasma membrane protein (A) and whole protein cell lysate (B) of soleus muscle of mice after oral administration of **BM10** are illustrated in Figure 6-7. It was confirmed that **BM10** had the ability to promote translocation of GLUT 4 in the skeletal

muscle of a living organism actually administered this metabolite orally. Regarding in vivo activation of signaling proteins involved in GLUT4 translocation, **BM10** could significant increase in the phosphorylation level of both p-AMPK/AMPK in the 32 mg/kg body weight dosed group (Fig. 6-8 A), while could not increase the phosphorylation level of p-PI3K/PI3k, p-Akt /Akt (Ser 473) and p-Akt /Akt (Thr 308) (Figure 6-8 B, 8 C). These results supported the result that a significant suppression of postprandial blood glucose level was confirmed in the 32 mg/kg oral administration of **BM10** group in the OGTT (Fig. 6-6).

The effective concentration at which **BM10** showed significant GLUT4 translocation to the plasma membrane (Figure 6-7) was consistent with the concentration at which significant suppression of postprandial hyperglycemia was observed in the OGTT (Figure 6-6). From these in vivo examinations, **BM10** was demonstrated to have the potential for effective improvement of glucose tolerance in mice by promoting GLUT 4 translocation through phosphorylation of the AMPK-signaling pathway.
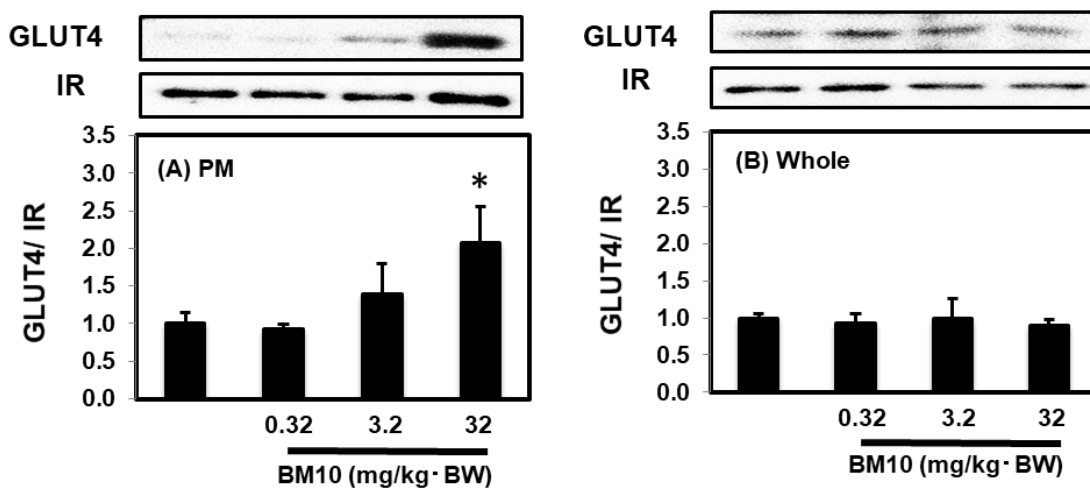

Figure 6-7. Effect of **BM10** on GLUT 4 translocation in skeletal muscle of ICR mice
ICR mice were treated with BM10 at 0.32, 3.2 and 32 mg/kg body weight or saline as a control. Skeletal muscle was removed 60 min after administration. The amounts of GLUT4 and IR proteins in the plasma membrane (A) and the tissue lysate (B) of the muscle were determined by western blot analysis. The density of each band was analyzed and normalized to that of GLUT1. The results are presented as the mean ± SEM (n=5). Asterisk indicates significantly different from the control group (*p <0.05, Dunnett's test).

DISCUSSION

As shown in Figure 6-2, significant glucose uptake ability in L6 myotubes was observed with **BM10** treated cells. It was found that **BM10** has higher activity of glucose uptake rather than that of **BM6**. The 2DG uptake value of the 0.3 μM treated with **BM10** (157.0 %) indicated higher than that of 0.1 μM insulin treated cell (144.1 %). In addition, the uptake ability in 1 μM of **BM10** treated cell (174.4 %) indicated higher than same concentration of 1 μM EGCG (13.6.2 %) which used as a positive control. As for the glucose uptake in L6 myotubes, **BM10** was found to have a significant uptake at the low concentration of 0.3 μM.

Figure6-3 demonstrates the promotive effect of **BM10** on GLUT4 translocation, and Figure 6-4 indicates the activation of signaling pathway accompanying GLUT4 translocation. As shown in both figure 6-3 and figure 6-4, **BM10** showed significant GLUT4 translocation activity and AMPK phosphorylation activity both even at a lower concentration of 0.3 μM. Particularly, as shown in Figure 6-4, the AMPK phosphorylation activity value of p-AMPK / AMPK was 4.15 in the positive control of 0.1 μM AICAR-treated L6 myotubets, while that of the 0.3 μM **BM10** treated was 3.44. From this result, it was shown that **BM10** has a strong AMPK activation action.

According to **BM6** as descrived in Chapter 5, significant glucose uptake ability on L6 myotube was found from the concentration at 1μM. GLUT 4 translocation activity and, but **BM10** was more effective at lower concentrations, indicating that **BM10** is more effective than **BM6**. From the *in vitro* results shown in Figure 6-2, Figure 6-3 and Figure 6-4, **BM10** showed a significantly higher promotive effect at a lower concentration than that of **BM6** (Figure 5-3), and **BM10** was found to have superior promotive effects on GLUT4 membrane translocation via high AMPK phosphorylation activity, and on glucose uptake into L6 myotubes.
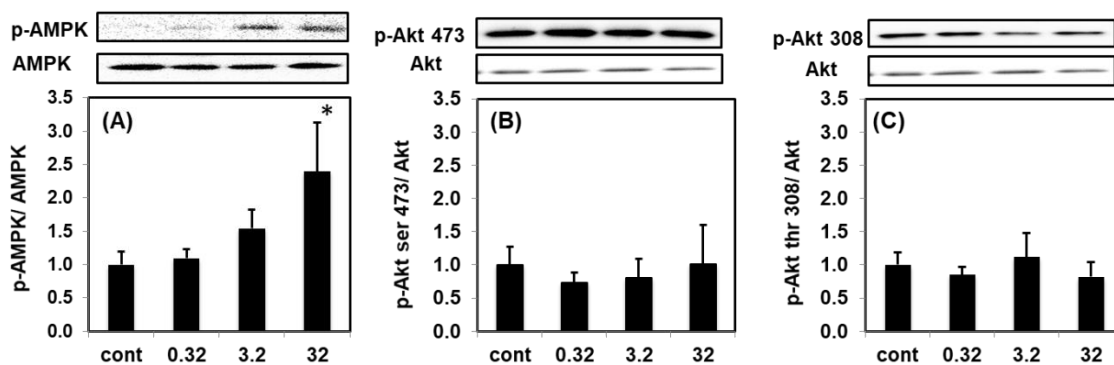
Figure 6-8 Effect of **BM10** on phosphorylation of PI3K and AMPK in skeletal muscle of mice ICR mice were treated with BM10 at 0.32, 3.2 and 32 mg/kg body weight or saline as a control. Tissue lysate of skeletal muscle was prepared 60 min after the administration and subjected to western blot analysis to determine (A) p-AMPK and AMPK and the density of each band was analyzed and normalized. The results are presented as the mean ± SEM (n=5). Asterisks indicate significantly different from the control group (*p <0.05, Dunnett's test).

Furthermore, according to *in vivo* glucose tolerance tests conducted by oral administration of **BM10**, a significant inhibitory effect on elevation of postprandial blood glucose level was confirmed at 15 and 30 minutes after administration in the 32 mg / kg dosed group. Four different doses of **BM10**, 0.32, 3.2, 32.0 and 64.0 mg/kg/BW were tested in this study, but only the 32 mg/kg/BW dosed group showed a significant anti-hyperglycemic effect. Furthermore the group administered with the highest dose of 32.0 mg/kg/BW did not show a significant effect on blood glucose levels at any of the time points measured at 15, 30, 60, and 120 minutes post administration. Also, **BM6** (in Chapter 5) the significant increase in the suppression of postprandial glucose levels, and the promotion of GLUT4 translocation have been shown to be stronger in the 32 mg/kg/BW dosed group rather than in the 64 mg/kg/BW dosed group. Thus in this Chapter, it was obviously demonstrated that there was suitable concentration for the glucose uptake effect of phenyl-γ-valerolactones in the body. These observations of **BM10** involved in improvement of glucose tolerance in this Chapter 6 agreed with the **BM6** results in Chapter 5, which confirmed the existence of an optimum concentrationfor the promotive effect of phenyl-γ-valerolactones on their glucose uptake activity in the body.

AMPK activation is an important factor for improvement of insulin resistance and is also deeply associated with stimulation of both fat and glucose metabolism (97). Therefore, screening of compounds having AMPK phosphorylation activity is ongoing in the medical and food nutritional fields with the purpose of discovering ways to counteract lifestyle-related diseases. Compounds known to have AMPK phosphorylation activity are hormone-like substances such as adiponectin and leptin which are secreted from adipocytes, and among food ingredients, cocoa polyphenols, resveratrol, procyanidins, etc. have been reported to

possess AMPK phosphorylation activity. It has been reported (111) that adiponectin phosphorylates AMPK and PPARα by binding to membrane receptors type 1 (AdipoR1) and type 2 (AdipoR2) on skeletal muscle cells, which results in the promotion of glucose uptake and oxidation of fatty acids. Resveratrol, a plant polyphenol contained in red wine, has been reported to inhibit activation of phosphodiesterase 4 (PDE4) by binding to PDE4 and causing intracellular cAMP and Ca2$^+$ levels to increase, resulting in increased AMPK and SIRT1 phosphorylation activities (112). In this Chapter, **BM10** showed high AMPK phosphorylation activity at a lower concentration than **BM6** in L6 skeletal muscle cells *in vitro*. Therefore, it is thought to be likely that receptor-mediated AMPK activation as in adiponectin or activation via signal transduction by inhibiting PDE4 activation as in resveratrol occurs. Therefore, the reason that **BM10** had higher AMPK phosphorylation activity than **BM6**, may be because the pyrogallol structure of **BM10** is more favorable than **BM6** for binding to proteins such as receptors or PDE4. However, little is known about the affinity of the pyrogallol structure of **BM10** and the catechol structure of **BM6** to proteins, and therefore further investigation of microbial metabolites is necessary.

In OGTT in ICR mice, a significant reduction in post-prandial hyperglycemia was observed only in the 32.0mg/kg/BW (**BM10**) dosed group. This result is in accordance with **BM6** and it is confirmed that there was an optimum concentration of phenyl-γ-valerolactones for improving glucose metabolism in the body. Concerning to extensive concentration range for phenyl-γ-valerolactones in body, further investigation will be necessary in each function.

Recently, with the advancement of metabolomic analytical techniques, there has been increasing reports on intestinal flora analysis and intestinal bacterial metabolites. Studies have reported that phenyl-γ-valerolactones such as **BM6** and **BM10** have are the common colonic metabolites of dietary polyphenols which have flavan-3-ol as a fundamental structure (108, 109). Procyanidin, which is one of the functional plant polyphenols, has a structure of polymerized flavan-3-ol, and is reported to have various beneficial functions such as drug metabolism promoting action, lipid metabolism promoting action, and sugar metabolism promoting action. In recent years, 5-(3,4-dihydroxyphenyl)-γ-valerolactone has been identified as a major metabolite in human urine after procyanidin consumption (113, 114) . According to reports by Zang L *et al* (113) is thought that procyanidin is degraded to the monomeric-forms epicatechin and catechin at low pH (pH 2.0), as found in gastric acid, and then metabolized to 2-(3,4-dihydroxyphenyl) acetic acid and 5-(3,4-dihydroxyphenyl)-γ-valerolactone by intestinal bacteria. Pycnogenol, a natural functional material extracted from pine bark on the French coast, is known to have strong antioxidative activity, and 5-(3,4-dihydroxyphenyl)-γ-valerolactone is reported to be a major metabolite found in human urine after consuming pine bark extract (115, 116). Thus, phenyl-γ-valerolactones are reported as multiple common microbial metabolites in the body

after consumption of polyphenols which have flavan-3-ol as a fundamental structure. This fact indicates that phenyl-γ-valerolactones may commonly contribute to functionality in the body after intake of dietary flavan-3-ols souses.

Phenyl-γ-valerolactones detected in urine are almost all conjugated, and the numbers of hydroxyl moieties in the benzene ring and the binding sites of such hydroxyl groups vary (108). Such structural differences are due to the differences in the structure of the catechol type or the pyrogallol type of catechins, beside the presence of electron donors released from symbiotic bacteria for C-ring cleaving bacteria. Therefore, the production rate in the body of **BM10** and **BM6** which were evaluated on glucose uptake ability in this Chapter, was predicted to show individual differences due to the variety of intestinal flora in human. It was then revealed that **BM10** possessed glucose uptake activity in skeletal muscle by GLUT4 translocation via phosphorylation of AMPK pathway in the same way as **BM6**, and also **BM6** was found to have the ability to reduce postprandial hyperglycemia in the body.

In conclusion, **BM10** which is one of the major urinary metabolites of EGCG degraded by intestinal flora, could promote GLUT4 translocation accompanying AMPK phosphorylation at a lower concentration than **BM6** and showed higher glucose uptake activity into L6 myotubes than **BM6**. Moreover, the reducing effect of **BM10** on postprandial hyperglycemia was in accordance with the effect of **BM6** in Chapter 5. Thus, it was suggested that **BM10** may also contribute to the anti-hyperglycemic effect after green tea consumption.

Chapter 7

General Disucussion

Green tea is very familiar beverage in Japanese daily life. There are many types of green teas, such as sen-cha, hoji-cha, and matc-cha, and they are all consumed by many people daily and are especially favored by people throughout Japan. The health benefits of green tea are often attributed to the actions of tea catechins, which are green tea polyphenols. Green tea catechins, the polyphenols contained in green tea, are well-known for their variety of health benefit functions including antioxidative (117, 89), blood cholesterol lowering (118), hypoglycemic (91), cancer preventive (119) and blood pressure lowering activities (120,121). However, it has been reported that the absorption rate of EGCG was 0.1−1.6% of the oral dose in rats (15). In a previous paper, the bioavailability of intact EGCG, including its conjugates, was estimated to be 0.26% after oral administration of (−)-[4-^{3}H]EGCG in rats (15). Del Rio *et al* (119) have reported the bioavailability of tea catechins including EGCG, EGC, ECG, and EC would be <4% in humans. Thus, these studies have suggested that tea catechins, particularly EGCG, are poorly absorbed in the body. Therefore despite its strong activity in vitro, there are some cases when it is questionable whether intact EGCG would show favorable biological activity in the body.

Accordingly, this author focused on EGCG, which among green tea catechins is the most abundant and possesses the highest functionality. In this study, the author first investigated the metabolic pathway of EGCG in the rat intestine. In addition, quantitative analysis of fecal metabolites after oral administration of EGCG was performed, and it was confirmed that the metabolic pathway presumed by *in vitro* examinations is reflected *in vivo* (Chapter 2). In Chapter 3, the author confirmed the conversion of **BM5**, the main metabolite in the gut tract, to **BM6** in the body. Next, isolation and identification of enteric bacteria associated with the metabolism of EGCG was performed. With regard to isoflavone-metabolizing bacteria closely related to catechin-metabolizing bacteria, it was confirmed that isoflavone-metabolizing bacteria could catabolize EGC (Chapter 4). Furthermore, research into the anti-hyperglycemic effect of EGCG metabolites, mainly focused on main metabolite **BM6**, in order to investigate whether EGCG microbial metabolites produced in gut intestine are involved in *in vivo* effects following green tea consumption (Chapter 5).

The metabolism of EGCG by rat intestinal flora is described in Chapter 3 and Chapter 4. In the first step, EGCG is decomposed to yield EGC and gallic acid by the tannase activity of enteric bacteria, such as *Enterobacter aerogenes*, *Raoultella planticola (Klebsiella planticola)*, *K. pneumoniae susp. pneumoniae*, and *Bifidobacterium longum subsp. infantis (B. infantis)*. We isolated and identified *Adlercreutzia equolifaciens* MT4s-5 as the C-ring cleaving bacteria

of EGC. *A. equolifaciens* MT4s-5 and *Eggerthella lenta* JCM 9979 were found to convert EGC into **BM3**, but also to catalyze the subsequent 4'-dehydroxylation of the above metabolite to yield **BM4** in the presence of hydrogen or formate, supplied by symbiotic bacteria. This is a conversion that occurs when an electron donor of hydrogen and/or formic acid is donated by a symbiotic bacterium, such as *Escherichia coli*, *Butyricimonas synergistica*, or *Butyricimonas virosa*, to a bacterium having the above-mentioned ring-opening ability. Such communication between bacteria via electron donors is a typical symbiotic action found in anaerobic bacteria, and is called interspecific hydrogen transfer or interspecific formic acid transfer. Then, *Flavonifractor plautii* MT42 degraded the phloroglucinol moiety of the propan-2-ols of above-mentioned **BM3** and **BM4**, results and simultaneously produced their corresponding 4-hydroxy-5-hydroxyphenylvaleric acids (**BM5** and **BM9**) and 5-hydroxyphenyl-γ-valerolactones (**BM6** and **BM10**). This decomposition reaction by *Flavonifractor plautii* is presumed to be the same reaction as reported during gallic acid catabolism by *Eubacterium oxidoreducens*. Thus after ring fission of phloroglucinol moiety of **BM3** and **BM4**, it was speculated that methylene chain consumption occurs by β-oxidation reaction, resulting in formation of **BM5** and **BM9**. During this study, *in vitro* metabolism analyses were repeated several times. Due to differences in the intestinal flora, several patterns of metabolic pathways are thought to exist. One of the metabolic patterns among these was when the compound metabolism was advanced to generate hydroxyl-valeric acids (**BM11**, **BM12**, and **BM13**) from 4-hydroxy-5-hydroxyphenylvaleric acids (**BM5** and **BM9**).

Additionally, the author investigated the conversion of the main EGCG metabolite in the living body. The main fecal metabolite after oral administration of EGCG was confirmed as **BM5** in Chapter 2. On the other hand, **BM6** has been reported as the main metabolite in the urine. Then, in order to examine the discrepancy in which the main metabolites used in feces and urine is different, examinations on lactonization of **BM5** in blood circulation were conducted by intravenous administration of **BM5** to rat, and on absorption from digestive tract of **BM5** and **BM6** by everted gut sac method. As a result, it was revealed that **BM5** was unlikely to be lactonized during blood circulation, while in the absorption process **BM6** could more easily pass through digestive tract than **BM5**. It was found that most of **BM6** which passed through the intestine underwent glucronide conjugation. From these results, although **BM5** was the main product of EGCG in the gut tract, it was **BM6** that was absorbed predominantly, undergoing conjugation in the absorption process, and as a result, after oral dosage of EGCG conjugated **BM6** was the major metabolite detected in the urine finally. Therefore, the main metabolites circulating in the body after oral administration of EGCG are considered to be mainly the **BM6** conjugates. Then in this study, as the main metabolite degraded from EGCG in body is considered as **BM6** conjugates. Subsequently, in the next

chapter, the author examined the physiological function of microbial metabolites. From the results up to this point, the main metabolite in the body produced from EGCG was considered to be the **BM6** conjugates. Therefore, in the functional study in the next Chapter, we mainly focused on **BM6** as the main metabolite derived from EGCG. Basically, as a first step of evaluation, the biological functionality was assessed using aglycone **BM6**.

There are various reports on the beneficial health effects of catechin metabolites as described in Chapter 1. As the functional target in this study, anti-diabetic effect of these metabolites was investigated because lifestyle-related diseases are recognized to have become an increasingly serious problem due to an aging population. In Chapter 6, glucose uptake ability into L6 skeletal muscle cell was examined with microbial metabolites of EGCG produced by intestinal bacteria and several metabolites have been found to promote uptake of glucose into L6 myotubes significantly. **BM6**, which is one of the major ring fission metabolites of EGCG, was also found to have a promotive effect on glucose transporter 4 (GLUT4) translocation accompanied by phosphorylation of AMPK signaling pathway in skeletal muscle both *in vivo* and *in vitro*. Furthermore, the effect of oral single dosage of **BM6** on glucose tolerance test with ICR mice was examined and significant suppression of hyperglycemia was observed. As mentioned in discussion of Chapter 6, AMPK phosphorylation occurs via a non-insulin-dependent signal transduction pathway, and it is known that its phosphorylation is usually triggered by various stimuli, such as exercise. AMPK is known to be activated when intracellular ATP is decreased and AMP is increased in cells. It is a key energy-sensitive enzyme that acts as a key regulator in cellular energy homeostasis. Since activation of AMPK leads not only to promotion of glucose metabolism but also promotion of lipid metabolism, it can be expected that AMPK activation will be effective in the improvement of lifestyle-related diseases. Several studies on promoting effects of lipid metabolism by green tea catechins have already been reported (113, 122, 123). Therefore, **BM6** is also expected to have a lipid metabolism promoting action through AMPK activation. Further efforts are required to examine the effect of EGCG metabolites on body fat metabolism, with the purpose of investigating the contribution of microbial metabolites to lipid metabolism improvement following green tea consumptions. In this evaluation, the author mainly examined the glucose tolerance using the main metabolite **BM6**. The in vivo examination in this study confirmed the significant AMPK activation action in the body after oral administration of **BM6**, promotive effects of GLUT4 transflocation, and the suppression of postprandial hypergrycemia. After oral dosage of **BM6** for 60 minutes, aglycone and sulfate and glucuronide conjugates of **BM6** were detected as the plasma metabolites. In this way, the phenyl-γ-valerolactone metabolites are detected mainly in the conjugated form *in vivo*. Therefore, it was necessary to evaluate the effect of conjugated **BM6** as the next step.

From results, it was suggested that the phenyl-γ-valerolactone metabolite such as BM6

could contribute to an anti-hyperglycemic effect in the body, one of the beneficial effects of green tea consumption which have been reported. From the results of this study, it was confirmed that the metabolite itself is a functional factor in the body.

Recently, with the advancement of metabolomic analysis technologies, there has been increasing research on intestinal flora analysis and intestinal bacterial metabolites. Studies have reported that phenyl-γ-valerolactones such as **BM6** and **BM10** have are the common colonic metabolites of dietary polyphenols which have flavan-3-ol as a fundamental structure. (115, 124) Procyanidin, which is one of the functional plant polyphenols, has a structure of polymerized flavan-3-ol, and is reported to have various beneficial functions such as drug metabolism promoting action, lipid metabolism promoting action, and sugar metabolism promoting action. In recent years, 5-(3′,4′-dihydroxyphenyl)-γ-valerolactone has been identified as a major metabolite in human urine after procyanidin consumption (116, 125). According to reports by Zang L *et al* (113), is thought that procyanidin is degraded to the monomeric-forms epicatechin and catechin at low pH (pH 2.0), as found in gastric acid, and then metabolized to 2-(3′,4′-dihydroxyphenyl) acetic acid and 5-(3′, 4′-dihydroxyphenyl)-γ-valerolactone by intestinal bacteria. Pycnogenol, a natural functional material extracted from pine bark on the French coast, is known to have strong antioxidative activity, and 5-(3′, 4′-dihydroxyphenyl)-γ-valerolactone is reported to be a major metabolite found in human urine after consuming pine bark extract (116, 115). Thus, phenyl-γ-valerolactones are reported as multiple common microbial metabolites in the body after consumption of polyphenols which have flavan-3-ol as a fundamental structure. This fact indicates that phenyl-γ-valerolactones may commonly contribute to functionality in the body after intake of dietary flavan-3-*ols* souses.

There are several research reports on urinary metabolites in human after consumption of green tea catechins. Justin JJ van der Hooft *et al* (60) identified 138 kinds of metabolites including 48 kinds of γ-valerolactone-based metabolites as the urinary metabolite detected from four human volunteers after green tea consumptions. Among them, glucuronide conjugates of BM6 (5-30 μmol/mL) and glucuronide conjugates of BM10 (50-150 μmol/mL) were reported to be detected at high concentrations accumulated in urine 26 hours after green tea intake. In addition, Luca Calani *et al* (125) investigated for up to 48 hours, the urine of of 20 healthy volunteers who drank RTD green tea that mainly contains (-)-EGCG, (-)-EGC, and (-)-ECG. They identified the conjugates of **BM6**, **BM10**, 5-(3', 4-dihydroxyphenyl)-γ-valerolactone, and 5-(3-hydroxyphenyl) -γ-valerolactone as the major urinary metabolites. The binding positions and number of hydroxyl moieties on benzoic acid of phenyl-γ-valerolactone are derived from the structure of substrate catechins, making 5-(3', 4-dihydroxyphenyl)-γ-valerolactone and 5-(3'-hydroxyphenyl)–γ-valerolactone the metabolic compounds of catechol-type catechins, as such (-)-EC and (+)-C. This indicated that, in the

large intestine, most of the phenyl-γ-valerolactones produced by metabolism of intestinal bacteria is likely to be absorbed from gut tract into blood circulation. However, there is still limited information on the role of these metabolites in the body.

Concerning the effects of microbial metabolites of EGCG, studies have already reported the in vitro functions for antioxidant activity against 2,2'-azinobis -(3-ethyl-benzothiazoline-6-sulfonic acidate) (ABTS) radical cation (126), neurogenic activity in human neuroblastoma SH-SY5Y cells (127), activation of splenic CD4+ cells (128), inhibition of matrix metalloproteinases (129), inhibition of NO production (129), and inhibition of angiotensin I converting enzyme (ACE) activity (130). Furthermore, the in vivo functions of anti-hypertension in spontaneously hypertensive rats (SHR) (130) and immune regulatory effects on natural killer cells in BALB/c mice (128) have been reported. As the newly discovered functions of EGCG degraded metabolites, glucose uptake ability into L6 skeletal muscle cells, and improvement of glucose tolerance in body were found in this study. Previous reports and this report clearly indicated that the EGCG microbial metabolites will perform as a functional factor in the body following green tea consumption. Thus, it is reasonable to consider that the microbial metabolites are important contributors to physiological function following green tea consumptions. However, there are still limited reports concerning the effects of microbial metabolites, and further studies on this topic are needed in the future.

In this study, the author has tried to elucidate the metabolic pathway of EGCG in rat intestinal bacterium, isolation and identification of the intestinal bacteria involved in EGCG metabolism, and functionally verified the degraded metabolites for the purpose of examining the mechanism of action of green tea catechins. In conclusion, the metabolic pathway in the rat intestine has became clarified and isolating and identifying enteric bacteria involved in EGCG metabolism have identified in this study. As a result, it became reveal that the intestinal bacterial metabolites are also having physiological functions, indicating that they may be involved in mediating the beneficial effects of green tea. In the future, continuing studies are necessary to clarify the role of phenyl-γ-valerolactone in the body, as the common microbial metabolite of the flavan-3-ols.

Refferences

1. 村松敬一郎編「茶の科学」朝倉書店 1991
2. 松崎芳郎編著「茶年表の世界史」八坂書房 2012
3. 林屋辰三郎著「日本の茶書1」平凡社 1995
4. 林屋辰三郎著「日本の茶書2」平凡社 1996
5. 古田紹欽著「栄西 喫茶養生記」講談社学術文庫 2000
6. 岩間眞知子著「茶の医薬史ー中国と日本ー」株式会社思文閣出版 2009
7. 袴田勝弘編著「お茶の力 暮らしの中のお茶と健康」化学工業日報社 2003
8. NPO法人 日本茶インストラクター協会 企画・編集 「日本茶のすべてがわかる本」社団法人農村村文化協会 2008
9. 伊奈和夫、坂田完三編「緑茶・中国茶・紅茶の化学と機能」㈱アイ・ケイコーポレーション 2007
10. 伊奈和夫、坂田完三, 富田勲、伊勢村護共編 [茶の化学成分と機能」弘学出版株式会社 2002
11. 村松敬一郎、小国伊太郎、伊勢村護、杉山公男、山本（前田）万里編「茶の機能 生体機能の新たな可能性」㈱学会出版センター 2002
12. Eng Q Y, Thanikachalam P V, Ramamurthy S. Molecular understanding of Epigallocatechin gallate (EGCG) in cardiovascular and metabolic diseases. *J. Ethnopharmacol.* 2018, 210, 296-310
13. Yang C S, Wang H. Cancer preventive activities of tea catechins. *Molecules.* 2016, 21, E1679
14. Li C, Lee M-J, Sheng S, Meng X, Prabhu S, Winnik B, Huang B, Chung J Y, Yan S, Ho C-T, Yang C S. Structural identification of two metabolites of catechins and their kinetics in human urine and blood after tea ingestion. *Chem. Res. Toxicol.* 2000, 13, 177−184
15. Kohri T, Matsumoto N, Yamakawa M, Suzuki M, Nanjo F, Hara Y, Oku N. Metabolic fate of (−)-[4-^{3}H]epigallocatechin gallate in rats after oral administration. *J. Agric. Food Chem.* 2001, 49, 4102−4112
16. Unno T, Tamemoto K, Yayabe F, Kakuda T, Urinary excretion of 5-(3',4'-dihydroxyphenyl)-g-valerolactone, a ring-fission metabolite of (-)-epicatechin, in rats and its in vitro antioxidant activity. *J. Agric. Food Chem.* 2003, 51, 6893-6898
17. Kohri T, Suzuki M, Nanjo F. Identification of Metabolites of (-)-Epicatechin Gallate and Their Metabolic Fate in the Rat. *J. Agric. Food Chem.* 2003, 51, 5561-5566
18. Luca C, Daniele D R, Maria L C, Lorenzo M, Furio B. Updated bioavailability and 48h excretion profile of flavan-3-ols from green tea in humans. *Int. J. Food Sci. Nutr.* 2011, 1-9

19. Sang S, Yabg C S. Structural identification of novel glucoside and glucuronide metabolites of (-)-epigallocatechin-3-gallate in mouse urine using liquid chromatography/electrospray. *Rapid Commun. Mass Spectrom*. 2008, 22, 3693-3699

20. Llorach R, Garrido I, Monagas M, Urpi-Sarda M, Tulipani S, Bartolome B, Andres-Lacueva C. Metabolomics study of human urinary metabolome modifications after intake of almond (Prunus dulcis (Mill.) D.A. Webb) skin polyphenols. *J. Prot. Res.* 2010, 9, 5859-5867

21. Sanchez-Patan F, Cueva C, Monagas M, Walton G E, Gibson G R, Martín-Alvarez P J, Victoria Moreno-Arribas M, Bartolome B. Gut microbial catabolism of grape seed flavan-3-ols by human faecal microbiota. Targetted analysis of precursor compounds, intermediate metabolites and end-products. *Food Chem.* 2012, 131, 337-347

22. Iso H, Date C, Wakai K, Fukui M, Tamakoshi A, JACC Study Group. The relationship between green tea and total caffeine intake and risk for self-reported type 2 diabetes among Japanese adults.   *Ann. Intern. Med*. 2006, 144, 554-562

23. Fukino Y, Ikeda A, Maruyama K, Aoki N, Okubo T, Iso H. Randomized controlled trial for an effect of green tea-extract powder supplementation on glucose abnormalities. *Eur. J. Clin. Nutr*. 2008, 62, 953-960

24. Ryu O H, Lee J, Lee K W, Kim H Y, Seo J A, Kim G, Kim N H, Baik S H, Choi D S, Choi K M. Effects of green tea consumption on inflammation, insulin resistance and pulse wave velocity in type 2 diabetes patients. *Diabetes Res. Clin. Pract.* 2006, 71, 356-358

25. Tsuneki H, Ishizuka M, Terasawa M, Wu J B, Sasaoka T, Kimura I. Effect of green tea on blood glucose levels and serum proteomic patterns in diabetic (db/db) mice and on glucose metabolism in healthy humans. *BMC Pharmacol*. 2004, 4, 18

26. Honda M, Nanjo F, Hara Y. Inhibition of Saccharide Digestive Enzymes by Tea Polyphenols. *Agric. Biol. Chem*.1990, 9, 83-89

27. Wang Y, Huang S, ShaoS, Qian l, Xu P.   Studies on bioactivities of tea (Camellia sinensis L.) fruit peel extracts: Antioxidant activity and inhibitory potential against α-glucosidase and α-amylase in vitro. Industrial. *Crops. Products*. 2012, 37, 520-526

28. Anderson R A, Polansky M M. Tea enhances insulin activity. *J. Agric. Food Chem*. 2002, 50, 7182-7186

29. Waltner-L M E, Wang X L, Law B K, Hall R K, Nawano M, Granner D K. Epigallocatechin gallate, a constituent of green tea, represses hepatic glucose production. *J. Biol. Chem*. 2002, 277, 34933-34940

30. Collins Q F, Liu H Y, Pi J, Liu Z, Quon M J, Cao W. Epigallocatechin-3-gallate (EGCG), a green tea polyphenol, suppresses hepatic gluconeogenesis through 5'-AMP-activated protein kinase. *J. Biol. Chem*. 2007, 282, 30143-30149

31. Yasui K, Tanabe H, Okada N, Fukutomi R, Ishigami Y, Isemura M. Effects of catechin-rich green tea on gene expression of gluconeogenic enzymes in rat hepatoma H4IIE cells. *Biomed. Res*. 2010, 31, 183-189

32. Saltiel A R, Kahn C R. Insulin signaling and the regulation of glucose and lipid metabolism. *Nature*. 2001, 414, 799–806

33. Phielix E, Mensink M. Type 2 diabetes mellitus and skeletal muscle metabolic function.*Physiol Behav*. 2008, 94, 252-258

34. DeFronzo R A, Tripathy D. Skeletal Muscle Insulin Resistance Is the Primary Defect in Type 2 Diabetes. *Diabetes Care*. 2009, 32(Suppl 2), S157–S163

35. Winder W.W. Energy-sensing and signaling by AMP-activated protein kinase in skeletal muscle. *J Appl. Physiol.* 2001, 91, 1017-1028

36. Ueda M, Nishiumi S, Nagayasu H, Fukuda I, Yoshida K, Ashida H. Epigallocatechin gallate promotes GLUT4 translocation in skeletal muscle. *Biochem. Biophys. Res. Commun*. 2008, 377, 286-90

37. Zhang Z F, Liang Q J, Dai X Q, Ding Y, Wang J B, Li Y. Epigallocatechin -3-O-gallate (EGCG) protects the insulin sensitivity in rat L6 muscle cells exposed to dexamethasone condition. *Phytomedicine*, 2010, 17, 14-18

38. Hara Y. Prophylactic functions of tea. *ASC symp.ser*. 1994, 547, 34-50

39. Gupta J, Siddique Y H, Beg T, Ara G, Afzal M. A review on the benefical effects of tea polyphenols on human health. *Int.J.Pharmacol*. 2008, 4, 314-338

40. Naghma K, Hasan M. Tea polyphenols for health promotion. *Lif.Sci*. 2007, 81, 519-533

41. Carmen C, Reyes A, Rafael G. Benefical effects of green tea- A review. *J Am.Coll.Nutr*. 2006, 25, 79-99

42. Lee M-J, Wang Z-Y, Li H, Chen L, Sun Y, Gobbo S, Balentine D A, Yang, C S. Analysis of plasma and urinary tea polyphenols in human subjects. *Cancer Epidemiol. Biomerk. Prev*. 1995, 4, 393–399

43. Okushio K, Matsumoto N, Kohri T, Suzuki M, Nanjo F, Hara Y. Absorption of tea catechins into rat portal vein. *Biol. Pharm. Bull*. 1996, 19, 326–329

44. Unno T, Takeo T. Absorption of (-)-epigallocatechin gallate into circulation system of rats. *Biosci. Biotech. Biochem*. 1995, 59, 1558–1559

45. Yang C S, Chen L, Lee M-J, Balentine D, Kuo M C, Schantz S P. Blood and urine levels of tea catechins after ingestion of different amounts of green tea by human volunteers. *Cancer Epidemiol. Biomark. Prev*. 1998, 7, 351–354

46. Unno T, Kondo K, Itakura H, Takei T. Analysis of (-)-epigallocatechin gallate in human serum obtained after ingesting green tea. *Biosci. Biotech. Biochem*. 1996, 60, 2066–2068

47. Nakagawa K, Miyazawa T. Absorption and distribution of tea catechin, (-)-epigallocatechin-3-gallate, in the rat. J. Nutr. Sci. Vitaminol. 1997, 43, 679 - 684

48. Suganuma M, Okabe S, Oniyama M, Tada Y, Ito H, Fujiki H. Wide distribution of [^{3}H](-)-epigallocatechin gallate, a cancer preventive tea polyphenol, in mouse tissue. *Carcinogenesis*, 1998, 19, 1771–1776

49. Kida K, Suzuki M, Matsumoto N, Nanjo F, Hara Y. Identification of biliary metabolites of (-)-epigallocatechin gallate in rats. *J. Agric. Food Chem*. 2000, 48, 4151–4155

50. Sang S, Lambert J D, Hong J, Tian S, Lee M-J, Stark R E, Ho C-T, Yang C S. Synthesis and structure identification of thiol conjugates of (-)-epigallocatechin gallate and their urinary levels in mice. *Chem. Res. Toxicol*. 2005, 18, 1762 –1769

51. Sang S, Lee M-J, Yang I, Buckley B, Yang C S. Human urinary metabolite profile of tea polyphenols analyzed by liquid chromatography/electrospray ionization tandem mass spectrometry with data-dependent acquisition. *Rapid Commun. Mass Spectrom*. 2008, 22, 1567–1578

52. Wang L-Q, Meselhy M R, Li Y, Nakamura N, Min B-S, Qin G-W, Hattori M. The heterocyclic ring fission and dehydroxylation of catechins and related compounds by Eubacterium sp. Strain SDG-2, a human intestinal bacterium. *Chem. Pharm. Bull*. 2001, 49, 1640–1643

53. Hattori M. Metabolism of epicatechin 3-O-gallate and epicatechin 3-O-gallate by human intestinal flora. *Proceedings of 2001 International Conference on O-CHA (Tea) Culture and Science, Session III Health and Benefits*. 2001, October 5-8, 38- 41

54. Meselhy M R, Nakamura N, Hattori M. Biotransformation of (-)-epicatechin 3-O-gallate by human intestinal bacteria. *Chem. Pharm. Bull*. 1997, 45, 888 – 893

55. Auger C, Mullen W, Hara Y, Crozier A. Bioavailability of Polyphenon E flavan-3-ols in humans with an lleostomy 1-4. *J. Nutr*. 2008, 138, 1535s-1542s

56. Griffiths L A. Mammalian metabolism of flavonoids. In The Flavonoids: Advances in Research; Harbone, J. B., Mabry, T. J., Eds; Chapman and Hall: London, 1982, 681-718

57. Hackett A M, Griffiths L A. The metabolism and excretion of 3-O-mrthyl-(+)-catechin in the rat, mouse, and marmoset. *Drug. Metab.Dispos*. 1981, 9 54-59

58. Meng X, Sang S, Zhu N, Lu H, Sheng S, Lee M-J, Ho C-T, Yang C S. Laboratory for Identification and Characterization of Methylated and Ring-Fission Metabolites of

Tea Catechins Formed in Humans, Mice, and Rats. *Chem. Res. Toxicol.* 2002, 15, 1042–1050

59. Mohd A A, Fahad I A-J, Abdullah M. A-M. Everted gut sac model as a tool in pharmaceutical research: limitations and applications *J.Pharm. Pharmacol*. 2012, 64, 326–336

60. Van der Hooft JJ, De Vos R C, Mihaleva V, Bino R J. Structural elucidation and quantification of phenolic conjugates present in human urine after tea intake. *Anal. Chem.* 2012, 84, 7263-7271

61. Vaidyanathan J B, Walle T. Cellular uptake and efflux of the tea flavonoid (-)epicatechin-3-gallate in the human intestinal cell line Caco-2. *J. Pharmacol. Exp. Ther.* 2003, 307, 745-752

62. Konishi Y, Kobayashi S, Shimizu M. Transepithelial transport of p-coumaric acid and gallic acid in Caco-2 cell monolayers. *Biosci. Biotechnol. Biochem*. 2003, 67, 2317-2324

63. Konishi Y, Kobayashi S. Transepithelial transport of chlorogenic acid, caffeic acid, and their colonic metabolites in intestinal caco-2 cell monolayers. *J. Agric. Food Chem.* 2004, 52, 2518-2526

64. Sakamoto M, Takagaki A, Matsumoto K, Kato Y, Goto K, Benno Y. Butyricimonas synergistica gen. nov., sp. nov. and Butyricimonas virosa sp. nov., butyric acid-producing bacteria in the family 'Porphyromonadaceae' isolated from rat faeces. *Int. J. Syst. Evol. Microbiol*. 2009, 59, 1748-1753

65. Takagaki A, Nanjo F. Metabolism of (-)-epigallocatechin gallate by rat intestinal flora. *J. Agric. Food Chem*. 2010, 58, 1313-1321

66. Jin J-S, Zhao Y-F, Nakamura N., Akao T, Kakiuchi N, Min B-S, Hattori M. Enantioselective dehydroxylation of enterodiol and enterolactone precursors by human intestinal bacteria. *Biol. Pharm. Bull*. 2007, 30, 2113-2119

67. Jin J-S, Hattori M. Isolation and characterization of a human intestinal bacterium Eggerthella sp. CAT-1 capable of cleaving the C-ring of (+)-catechin and (-)-epicatechin, followed by p-dehydroxylation of the B-ring. *Biol. Pharm. Bull*. 2012, 35, 2252–2256

68. Kutschera M, Engst W, Blaut M, Braune A. Isolation of catechin-converting human intestinal bacteria. *J. Appl. Microbiol*. 2011, 111, 165-175

69. Takagaki A, Nanjo F. Manufacture of 5-phenyl-4-hydroxyvaleric acid and/or 5-phenyl-g-valerolactone from catechin derivatives with microorganisms. *Jpn Tokkyo Koho,* 2011 JP 2011087486

70. Maruo T, Sakamoto M, Ito C, Toda T, Benno Y. Adlercreutzia equolifaciens gen. nov., sp. nov., an equol-producing bacterium isolated from human faeces, and

emended description of the genus Eggerthella. *Int. J. Syst. Evol. Microbiol*. 2008, 58, 1221–1227

71. Minamida K, Tanaka M, Abe A, Sone T, Tomita F, Hara H, Asano K. Production of equol from daidzein by gram-positive rod-shaped bacterium isolated from rat intestine. *J. Biosci. Bioeng*. 2006, 102, 247–250

72. Minamida K, Ota K, Nishimukai M, Tanaka M, Abe A, Sone T, Tomita F, Hara H, Asano K. Asaccharobacter celatus gen. nov., sp. nov., isolated from rat caecum. *Int. J. Syst. Evol. Microbiol.* 2008, 58, 1238–1240

73. Jin J-S, Nishihara T, Kakiuchi N, Hattori M. Biotransformation of c-glucosylisoflavone puerarin to estrogenic (3S)-equol in co-culture of two human intestinal bacteria. *Biol. Pharm. Bull.* 2008, 31, 1621–11625

74. Jin J-S, Kitahara M, Sakamoto M, Hattori M, Benno Y. Slackia equolifaciens sp. nov., a human intestinal bacterium capable of producing equol. *Int. J. Syst. Evol. Microbiol.* 2010, 60, 1721–1724

75. Matthies A, Blaut M, Braune A. Isolation of a human intestinal bacterium capable of daidzein and genistein conversion. *Appl. Environ. Microbiol.* 2009, 75, 1740–1744.

76. Altschul S F, Gish W, Miller W, Myers E W, Lipman D J. Basic local alignment search tool. *J. Mol. Biol*. 1990, 215, 403-410

77. Thompson J D, Higgins D G, Gibson T J, Clustal W. Improving the sensitivity of progressive multiple sequence alignment through sequence weighting, positions-specific gap penalties and weight matrix choice. *Nucleic. Acids Res*. 1994, 22, 4673-4680

78. Hall T A, BioEdit: a user-friendly biological sequence alignment editor and analysis program for Windows 95/98/NT. *Nucl Acids Symp Ser* 1999, 41, 95-98

79. Tamura K, Dudley J, Nei M, Kumar S. MEGA4: Molecular Evolutionary Genetics Analysis (MEGA) software version 4.0. *Molecular Biology and Evolution* 2007, 24, 1596-1599

80. Kimura M. A simple method for estimating evolutionary rates of base substitution through comparative studies of nucleotide sequences. *J. Mol. Evo.* 1980, 16, 111-120.

81. Ohno M, Okano I, Watsuji T, Kakinuma T, Ueda K, Beppu T. Establishing the independent culture of a strictly symbiotic bacterium Symbiobacterium thermophilum from its supporting Bacillus strain. *Biosci. Biotechnol. Biochem*. 1999, 63, 1083-1090

82. Ito K, Ishida H, Takagaki A, Nanjo F, Maruo T, Ito C. Metabolism of isoflavone from soy bean by Eggerthella sp. MT4s-5, Part 1 Metabolism of daidzein, glycitein, and genistein. *The 128th Annual Meeting of the Pharmaceutical Society of Japan, Abstract 2*, 2008, 87

83. Krumholz L R, Bryant M P. Eubacterium oxidoreducens sp. nov. requiring H_2 or formate to degrade gallate, pyrogallol, phloroglucinol and quercetin. *Arch. Microbiol.* 1986, 144, 8-14

84. Stams A J M, Bok F A M, Plugge C M, Eekert M H A., Dolfing J, Schraa G. Exocellular electron transfer in anaerobic microbial communities. *Environ. Microbiol.* 2006, 8, 371-382

85. Decroos K, Vanhemmens S, Boon S C N, Verstraete W. Isolation and characterization of an equol-producing mixed microbial culture from a human faecal sample and its activity under gastrointestinal conditions. *Arch. Microbiol*. 2005, 183, 45-55

86. Bolca S, Verstraete W. Microbial equol production attenuates colonic methanogenesis and sulphidogenesis in vitro. *Anaerobe.* 2010, 16, 247-252

87. Goto K, Kanaya S., Nishikawa T, Hara H, Terada A, Ishigami T, Hara Y. The influence of tea catechins on fecal flora of elderly residents in long-term care facilities. *Annals of Long-Term Care*. 1998, 6, 43-48

88. Thawornkuno C, Tanaka M, Sone T, Asano K. Biotransformation of daidzein to equol by crude enzyme from Asaccharobacter celatus AHU 1763 required an anaerobic environment. *Biosci. Biotechnol. Biochem*. 2009, 73, 1435-1438

89. Takagaki A, Kato Y, Nanjo F. Rat intestinal bacteria involved in biotransformation of (-)-epigallocatechin gallate. *Arch. Microbiol*. 2014, 196, 681–695

90. Wolfram S, Raederstorff D, Wang Y, Teixeira S R, Elste V, Weber P. TEAVIGOTM (Epigallocatechin Gallate) Supplementation Prevents Obesity in Rodents by Reducing Adipose Tissue Mass. *Ann. Nutr. Metab*. 2005, 49, 54-63

91. Matsumoto N, Ishigaki F, Ishigaki A, Iwashina H, Hara Y. Reduction of blood glucose levels by tea catechin. *Biosci. Biotechnol. Biochem*. 1993, 57, 525−527.

92. Igarashi K, Honma K, Yoshinaga O, Nanjo F, Hara Y. Effect of dietary catechins on glucose tolerance, blood pressure and oxidative status in Goto-Kakizaki rats. *J. Nutr. Sci. Vitaminol.* 2007, 53, 496-500

93. Henrik Ortsäter H, Grankvist N, Wolfram S, Kuehn N, Sjöholm A. Diet supplementation with green tea extract epigallocatechin gallate prevents progression to glucose intolerance in db/db mice. *Nutr. Metab*, 2012, 9, 11, DOI:10.1186/1743-7075-9-11

94. DeFronzo R A, Bonadonna R C, Ferrannini E. Pathogenesis of NIDDM. A balanced overview. *Diabetes Care.* 1992, 15, 318-368

95. Yamamoto N, Yamashita Y, Yoshioka Y, Nishiumi S, Ashida H. Rapid Preparation of a Plasma Membrane Fraction: Western Blot Detection of Translocated Glucose

Transporter 4 from Plasma Membrane of Muscle and Adipose Cells and Tissues. *Curr. Protoc. Protein. Sci.*, 2016, 85:29.18.1-29.18.12., DOI: 10.1002/cpps.13

96. Nishiumi S, Ashida H. Rapid Preparation of a Plasma Membrane Fraction from Adipocytes and Muscle Cells: Application to Detection of Translocated Glucose Transporter 4 on the Plasma Membrane. *Biosci. Biotechnol. Biochem*. 2007, 71, 2343–2346

97. Yamauchi T, Kamon J, Minokoshi Y, Ito Y, Waki H., Uchida S, Yamashita S, Noda M, Kita S, Ueki K, Eto K, Akanuma Y, Froguel P, Foufelle F, Ferre P, Carling D, Kimura S, Nagai R, Kahn B B, Kadowaki T. Adiponectin stimulates glucose utilization and fatty-acid oxidation by activating AMP-activated protein kinase. Nat Med. 2002, 8, 1288-1295

98. Faubert B, Vincent E E, Poffenberger M C, Jones R G. The AMP-activated protein kinase (AMPK) and cancer: many faces of a metabolic regulator. *Cancer Lett.* 2015, 356, 165-170

99. Kim J, Yang G, Kim Y, Kim J, Ha J. AMPK activators: mechanisms of action and physiological activities. *Experimental & Molecular Medicine.* 2016, 48, e224; DOI:10.1038/emm.2016.16

100. Yamashita Y, Okabe M, Natsume M, Ashida H. Cacao liquor procyanidin extract improves glucose tolerance by enhancing GLUT4 translocation and glucose uptake in skeletal muscle. *J. Nutr. Sci.* 2012, vol 1, e2. DOI: 10.1017/jns.2012.2

101. Honda, M, Nanjo F, Hara Y. Inhibition of Saccharide Digestive Enzymes by Tea Polyphenols. *Agric. Biol. Chem*.1990, 9, 83-89

102. Wang Y et al. Studies on bioactivities of tea (Camellia sinensis L.) fruit peel extracts: Antioxidant activity and inhibitory potential against α-glucosidase and α-amylase in vitro. Industrial. *Crops. Products*. 2012, 37, 520-526

103. Anderson R A et al. Tea enhances insulin activity. *J. Agric. Food Chem*. 2002, 50, 7182-7186

104. Waltner-L, M.E et al. Epigallocatechin gallate, a constituent of green tea, represses hepatic glucose production. *J. Biol. Chem*. 2002, 277, 34933-34940

105. Han MK. Epigallocatechin gallate, a constituent of green tea, suppresses cytokineinduced pancreatic beta-cell damage. *Exp Mol Med*. 2003, 35, 136-139. [12754418]

106. Calani L, Del Rio D, Luisa Callegari M, Morelli L, Brighenti F. Updated bioavailability and 48 h excretion profile of flavan-3-ols from green tea in humans. *Int. J. Food Sci. Nutr.* 2012, 63(5), 513-521

107. Takagaki A, Nanjo. F. Catabolism of (+)-Catechin and (−)-Epicatechin by Rat Intestinal Microbiota. *J. Agric. Food Chem* 2013, 61, 4927−4935

108. Mena P, Bresciani L, Brindani N, Ludwig I A, Pereira-Caro G, Angelino D, Llorach R, Calani L, Brighenti F, Clifford M N, Gill C I R, Crozier A, Curtia C, Del Riobj D. Phenyl-γ-valerolactones and phenylvaleric acids, the main colonic metabolites of flavan-3-ols: synthesis, analysis, bioavailability, and bioactivity. *Natural Product Reports.* 10.1039/C8NP00062J

109. Borges G, Ottaviani J I, van der Hooft J J J, Hagen Schroeter, Crozier A. Absorption, metabolism, distribution and excretion of (−)-epicatechin: A review of recent finding. *Molecular Aspects of Medicine*, 2018, 61, 18-30

110. Takagak A, Yoshioka Y, Yamashita Y, NaganoT, Ikeda M, Hara-Terawaki A, Seto R, Ashida H. Effects of microbial metabolites of (--)-Epigallocatechin gallate on glucose uptake in L6 skeletal muscle cell and glucose tolerance in ICR mice. *Biol. Pharm. Bull.* 2019, 42, 212–221

111. Yamauch T, Kamon J, Ito Y, Tsuchida A, Yokomizu T, Kita S, Sugiyama T, Miyagishi M, Hara K、Tsunoda M, Murakami K, Ohteki T, Uchida S, Takekawa S, Waki H, Nelson H. TsunoY, Shibata Y, Y Terauchi, Froguel P, Tobe K, Koyasu S, Taira K, Kitamura T, Shimizu T, Nagai R, Kodowaki T. Cloning of adiponectin receptors that mediate antidiabetic metabolic effects. *Nature*, 2003, 423, 762-769

112. Nathan L. Price Ana P. Gomes, Alvin J.Y. Ling, Filipe V. Duarte, Alejandro Martin-Montalvo, Brian J. North, Beamon Agarwal, Lan Ye, Giorgio Ramadori, Joao S. Teodoro, Basil P. Hubbard, Ana T. Varela, James G. Davis, Behzad Varamini, Angela Hafner, Ruin Moaddel, Anabela P. Rolo, Roberto Coppari, Carlos M. Palmeira, Rafael de Cabo, Joseph A. Baur, and David A. Sinclair, SIRT1 Is Required for AMPK Activation and the Beneficial Effects of Resveratrol on Mitochondrial Function. *Cell Metabolism* 2012, 15, 675–690

113. Zhang L, Wang Y, Li D, Ho C T, Li J, Wan X. The absorption, distribution, metabolism and excretion of procyanidins. *Food Funct.* 2016, 7, 1273-1281.

114. Maaike M. Appeldoorn, Jean-Paul Vincken, Anna-Marja Aura, Peter C. H. Hollman, Harry Gruppen. Procyanidin Dimers Are Metabolized by Human Microbiota with 2-(3,4-Dihydroxyphenyl)acetic Acid and 5-(3,4-Dihydroxyphenyl)-γ-valerolactone as the Major Metabolites. *J. Agric. Food Chem*. 2009、57, 1084–1092

115. Duweler K G, Rohdewald P. Urinary metabolites of French maritime pine bark extract in humans. Pharmazie, 2000, 55, 364-368

116. Rohdewald P. A review of the French maritime pine bark extract (Pycnogenol), a herbal medication with a diverse clinical pharmacology. *International journal of clinical pharmacology and therapeutics,* 2002, 40, 158-168

117. Nanjo F, Honda M, Okushio K, Matsumoto N, Ishigaki F, Ishigami T, Hara Y. Effects of dietary tea catechins on α-tocopherol levels, lipid peroxidation, and erythrocyte deformability in rats fed on high palm oil and perilla oil diets. *Biol. Pharm. Bull.* 1993, 16, 1156−1159

118. Negishi H., Xu J-W, Ikeda K, Njelekela M, Nara Y, Yamori Y. Black and green tea polyphenols attenuate blood pressure increases in stroke-prone spontaneously hypertensive rats. *J. Nutr.* 2004, 134, 38−42

119. Del Rio D, Calani L, Cordero C, Salvantore S, Pellegrini N, Brighenti F. Bioavailability and catabolism of green tea flavan-3-olsin humans. *Nutrition.* 2010, 26, 1110−1116

120. Hase T, Komine Y, Meguro S, Takeda Y, Takahashi H, Matsui Y, Inaoka S, Katsuragi Y, Tokimitsu I, Shimasaki H, Itakura H. Anti-obesity effects of tea catechins in humans. *J Oleo. Sci.* 2001, 50, 599-605

121. Nagao T, Meguro S, Soga S, Otsuka A, Tomonobu K, Fumoto S, Chikama A, Mori K, Yuzawa M, Watanabe H, Hase T, Tanaka Y, Tokimitsu I, Shimasaki H, Itakura H. Tea catechins suppress accumulation of body fat in humans. *J. Oleo. Sci.* 2001, 50, 717-728

122. Mena P, Bresciani L, Brindani N, Ludwig I A, Pereira-Caro G, Angelino D, Llorach R, Calani L, Brighenti F, Clifford M.N, Gill C I R, Crozier A, Curtia C, Del Rio D. Phenyl-γ-valerolactones and phenylvaleric acids, the main colonic metabolites of flavan-3-ols: synthesis, analysis, bioavailability, and bioactivity. *Natural Product Reports.* 2019, 36, 714-752

123. Borges G, Ottaviani J I, Van der Hooft J J J, Schroeter H, Crozier A. Absorption, metabolism, distribution and excretion of (−)-epicatechin: A review of recent finding. *Molecular Aspects of Medicine,* 2018, 61, 18-30

124. Appeldoorn M M, Vincken J P, Aura A M, Hollman P C, Gruppen H. Procyanidin Dimers Are Metabolized by Human Microbiota with 2-(3,4-Dihydroxyphenyl)acetic Acid and 5-(3', 4'-dihydroxyphenyl)-g-valerolactone as the Major Metabolites. *J. Agric. Food Chem.* 2009, 57, 1084–1092

125. Calani L, Del Rio D, Luisa Callegari M, Morelli L, Brighenti F. Updated bioavailability and 48 h excretion profile of flavan-3-ols from green tea in humans. *Int. J. Food Sci. Nutr.* 2012, 63, 513-521

126. Takagaki A, Otani S, Nanjo F. Antioxidative activity of microbial metabolites of (−)-epigallocatechin gallate produced in rat intestines. *Biosci. Biotechnol. Biochem.* 2011, 75, 582−585

127. Unno K, Pervin M, Nakagawa A, Iguchi K, Hara A, Takagaki A, Nanjo F, Minami A, Nakamura Y. Blood–Brain Barrier Permeability of Green Tea Catechin Metabolites

and their Neuritogenic Activity in Human Neuroblastoma SH-SY5Y Cells. *Mol. Nutr. Food Res*. 2017, 61, ID: 1700294. DOI: 10.1002/mnfr.201700294

128.Kim Y-H, Won Y-S, Yang X, Kumazoe M, Yamashita S, Hara A, Takagaki A, Goto K, Nanjo F, Tachibana H. Green Tea Catechin Metabolites Exert Immunoregulatory Effects on CD4+ T Cell and Natural Killer Cell Activities. *J. Agric. Food Chem*. 2016, 64, 3591−3597

129.Yang C. S, Lambert J D, Hou Z, Ju J, Lu G, Hao X. Molecular targets for the cancer preventive activity of tea polyphenols. *Mol. Carcinog*. 2006, 45, 431−435

130.Takagaki A, Nanjo F. Effects of Metabolites Produced from (−)-Epigallocatechin Gallate byRat Intestinal Bacteria on Angiotensin I‑Converting Enzyme Activity and Blood Pressure in Spontaneously Hypertensive Rats. *J. Agric. Food Chem.* 2015, 63, 8262−8266

Acknowledgment

List of Publications

➢ Sakamoto M, Takagaki A, Matsumoto K, Kato Y, Goto K, Benno Y. Butyricimonas synergistica gen. nov., sp. nov. and Butyricimonas virosa sp. nov., butyric acid-producing bacteria in the family 'Porphyromonadaceae' isolated from rat faeces. *International Journal of Systematic and Evolutionary Microbiology*, 59(7), 2009, 1748-1753

➢ Akiko Takagaki, Fumio Nanjo. Metabolism of (-)-Epigallocatechin Gallate by Rat Intestinal Flora. *Journal of Agricultural Food Chemistry*, 58,(2), 2010, 1313-1321

➢ Akiko Takagaki, Fumio Nanjo. Catabolism of (+)-Catechin and (-)-Epicatechin by Rat Intestinal Microbiota. *Journal of Agricultural Food Chemistry*, 61(20), 2013, 4927-4935

➢ Akiko Takagaki, Shuichi Otani and Fumio Nanjo. Antioxidant Activity of Microbial Metabolites of (-)-Epigallocatechin Gallate Produced in Rat Intestine. *Bioscience, Biotechnology, and Biochemistry*. 75(3), 2011, 582-585

➢ Akiko Takagaki, Yuko Kato, Fumio Nanjo. Isolation and Characterization of Rat Intestinal Bacteria Involved in Biotransformation of (-)-Epigallocatechin and (-)-Epigallocatechin. *Archives of Microbiology*, 196(10), 2014, 681-695

➢ Akiko Takagaki, Fumio Nanjo. Bioconversion of (-)-Epicatechin, (+-)-Epicatechin, (-)-Catechin, and (+)-Catechin by (-)-Epigallocatechin-Metabolizing Bacteria. *Biological and Pharmaceutical Bulletin*. 38(5), 2015, 789-794

➢ Akiko Takagaki, Fumio Nanjo. Biotransformation of (-)-Epigallocatechin and (-)-Gallocatechin by Intestinal Bacteria Involved in Isoflavone Metabolism. *Biological and Pharmaceutical Bulletin*. 38(2), 2015, 325-330

➢ Akiko Takagaki, Fumio Nanjo. Effects of Metabolites Produced from (−)-Epigallocatechin Gallate by Rat Intestinal Bacteria on Angiotensin I Converting Enzyme Activity and Blood Pressure in Spontaneously Hypertensive Rats. *Journal of Agricultural Food Chemistry*. 63, **2015**, 8262-8266

➢ Akiko Takagaki, Fumio Nanjo. Biotransformation of (−)-epicatechin, (+)-epicatechin, (−)-catechin, and (+)-catechin by intestinal bacteria involved in isoflavone metabolism. *Bioscience, Biotechnology, and Biochemistry*, 80(1), 2016, 199-202

➢ Yoon Hee Kim, Yeong-Seon Won, Xue Yang Motofumi Kumazoe, Shuya Yamashita, Aya Hara, Akiko Takagaki, Keiichi Goto, Fumio Nanjo, and Hirofumi Tachibana. Blood brain barrier permeability of (−)-epigallocatechin gallate, its proliferation-enhancing activity of human neuroblastoma SH-SY5Y cells, and its preventive effect on age-related cognitive dysfunction in mice. *Biochemistry and Biophysics Reports*. 9, 2017, 180-186

➢ Keiko Unno, Monira Pervin, Aimi Nakagawa, Kazuaki Iguchi, Aya Hara, Akiko Takagaki,Fumio Nanjo, Akira Minami, and Yoriyuki Nakamura. Blood-Brain Barrier Permeability of Green Tea Catechin Metabolites and their Neuritogenic Activity in Human Neuroblastoma SH-SY5Y Cells.

Molecular Nutrition Food Research, 61(12), 2017, 1700294. doi.org/10.1002/mnfr.201700294

➢ Pervin M, Unno K, Nakagawa A, Takahashi Y, Iguchi K, Yamamoto H, Hoshino M, Hara A, <u>Takagaki A</u>, Nanjo F, Minami A, Imai S, Nakamura Y. Blood-brain barrier permeability of (-)-epigallocatechin gallates, its proliferation-enhancing activity of human neuroblastoma SH-SY5Y cells, and its preventive effect on age-related cognitive dysfunction in mice. *Biochemistry and Biophysics Reports*, Vol 9, 2017, 180-186

➢ Aya Hara-Terawaki, <u>Akiko Takagaki</u>, Hirotsugu Kobayashi, and Fumio Nanjo. Inhibitory Activity of Catechin Metabolites Produced by Intestinal Microbiota on Proliferation of HeLa Cells. *Biological and Pharmaceutical Bulletin*, 40(8), 2017, 1331-1335

➢ <u>Akiko Takagaki</u>, Yasukiyo Yoshioka, Yoko Yamashita, Tomoya Nagano, Masaki, Aya Hara-Terawaki, Ryota Seto, Hitoshi Ashida. Effects of Microbial Metabolites of (−)-Epigallocatechin Gallate on Glucose Uptake in L6 Skeletal Muscle Cell and Glucose Tolerance in ICR Mice. *Biol.Pharm.Bull*. 42(2), 2019, 212-221